The University Of Sheffield.

Understanding the effects of compositional changes in ion exchange

By:

Hande Özbayraktar

A thesis submitted in partial fulfilment of the requirements for the degree of Doctor of Philosophy

The University of Sheffield
Faculty of Engineering
Department of Materials Science and Engineering

APRIL 2021

Acknowledgments

First and foremost, I gratefully acknowledge the financial support for my doctoral study provided by Mr Erol Güral, Deputy Chairman of Gürok Company.

I would like to express my gratitude and sincere thanks to my supervisor, Professor Russel J. Hand for, his kind supervision throughout my research. I could not have completed this thesis without his guidance, support, encouragement and patience.

I would also like to express my sincere gratitude to my second supervisor Dr Adrian Leyland for his kind support and encouragement.

Special thanks to our wonderful technicians and people at the University of Sheffield, especially Dr Lisa Hollands for glass melting, Neil Hind for helping me out with the heat treatment, Dr Dawn Bussey for her guidance during my indentation runs, Tes Monaghan for micro preparation, Dr Nik Reeves-McLaren for Raman Spectroscopy and XRF.

Special thanks to all my great friends for all the good times we had together in Sheffield.

I would like to express my gratitude and appreciation to my mum, Sadiye, my dad, Gürbüz and my brother, Eray, for their unconditional love, understanding, constant support and encouragement. I owe special thanks to my beloved husband Semih for his love, continual support, encouragement and patience, especially during difficult times. Last, but of course, not least, I thank my precious daughter, Zeynep who joined us right after I finished my PhD.

Abstract

The primary methods for consistently improving the strength of silicate glasses is the use of thermally or chemically introduced residual stresses, with the latter technique having become increasingly important in recent years. Chemical strengthening is based on ion exchange which is mainly a diffusional process, takes place in a molten salt by exchanging larger alkali for smaller ones to generate surface compression below the glass transition temperature. Commonly the focus is on the level of stresses that can be introduced by ion exchange, with relatively little attention being paid to other structural and property changes that arise from the compositional changes inherent in ion exchange.

This project involves investigation of the effects of exchanging pairs of ions, ionic species, process time and temperature on the enhancement of mechanical properties of ion-exchanged strengthened alkali – alkaline earth silicate glasses as well as the effects of compositional changes arising from ion exchange by making bulk glasses with equivalent compositions to glasses produced by ion exchange. The structures of these bulk glasses have been assessed using Raman and IR spectroscopies and the results compared to those obtained on the ion exchanged glasses. In addition, the mechanical properties, including fracture toughness, of the bulk glasses have also been assessed. In this research the primary focus has been Na/K ion exchange but ion exchange of different alkali ions such as Na^+ for Li^+, K^+ for Na^+, Cs^+ for Na^+ or K^+ have been examined using a salt paste method.

Modifications in the Na^+ - K^+ ion–exchanged glasses are observed to be associated with structural band changes in the silica network structure; notably Q^n distribution changes based on ion-exchange temperature and time. However, the structural changes cannot all be a direct consequence of ion-exchange; some of the changes shown should be due to the stress. The Raman Spectroscopy and FTIR reflectance spectra suggest observation of similar features in both ion exchange glasses and the as-melted glasses. The ion – exchange process aids to improve mechanical properties; however, as the amount of potassium content increases in the glass composition, toughness, hardness, elastic moduli all decrease. Consequently, it can be seen that although the structural changes are similar in both Na^+-K^+ ion-exchanged glasses and equivalent potassium-containing as-melted glasses, examination of the mechanical properties gave better results for the ion-exchange strengthened glasses.

Table of Contents

List of Tables

Table of Figures

Chapter 1. Introduction

Due to a combination of durability, transparency and optical properties glasses are unique materials used in a wide variety of application, despite the fact that many glasses are brittle. As well as flat glass and container glass or glass fibres, which are well-known areas of glass usage commercially, glasses are also used for high-value products for high technology applications such as biological implants, smartphone screens, opto-electronics.

Theoretically, most oxide glasses can be considered as having high strength due to the strong covalent bonds of the network forming oxides. For instance, it was established that vitreous silica has a tensile strength of up to 26 GPa (Kurkjian *et al.*, 2003). However, there is a great difference between experimental and theoretical values of glass strength due to the presence of small flaws which usually occur on the surface (LaCourse, 1987). These flaws can be scratches on the surface due to the mechanical interactions with materials which are harder than the glass, bubbles coming from the melting process, inhomogeneities related to insufficient annealing time, inclusions or any distinguishable mechanical phase. Essentially, for annealed soda-lime-silica glass as found in windows and bottles, the strength values vary between ~30 MPa for aged glass up to ~100 MPa (Varshneya, 2006). Therefore, the improvement of the mechanical properties of glasses is of significant interest. Modifications can be done by altering the material's surface or chemical composition or else modifying the processing of the material. The most reliable method of improving the practical strength of silicate glasses involves the introduction of compressive residual stresses at the glass surface through thermal or chemical processing, with thermally strengthened glass being known as safety glass (Amidon et al., 1983; As et al., 2005; Mognato et al., 2014). However, chemical strengthening by ion exchange is increasingly being used as higher surface compression can be obtained, on thinner and more complex shaped glass specimens while the optical quality of glass remains the same (Gy, 2008; Macrelli, 2015).

Ion exchange mostly involves exchanging of smaller alkali ions inside the glass by larger ones, at temperatures below the glass transition temperature, to give compressive stresses on the glass surface. Ion exchange has been extensively used to modify glass surfaces to enhance not only mechanical properties (Gy, 2008), but also electrical (Ramaswamy, 1988), optical (Speranza *et al.*, 2009) and chemical (Guldiren et al., 2016) properties. Chemical strengthening by ion exchange provides surface compression to prevent the formation of new cracks and propagation of

existing cracks on the glass surface. The strength of glass and glass strengthening methods which are thermal strengthening, acid etching, fire polishing, lamination, ceramming anc coating are reviewed in some papers (Karlsson et al., 2010; Varshneya, 2010a, 2018). For instance Karlsson et al., (2010) reported the technology of chemical stregthening applications which covers the advantage over the other strengthening techniques such as sol-gel coatings and thermal strengthening. Although sol-gel coatings are relatively inexpensive and easily controlled coating methods, the strengthening mechanism is not as effective as thermal or chemical tempering.

Conventionally, chemical strengthening via ion exchange is mostly done by immersion of the glass pieces in a salt bath for long hours. Experimentally many monovalent cations have been tested in the ion exchange experiments such as Li^+, Na^+, K^+, Rb^+, Cu^+, Ag^+ using different typezof alkali containing glasses for varying times and temperatures (Gy, 2008a; Varshneya, 2010b; Karlsson, 2012). There are a few studies that uses different ion exchange methods such as salt paste, physical vapor deposition as well as the electric field assisted ion exchange (Oven et al., 1999; Karlsson, 2012; Patschger and Rüssel, 2016). Structural and property changes that arise from compositional changes inherent in ion exchange has been given relatively less attention than mechanical property enhancement due to the ion exchange treatment. There are a few studies that examined the molecular dynamics for investigations of the structural changes induced by an ion-exchange process. (Kreski et al., 2012; Tandia et al., 2012)

Hence this thesis investigates the effects of anionic species, process time and temperature on the preparation of ion-exchanged soda-lime-silica glasses, using a single-side ion exchange process by salt-paste method. Salt paste method is used as an alternative to conventional salt bath method, since relatively less amount of salt needs to be used. Soda-lime-silica glasses are examined because they are used commercially in many applications and are relatively cheap. Due to the contact of the bottom side with the molten tin inside tin tank during float process, the composition of the one side of float glass contains tin oxide. Tin side of the glass is resistant to ion exchange due to the presence of tin in the surface, grinding and polishing presedure needs to be done prior to ion exchange. Glass slides which were used in this study checked for the presence of any thin in the surface by using a short wave, 180-280 nm, UV lamp. Under UV light tin side is expected to be flourescent and reflects milky white image.

However thin was not observed in the surface, therefore grinding and polishing was not necessary to remove the tin in the surface(Shelby, 2005; Varshneya, 2006)

In addition to ion exchange involving potassium, equivalent potassium containing glasses have been prepared to determine whether the features are a direct consequence of ion exchange or due to the presence of potassium in the glass composition with the aim of deconvoluting the effects of introducing residual stresses from compositional changes (Gonzalez Rodriguez and Hand, 2013). The comparative interpretation of mechanical and structural properties examined from various perpectives are thought to complement the contribution to the literature. Furthermore, this work has led to further research and development in the industry in terms of developing impact test resistance. Preliminary pilot-scale tests have been done, further experiments are planned.

This thesis is divided into five chapters. This chapter (Chapter One) provides the context and aims of this project. Chapter Two, the literature review, introduces first the structure of glass and secondly, mechanical properties such as strength, elastic moduli, hardness and fracture toughness are considered followed by an examination of the strengthening mechanisms which are used to improve the mechanical properties of glasses. This leads to a detailed consideration of strengthening arising from ion exchange. Chapter Three describes the experimental methods used throughout the work. This includes details procedures for the ion exchange process and glass production and also a variety of characterization techniques. The results obtained for ion exchange strengthening and different alkali metal containing glasses are presented in Chapter four. Also, the results are discussed and placed in the context of the wider literature in the same chapter. Finally, conclusions and recommendations for future work are presented in Chapter 5.

Chapter 2. Literature Review

2.1. Introduction

In the following, the structure of silicate glasses is firstly reviewed, followed by the mechanical properties of silicate glasses including elastic moduli, hardness, and fracture toughness. Finally, glass strengthening methods are reviewed, leading into a detailed consideration of chemical tempering or ion exchange strengthening.

2.2. Glass Structure

Glasses are one of the most important and impressive types of material with more than 5000 years of history of production. Glasses are generally known for having a good combination of transparency and mechanical stiffness. Although the brittleness of many glasses limits their use in some applications, glasses play a major role in modern technology as a result of their physical performance and unique structure. Soda-lime-silica glass is the most widely used in architectural windows, beverage containers, household lamps, thermal insulation as it has good chemical durability, transparency, and high electrical resistivity (Kearns *et al.*, 2010).

Originally the word glass derives from a Latin word “glaseum” meaning transparent and glossy material. A number of definitions of a “glass” have been made. The American Society for Testing and Materials (ASTM) defines glass as ‘‘an inorganic product of fusion which has been cooled to a rigid condition without crystallizing” (ASTM 2010). However, techniques such as sol-gel or chemical vapour deposition can also be used to fabricate glasses. In addition, other glasses such as metallic glasses and organic glasses can also be produced Zachariasen (1932). As a result, in 2017, Zanotto & Mauro suggested an improved definition namely *“Glass is nonequilibrium, non- crystalline condensed state of matter that exhibits a glass transition. The structure of glasses is similar to that of their parent supercooled liquids, and they spontaneously relax toward the supercooled liquid state. Their ultimate fate, in the limit of infinite time, is to crystallize.”* This definition does, of course, require a knowledge of the meaning of glass transition (see below).

There are several hypotheses related to glass structure and the conditions of formation of glass. One of the earliest is due to Zachariasen's (1932) who proposed the random network hypothesis which has become one of the most accepted theories of the structural formation of glass. According to Warren (1934) glass formation rules; oxygen atoms should not link to more than two cations; the coordination number of the glass forming atom should be small

(3 or 4); the cation polyhedra should share corners, not edges or faces. A supportive X-Ray diffraction study done by (A.Feltz, 2001) showed that the polyhedra should link in a three-dimensional network.

Hence oxide glasses are produced out of components which can be classified as network formers, network modifiers or intermediates. Common glassy materials capable of being produced using widely-accessible cooling rates, at least one network former must be present(Shelby, 2005). Network formers such as SiO_2, B_2O_3, and GeO_2, are able to form the glass on their own and have high electronegativity. Oxygens linking two formers are known as bridging oxygens. Network modifiers include alkali oxides (Li_2O, Na_2O, and K_2O) and alkaline earth oxides (MgO, CaO and BaO) and they reduce the connectivity of the network by creating non-bridging oxygens. The structure of sodium silicate glass can be seen schematically in Figure 2. 1

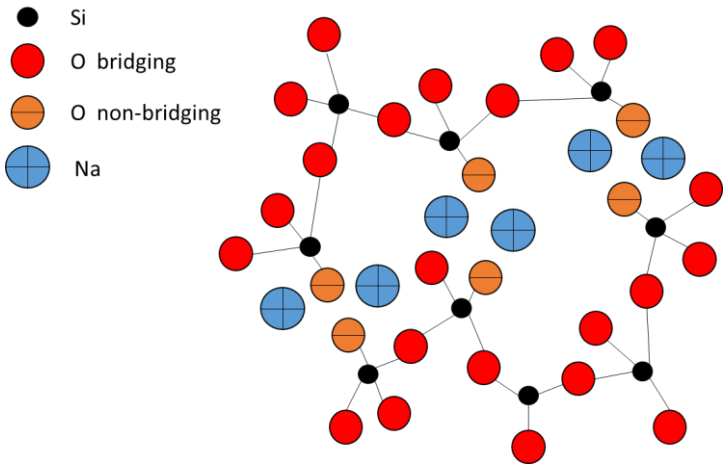

Figure 2. 1: Structure of sodium silicate glass

Thus, by adding network modifiers to the glass composition the connectivity and the processing temperature are reduced. Network intermediates or conditional glass formers are not able to form a glass on their own since they have a lower electronegativity than any network former. However, intermediates can be used to improve some of the mechanical and thermal properties. Al_2O_3, ZrO_2, PbO, and TiO_2 are examples of intermediates Sun (1947).

Sun (1947) stated the single bond strength of glass network formers is greater than 80 kcal mol^{-1} (336 kJ mol^{-1}). Intermediates, which can be both a network former and a modifier, have the single bond strength between 60 and 80 kcal mol^{-1} (252 kJ mol^{-1} – 336 kJ mol^{-1}). Network

modifiers have below 60 kcal mol^{-1} (252 kJ mol^{-1}) of bond strength. Thus, according to (Shelby, 2005), the higher bond strength means a better glass forming ability for a given oxide.

Apart from network formers, modifiers, and intermediates other oxides may also be present in the glass batch and the final glass. For example, colorants oxides such as FeO/Fe_2O_3, CuO/Cu_2O, CoO/Co_2O_3 may be present at low concentrations to absorb the light thus producing a colour. Fining agents are also used to improve the quality of the glass by aiding bubble removal during the glass melting process (Shelby, 2005; Varshneya, 2006). Fining agents are species such as arsenic, antimony or sulphate usually present at low concentrations.

Figure 2.2. shows a volume versus temperature diagram for a glass melt. If the molten material starts the path at point a, cools down and follows the *abc* path to below the melting temperature, crystallisation occurs. However, providing that the crystal growth rate is slow enough and the melt contains a relatively low number of nucleation sites, the volume of the liquid material may continue to shrink without crystallisation so that it remains liquid even below the melting temperature. In this region, it is a supercooled liquid. On further cooling below the supercooled liquid state, the liquid passes through the glass transition region to form an amorphous solid (points *g* and *h*). The cooling rate required for this to occur is linked to the volume, glass transition temperature and amount of disorder Varshneya (2006).

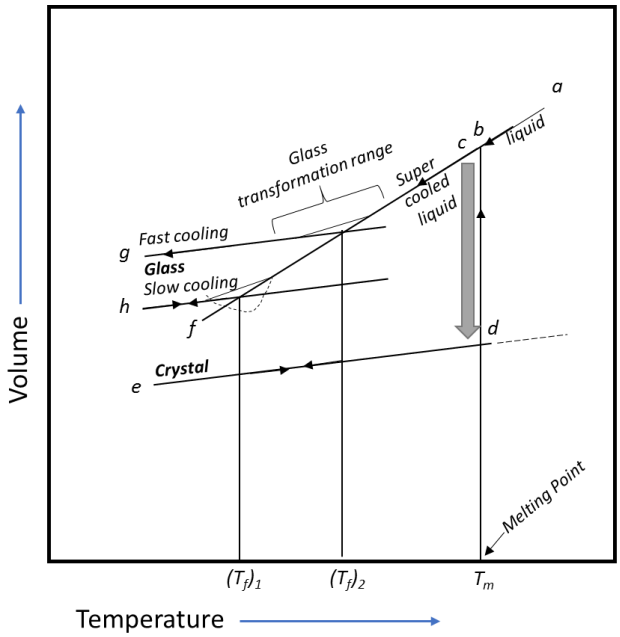

Figure 2. 2: The volume-temperature diagram for a glass-forming liquid adapted from(Kurkjian, 1985b; Lakin, 1991)

The structure of silicate glasses is based on a continuous random network of silicon-oxygen tetrahedra. This random network consists of SiO_4 tetrahedral units linked at their corners. The presence of non-bridging oxygens (NBOs) decreases the connectivity of the glass network, reduces the viscosity and eases the melting process Varshneya (2006). The number of NBOs can be determined through an assessment of Q^n species where n represents the number of Si-O-Si bonds and can vary from 0 to 4. For instance, a silicon atom is bonded via oxygen to four other silicon atoms (Q^4 units) in vitreous silica, meaning that the structure is fully polymerised and has high network connectivity. A silicon atom bond via oxygen to three other silicon atoms and via oxygen to a modifier (Q^3 units), means that the structure is less polymerised than if just Q^4 units are present. Whereas, Q^0 represents an isolated tetrahedron which does not have any bridging oxygens. Thus, the degree of polymerisation refers to the amount of Si-O-Si bonds. A schematic of Q^n species can be seen in Figure 2. 3.

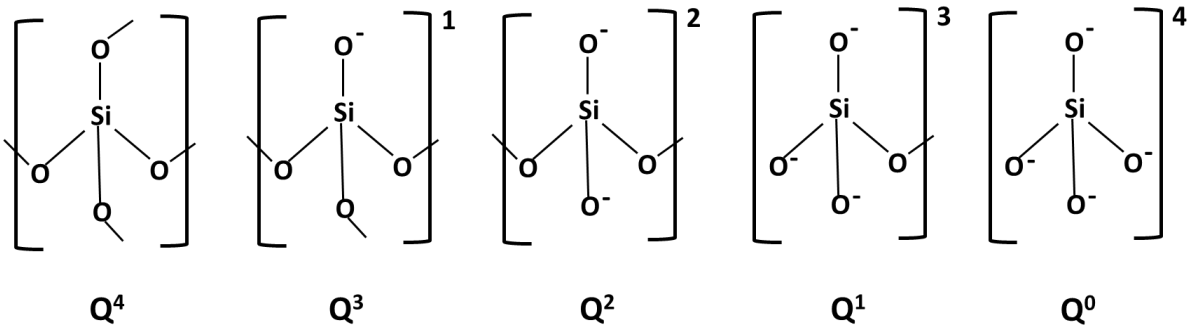

Figure 2. 3: Q^n species in the silicate glass network adapted from (Shelby, 1989)

In sodium aluminosilicate glasses both SiO_2 and Al_2O_3 are present as tetrahedral units. SiO_2 is the main network former, and Al_2O_3 is an intermediate. Alumina might also be a network modifier depending on the amount of alumina versus the amount of alkali and alkaline earth in the glass composition. (Day and Rindone, 1962). This is because the aluminium ions need charge balancing by an alkali or alkaline earth ion to form AlO_4 tetrahedra. As a result, by adding alumina into the glass non-bridging oxygens may be converted to bridging oxygens. A schematic of the structure of soda-lime aluminosilicate glass can be seen in Figure 2.4.

Hence in soda aluminosilicate glasses, aluminium ions can be either fourfold, fivefold or sixfold coordination depending on the aluminium / sodium ratio in the glass. (Xiang *et al.*, 2013). If the ratio of Al/Na ≤1, the aluminium ions will be mainly fourfold coordinated. If the ratio of Al/Na > 1, small amounts of five-fold coordinated aluminium ions will be present and

some aluminium ions will be sixfold coordinated (Uchino *et al.*, 1993). Sodium ions can be located in two different sites. They can either neutralize negatively charged AlO_4 units or work as a modifier and create NBOs (Kurkjian, 1985a; Shelby, 2005; Varshneya, 2006). The Al_2O_3 content of alkali aluminosilicate glasses is typically 10–25% with alkali contents exceeding 10%. Aluminosilicate glasses have excellent mechanical, chemical and thermal properties. Therefore, they are used in many applications such as pharmaceuticals, optoelectronics, crystal display substrates. However, in soda-lime-silica glasses all of the aluminium can be presumed to be charge balanced.

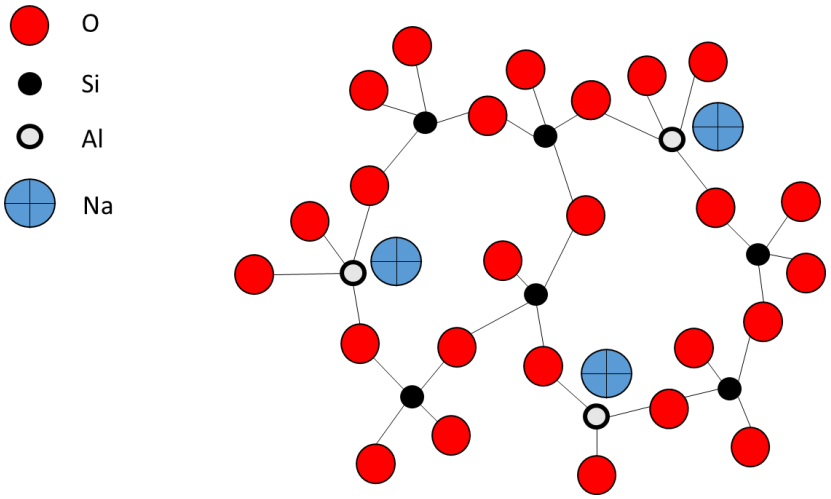

Figure 2. 4: Structure of Sodium-Aluminosilicate Glass

Total ion dynamics can be slow down by the addition of second alkali species which described as mixed-alkali effect in the literature. Properties of glasses such as viscosity, electrical resistivity, chemical durability, glass transition temperature and thermal expansion coefficient changes when a second alkali oxide is added depending on the mobility of ions. The mixed-alkali effect is usually studied on a series of glasses in which one alkali oxide is substituted for the other on a molar basis, the total alkali concentration remaining constant(DOREMUS, 1974; Calahoo, 2016a).

2.3. Mechanical Properties of Soda-Lime-Silica Glasses

Glasses are brittle materials, susceptible to stress concentrations and in general do not deform plastically, except under indentation. The fracture behaviour of glasses is therefore not an intrinsic property as it is controlled by environmental factors. The measurement method used to assess fracture strength, the environment and the treatment history of the

surface all affect the value of the fracture strength of glasses. Being brittle can also result in failure due to thermal shock (Lawn, 1993; Yarema, 1995; Varshneya, 2006; Macrelli, 2017).

2.3.1. Fracture Strength

Strength is defined as the applied stress at failure. Despite being highly resistant to compressive stresses, silicate glasses fail under low tensile stresses. Theoretically, most glasses should have high strength due to the strong covalent bonds of the network forming oxides. However, there is a great difference between experimental and theoretical values of glass strength due to the presence of small flaws which usually occur on the surface which control the strength of glass. Numerous papers have been published on the effects of surface flaws.

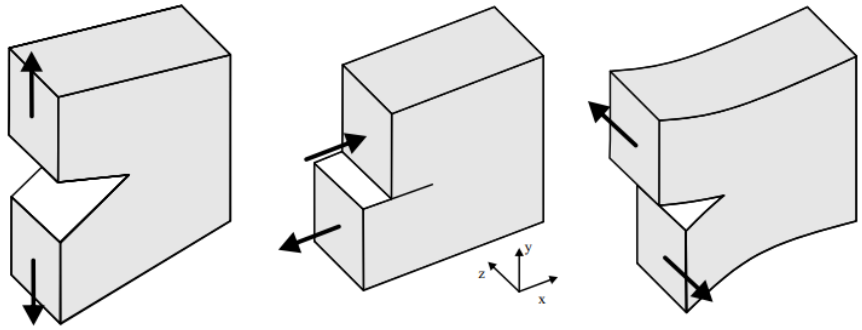

a) K_I : Mode I fracture b) K_{II} : Mode II fracture c) K_{III} : Mode III fracture

Figure 2. 5: Modes of crack extension

Critical values of the stress intensity factor depend on three different modes of crack extension which can be seen in Figure 2. 5. Mode I (opening displacement or tensile cracks) is opening in tension where the failure plane and the direction of propagation are perpendicular to the applied stress direction. Mode II (transverse shear cracks) is sliding in shear failure where the applied stress acts to slide fracture planes over each other along the direction of propagation. Mode III (longitudinal shear cracks) is tearing in shear where the direction of propagation is perpendicular to that of the stress, but the failure plane is parallel to shear stress direction. In general, for brittle solids and glass strength, only the first mode of crack extension is relevant Inglis (1913).

Griffith was one of the first researchers to realise the importance of stress concentrations. Afterwards, (Griffith, 1921) expanded the idea and hypothesized that glass strength depends

on the existence of flaws in 1921 Irwin (1958). He proposed the existence of a critical crack length and thus tensile strength for brittle materials. The larger a piece of glass, the lower the average strength and this situation is caused by the increase in the probability of finding faults on a larger glass surface. This is the main reason for the difference between the theoretical strength and the real strength in the glass and typically can be attributed to surface defects that occurred during or after production. Griffith derived an equation showing the stress that the glass can withstand without breaking (See Figure 2. 6).

$$\sigma_c = \sqrt{\frac{2E\gamma_s}{\pi a}} \qquad \textit{Equation 2. 1}$$

Where σ_c = the critical stress required for propagation of a brittle crack, a = material constant E = Young's Modulus, and γ_s = surface energy per unit area.

(Varshneya, 2006) modified Griffith's theory and introduced an expression called stress intensity factor. The effect of flaws on failure stress is justified through the stress intensity, mainly near the crack tip.

$$\sigma = \frac{K_{IC}}{Y\sqrt{\pi c}} \qquad \textit{Equation 2. 2}$$

Where σ=failure stress, c=flaw size in meters, K_{IC}=critical stress intensity factor/fracture toughness, and Y= geometric constant.

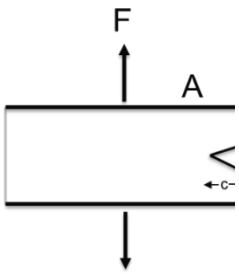

Figure 2. 6: Schematic diagram of an edge crack (flaw) of length c in a glass

Thus any damage or flaws on the glass surface as well as fracture toughness, static fatigue (crack growth due to attack by water), residual stress and bond strain are all parameters related to glass strength. Flaws reduce the strength of glass because they concentrate on

stress. However, anything which contacts the glass surface might be the reason to create a flaw, and it is not easy to produce glass products without touching anything. Thus, strengthening and toughening methods have been developed to enable the manufacture of glasses with higher strengths Varshneya (2018). Figure 2. 7 shows the relationship between the flaw size and failure strength of glass. As the flaw size increases, failure strength decreases relatively. The glass strength is strongly related to the state of the surface by the presence of flaws which extend generally from few up to tens of micron into the glass.

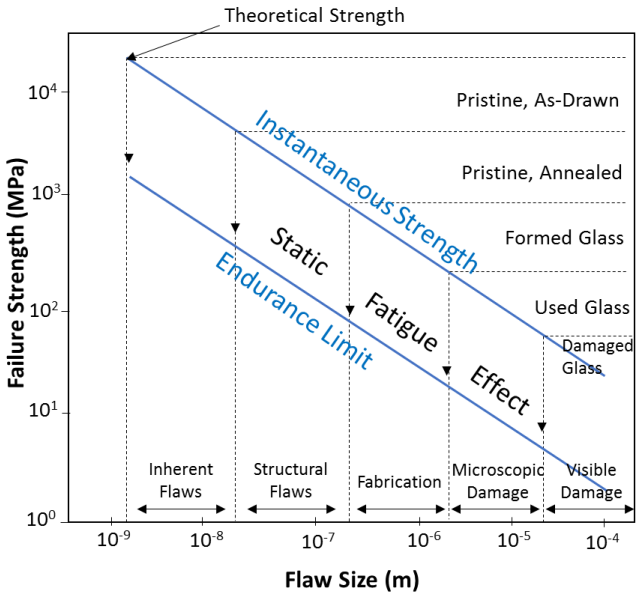

Figure 2. 7: Strength of glass products adapted from (Shelby, 2005)

Strength measurement generally consists of applying an increasing magnitude of stress to a sample of defined shape until failure occurs. Often glass strengths are measured by using a 3-point bending test as shown in Figure 2. 8, or preferably, 4-point bending test as shown in Figure 2. 9. Strengths measured using these tests may be referred to as modulus of rupture (MOR).

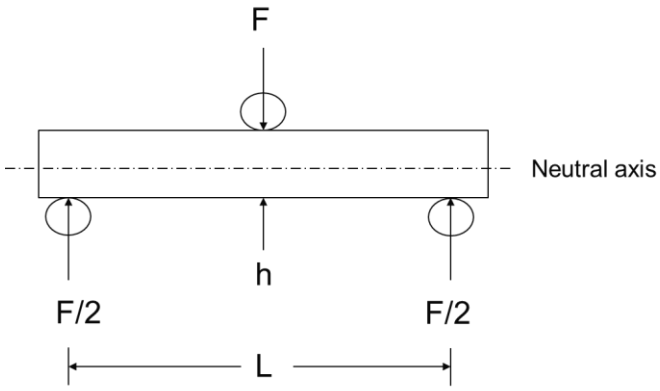

Figure 2. 8: Schematic diagram of three-point bending

The stress is obtained by multiplying the maximum bending moment by the half height of the rectangular over a geometric moment of the beam cross-section (See Equation 2.2). The maximum stress is at the third point and ideally the sample fails from that point. However, the strength controlling defect would not always be at the point of maximum applied stress.

$$\sigma = \frac{({}^{F}/_{2})({}^{L}/_{2})\, h/2}{b\, h^3/12} \qquad \textit{Equation 2. 3}$$

Where b=width, h=height

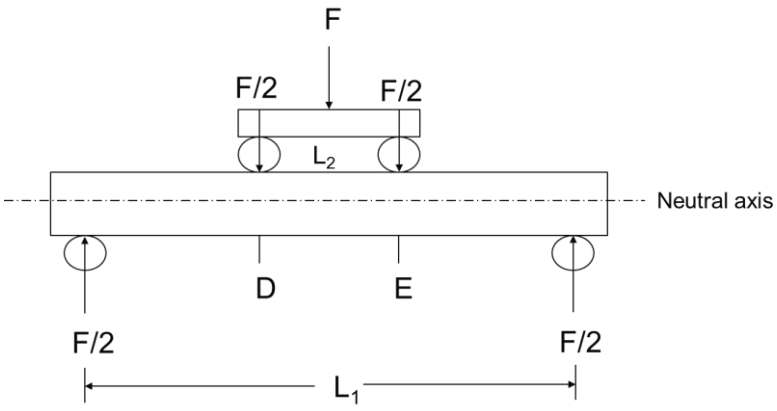

Figure 2. 9: Schematic diagram of four-point bending

For the 4-point bending test, the maximum bending stress is given by (Varshneya, 2006)

$$\sigma = \frac{(F/2)\,[(L_1 - L_2)/2]h/2}{b\, h^3/12} \qquad \textit{Equation 2. 4}$$

In four-point bending tests, the maximum flexural stress is spread over the section of the beam between the inner loading points.

2.3.2. Elastic Moduli

For an isotropic material such as glass, there are 4 elastic moduli; Young's modulus (E), bulk modulus (K), shear modulus (G) and Poisson's ratio (v) of which 2 are independent. The Young's modulus is defined as the ratio of tensile stress to tensile strain, and is also known as elastic modulus, E. The moduli are determined by the structure of the network and the individual bonds in the glass (Makishima and Mackenzie, 1973; Makishima and Mackenzie, 1975).

A good correlation between an equation to predict Young's modulus and experiments for several silicate glasses has been shown in different studies (Makishima and Mackenzie, 1973). The method is established on a consideration of the dissociation energy of the oxide constituents per unit volume and the packing density. The formula for determining the Young's modulus of an ionic crystal can be obtained as follows.

The electrostatic energy of attraction U, which is for a pair of ions with opposite signs is equal to,

$$U = -e^2/r_0 \qquad \textit{Equation 2. 5}$$

where e and r_0 are electronic charge and interatomic distance, respectively.

Description for many interactions between ions in a crystal lattice, U is multiplied by the Madelung constant α, giving the Madelung energy:

$$U_m = \alpha U \qquad \textit{Equation 2. 6}$$

The force between ions is equivalent to $\partial U_m/\partial r$ so the stress, σ is

$$\sigma \approx \frac{1}{r_0^2}\left[\frac{\partial U_m}{\partial r}\right] \qquad \textit{Equation 2. 7}$$

the change of stress for a change in r is $\partial\sigma/\partial r$ and hence

$$d\sigma = \frac{dr}{r_0^2}\left[\frac{\partial^2 U_m}{\partial r^2}\right] \qquad \textit{Equation 2. 8}$$

$$d\sigma = \frac{dr}{r_0^2}\frac{1}{r_0}\left[\frac{\partial^2 U_m}{\partial r^2}\right] \qquad \textit{Equation 2. 9}$$

The strain is $d\varepsilon = \frac{dr}{r_0}$ and $\frac{d\sigma}{d\varepsilon}$=E

$$U_m = -\frac{\alpha e^2}{r_0} \text{ and } \left[\frac{\partial^2 U_m}{\partial r^2}\right] = -\frac{2\alpha e^2}{r_0^3}$$ *Equation 2. 10*

and

$$E = \frac{d\sigma}{d\varepsilon} = \left[\frac{2\alpha e^2}{r_0^3}\right]\left[\frac{1}{r_0}\right] \approx 2\alpha\left[-\frac{e^2}{r_0}\right]\left[\frac{1}{r_0^3}\right]$$ *Equation 2. 11*

where $-\frac{e^2}{r_0} = U$

$$E = \frac{2\alpha}{r_0^3}\left[-\frac{e^2}{r_0}\right] = 2\alpha\frac{U}{r_0^3}$$ *Equation 2. 12*

According to Equation 2.12 the Young's Modulus is equal to two times of the binding energy U_m divided by the third power of atomic spacing r_0^3. Madelung energy divided by the third power of interatomic distance (U_m/r_0^3) is replaced by the average dissociation energy per unit volume (D_{av}) and packing density (C_g) (Green, 1998). Because the Madelung constant is not applicable for short-range order glasses.

$$E = 2C_g D_{av}$$ *Equation 2. 13*

Where packing density can be calculated

$$C_g = \frac{4}{3}\pi N_A \rho \frac{\sum f_i\left(X_i r_A^3 + y_i r_O^3\right)}{\sum f_i M_i}$$ *Equation 2. 14*

Where N_A is Avagadro's number, f_i is the molar fraction of the oxide $A_{x_i}O_{y_i}$, with molar mass M_i, r_A and r_O are the ionic radii.

The elastic modulus is known to be dependent on the atomic packing density and the interatomic bonding. In fact, the atomic energy per mol atom is connected to the bulk modulus and the atomic volume.

Shear modulus (G) is defined as shear stress over shear strain, which can be described as a material's tendency to the deformation of shape at constant volume under opposing forces. Whereas, bulk modulus (K) is described as a material's tendency to deformation in all directions when it is under loads in all directions.

If any two moduli are known the others can be calculated using relationships such as equation 2.15 and Equation 2.16 (Soga and Yamanaka, 1976; Lakin, 1991; Burkhard, 1997). Where v is Poisson's ratio, E is Young's modulus, K is bulk modulus, G is shear modulus.

$$K = \frac{E}{[3(1-2v)]} \qquad \textit{Equation 2. 15}$$

$$G = \frac{E}{2(1+v)} \qquad \textit{Equation 2. 16}$$

Typically, the addition of an alkali causes a reduction in Young's modulus. On the other hand, if the number of non-bridging oxygens higher than the number of bridging oxygens, Young's modulus and bulk modulus can actually increase (Shelby, 2005).

2.3.3. Hardness

Hardness is described as the resistance to deformation of a material under pressure. The hardness of glasses is determined by the function of the strength of individual bonds and the density of packing of the atoms in the structure. (Wiederhorn 1969) Vickers and Knoop indentation are the most widely used hardness measurement techniques for glasses. A Vickers hardness indenter is a square pyramid whereas Knoop hardness indenter is an elongated pyramid as seen in Figure 2. 10.

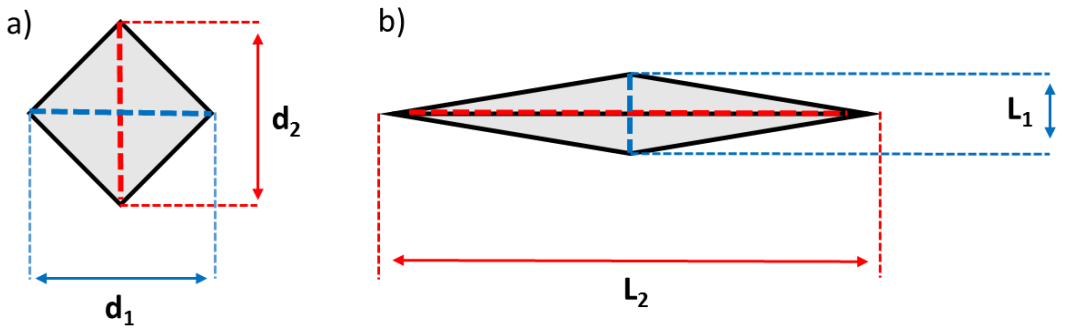

Figure 2. 10: Schematic of a) Vickers and b) Knoop indentation

For Vickers hardness:

$$H_v = 1.8555\frac{P}{d^2} \qquad \textit{Equation 2. 17}$$

Where P is indentation load in kg, and d is the average diagonal length of the impression.

For Knoop hardness:

$$H_k = 14.23 \frac{P}{{L_2}^2}$$ *Equation 2. 18*

Where P is indentation load in kg, and L_2 is the long diagonal.

Due to the exchange of smaller ions to the larger ones, ion exchange strengthened glass surfaces are expected to be harder than the non-ion exchanged surface. As the ion exchange process takes place at high temperature where the glass has a more open structure, the free volume increases. Thus, after the ion exchange process, the surface resists indentation penetration in favour of compression stress.

2.3.4. Fracture Toughness

Fracture toughness (K_{IC}) defines as an intrinsic resistance of a material to crack growth. Crack propagation occurs when stress intensity (K_I) equals to fracture toughness (K_{IC}). For glasses, the fracture toughness is usually within the range of 0.6 – 1.0 MPa·$m^{1/2}$, which is much lower than that of engineering metals is within the range of 20 to 200 MPa·$m^{1/2}$ (Griffith 1921; Evans and Charles 1976; Tadjiev et al. 2010), hence glasses are flaw sensitive. Fracture toughness theoretically depends mainly on intrinsic modulus surface energy for given material residual stresses modifying resistance to crack growth.

Combining the Griffith and Irwin approaches gives

$$K_{IC} = \sqrt{2E'(\gamma_e)}$$ *Equation 2. 19*

$$K_{IC} = C\sigma\sqrt{\pi a}$$ *Equation 2. 20*

Where σ is strength, a is crack depth, C is a geometric constant

Residual stresses would affect the results since

$$K_{IC} = C\sigma\sqrt{\pi a} + C'\sigma,\sqrt{\pi a}$$ *Equation 2. 21*

Relating the plane strain modulus to the Makashima and Mackenzie model gives

$$E' = \frac{E}{(1-v^2)} = \frac{2C_g D_{av}}{(1-v^2)}$$ *Equation 2. 22*

Where, hence the packing density is also linked to fracture toughness and D_{av} is the average dissociation energy per unit volume (Lawn and Marshall 1979).

2.3.5. Brittleness

The brittleness (B) is described as the ratio of hardness to the fracture toughness.

$$B = \frac{H_v}{K_{IC}} \qquad \textit{Equation 2. 23}$$

The ratio of median crack length to the diagonal length of a deformation impression is often used to estimate the brittleness. Sehgal and Ito (1999) found that the brittleness is directly correlated to the density and for so-called "normal" glasses brittleness increases with increasing density (Shelby, 2005; Kurkjian, Gupta and Brow, 2010; Varshneya, 2018).

2.4. Glass Strengthening Techniques

This section covers conventional techniques used for permanently strengthening glass. It is well known that the surface properties of all types of glasses depend on the composition and manufacturing conditions. The surface can be affected by mechanical contact and the atmosphere. However, it is not so easy to manufacture flaw-free glass products or to maintain them as flaw-free. Surface flaws can be caused by the contact of the surface with moulds, dies during the manufacturing, abrasion, moisture, water, chemicals. Typically, anything which contacts with a glass surface might therefore be the reason for the decreased functional strength of glass products as flaws concentrate stress, therefore, reduce the strength of glass. Thus, manufacturers tend to use strengthening or toughening methods. The literature associated with the strengthening of glass is extensive covering the range of different strengthening mechanisms that have been used over the years. In general, increasing the strength of the glass in practice is based on one of the following two approaches. The first one can be summarized as destroying or covering the existing cracks on the surface, and the second is to increase the strength of the glass by forming near surface compressive stresses which are greater than the tensile stresses on the surface and making it difficult to advance the cracks that may occur Varshneya (2006).

As stated by (Varshneya, 2010b), these include reducing the severity of flaws, decreasing the risk of surface damage, creating compressive stress on the surface, and crack pinning. In the literature, the most commonly used methods are coatings, thermal strengthening, surface crystallization, and chemical strengthening.

Fire polishing, surface etching, and surface coating are techniques that are all focused on reducing the density or the severity of pre-existing defects. Thus, fire polishing or etching can

be used to reduce the possibility of fracture during manufacturing by decreasing the harshness of flaws. Similarly, etching can be used in some production lines for removing flaws. However, these methods are temporary solutions since subsequent glass handling will still result in flaw generation (James et al. 1993; Barthel et al. 2005).

Improvement of fracture toughness (K_{IC}) could be another option for the strengthening of glass for instance by surface crystallisation. Surface crystallisation can also be used to strengthen a glass product. The thermal expansion mismatch between the bulk glass and the crystallised surface causes compressive stress development on the surface layer. As the name suggests, ceramming involves generating partially crystallised glass; this requires controlled heat treatment to obtain optimum crystalline particles inside the glass article (Liversidge et al. 1983).

Glass coatings have been investigated as a glass strengthening technique as well as for optical purposes such as antireflection. Some studies reported that strengthening of glass by the application of coatings is easier to implement than other techniques (Brzesowsky *et al.*, 1998; Mallick and Holland, 2005; El-Sayed and Hand, 2012). The effects of strengthening of glass by coatings have been attributed to the filling of the surface flaws as well as the possible presence of compressive stresses arising from the coating (Fabes *et al.*, 1986; Fabes and Uhlmann, 1990; Chen and Ellis, 1995; Hand *et al.*, 2003; Teisseire *et al.*, 2011). There are a variety of glass coating techniques which show a significant increase in glass strength that have been reported in the literature. For instance, alkoxide derived coatings, sol-gel coatings organosilane derived, organic-inorganic coatings, and epoxy coatings have all been reported to strengthen glass (Fabes and Uhlmann, 1990; Wang *et al.*, 1997; Hand, Wang and Ellis, 1998). Polymer coatings can be used to either reduce the size of the flaws on the surface or to prevent the growth of flaws (Gordon et al., 1996; Sundberg et al., 2019). Deposition of Al_2O_3 thin films on a glass surface by chemical vapour deposition have also been shown to result in provides an improvement in the mechanical properties (Uhlmann, 1980).

Thermal tempering was first observed in so-called Prince Rupert drops which have been known experimentally since the seventeenth century. Rapid cooling of glass droplets provided high surface compression with complementary interior tension stress; the high compressive stress results in high strength (Olcott, 1963; Uhlmann, 1980). For practical strengthening thermal tempering has been used since the 1870s (As et al., 2005). Thermal tempering involves

the heating up of the glass product to a uniform temperature above the annealing temperature such that the glass is in the viscoelastic state. Then the glass is cooled rapidly down to the room temperature usually by using cold air jets; this creates compression in the surface. During the process, a temperature gradient develops, and the glass surface cools faster than the interior (Lawn and Marshall, 1979; Anderson, 2005).

Figure 2. 11 shows a schematic diagram of the tension and compression zones in thermally tempered glass specimen. For mechanical stability, the induced compression stress in the glass near the surface must be balanced by intrinsic tensile stress in the glass body. The stress gradually decreases from the surface to inside of the glass. The residual stress distribution along the specimen thickness direction is given by:

$$\sigma(x,y) = -\sigma_R \left[1 - \frac{3x}{d} + \frac{3x^2}{2d^2}\right] \qquad \textit{Equation 2. 24}$$

Where σ_R defined as the surface compressive stress and d is the half thickness of the glass specimen. The compressive layer is approximately on a fifth of the specimen thickness.(Varshneya, 2006)

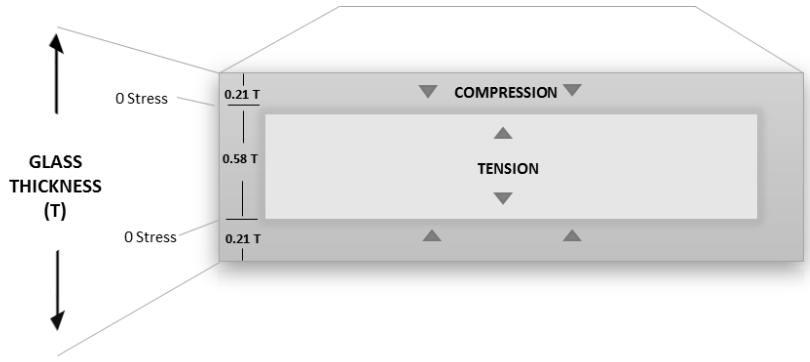

Figure 2. 11: Thermally tempered glass compression and tension zones

Surface compression can be between 70 to 200 MPa after thermal tempering, with most commercial fully tempered glasses having 100 MPa surface compression. This is because there is always a risk when developing higher interior stress which may be a reason for an internal or edge fracture during tempering hence 200 MPa surface compression is rarely achieved. However, there are some significant drawbacks to the process such as its inability

to strengthen complexly shaped glasses, and due to the limits of air cooling it is not easy to strengthen samples with glass that are less than 2 mm thick (Mognato, Brocca and Comiati, 2018). Thermally tempered glass is called “safety glass” because on fracture it breaks into small pieces which makes it much safer than large dagger-like pieces that are commonly produced when annealed glass is broken.

Thus, it is suitable to use tempered glasses in places such as emergency exits, entry areas, storefronts and high wind loads. According to the ASTM C 1048, thermally tempered glass must have a surface compressive stress over 70 MPa for 6 mm glass. However, to be considered as safety glass, it should offer at least 100 MPa compressive stress. (Gy, 2008a; Varshneya, 2010b) Glass strengthening techniques are summarised in Table 2. 1.

Glass Strengthening Technique	Advantages	Disadvantages	Reference
Thermal Tempering	Fast, thick compressive layers	Difficult for thin glass and non-symmetric shapes	(D.R. Uhlmann and N.J. Kreidl, 1980)
Chemical Strengthening	Easy for thin glass low tensile stress	Slow, thin compressive layers	(Urbain, Stemeri and Charles, 1966)
Acid etching	High strengths possible	Surface protection required	(Varshneya, 2006)
Fire polishing	Fast, no washing required	Difficult for thin glass	(Amidon *et al.*, 1983)
Lamination	Reliability, safety	Cost, weight	(Liversidge et al. 1983)
Ceramming	Increase fracture toughness	Cost, loss of transparency	(Fabes *et al.*, 1986)
Coatings	Protect from surface damage	Changes surface properties	(Kistler, 1962)

Table 2. 1: Glass Strengthening Techniques in a summary

2.4.1. Chemical strengthening

Chemical strengthening or ion-exchange strengthening (also known as chemical tempering) involves placing the glass in contact with a molten salt so that the alkali ions in the glass are replaced by larger alkali ions from the salt; once exchanged the larger ions produce surface compressive stresses that place a closure stress on surface flaws.

Studies related to ion exchange for strengthening glass date back to the early 1960s with Kistler (1962) reporting the first successful results obtained by heating soda-lime-silica glass

in potassium nitrate. Depending on the processing time and temperature of the glass article, it was reported that the glass strength could be doubled and sometimes tripled. As ion exchange is mainly a diffusional process, the main parameters controlling the process are the ion exchange temperature, ion exchange time and the exchanging pair of ions. Glass compositions should include mobile alkali ions such as Li^+, Na^+, K^+ for ion exchange. For sodium containing glasses, a KNO_3 (potassium nitrate) bath is usually used; for lithium-containing glasses, $NaNO_3$ (sodium nitrate) is used. Exchanging smaller ions is much more effective than exchanging larger ones. For instance, Na^+ (ionic radius 0. 98 Å) for Li^+ (ionic radius 0.68 Å) ions is more efficient than exchanging K^+ (ionic radius 1.33 Å) for Na^+ (ionic radius 0.98 Å)(Gy 2008; Varshneya 2010). Ion exchange has been used not only to strengthen the glass but also to enhance other mechanical properties of glass (Findakly, 1985) as well as electrical (Speranza *et al.*, 2009), optical (Guldiren et al., 2016; Özdemir Yanık et al., 2018) and chemical properties (Gy 2008; Varshneya 2010; Mazzoldi et al. 2013; Sglavo 2015; Calahoo et al. 2016; Macrelli 2017).

The most commonly used glass compositions for ion exchange strengthening are silica glasses, including aluminosilicate, borosilicate and soda-lime silica which contain sufficient amounts of mobile alkali ions. Mobile alkaline ions for ion exchange are Na^+, Li^+ and K^+. In studies, potassium sulphate (K_2SO_4), potassium iodide (KI), potassium chloride (KCl), sodium sulphate (Na_2SO_4), lithium chloride (LiCl), Lithium bromide (LiBr), Lithium sulphate (Li_2SO_4) salts reported as used in salt baths, but potassium nitrate (KNO_3), sodium nitrate ($NaNO_3$) and lithium nitrate ($LiNO_3$) are mostly preferred for the efficiency. Ion exchange on soda-lime-silica glasses has mainly concentrated on Na^+ - K^+ exchange. The ion-exchange process generally takes 50 to 200°C below the glass transition temperature, and the glass transition temperature varies according to the composition, so the process temperatures vary according to the determined glass transition temperatures. The temperature range for ion exchange for all glass compositions is 370 – 540 °C. Since the glass transition temperature of soda-lime-silica glass is at around 550 °C, the ion exchange process can be applied at the temperatures below 500°C. The exchanging pair of ions directly affects the rate of interdiffusion. Thus, the processing time of the ion exchange varies depending on the composition of the glass used and the alkali ions in the salt bath. Although there are extended process times reported

between 30 minutes to 400 hours, the most consistently used ones are 0.5 to 24 hours (Varshneya, 2010b).

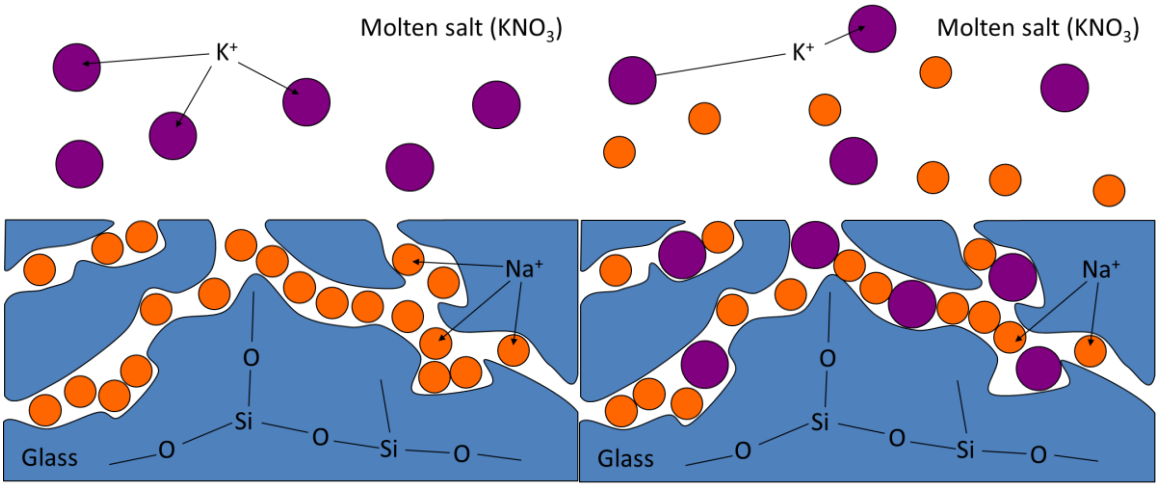

Figure 2. 12: Schematic Diagrams of the Ion Exchange Process

The main principle of ion exchange is the immersion of an alkali-containing glass into a molten alkali salt such as KNO_3 below the annealing temperature of the glass. On heating inter-diffusion occurs between the ions of glass and the ions from the salt as shown in Figure 2. 12. As the ions of the salt are larger than the ions that were originally present inside the glass, a high surface compressive stress is obtained. To achieve nearly 450 MPa surface compression a soda-lime glass should stay in a KNO_3 salt bath for 16 hours at a temperature of approximately 475°C (Schott, no date; Corning, 2016). Hence the process is high-cost and can only be used economically for high-value products. Common applications of ion-exchanged glasses are touch screen devices, mobile phone screens, displays, and pharmaceutical containers. Asahi (AGC) Dragontrail™, Corning® Gorilla® Glass and SCHOTT Xensation™ cover glass, Nippon Electric Glass Dinorex™, Sax-on Glass Ion-Armor™ are examples of some of the commercially available products. Karlsson (2012)

The stress profile, which is formed along the cross-section of an ion exchange strengthened glass sample, is given in Figure 2. 13 with a representation of residual compressive stresses at the surface with a balancing tensile stress in the interior.

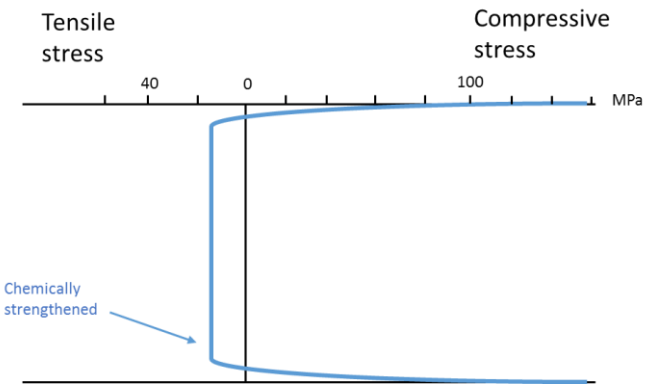

Figure 2. 13: Principal stress profiles for chemically strengthened flat glass viewed from the thickness cross-section adapted from (Gy 2008)

Chemical strengthening has some significant advantages over conventional thermal tempering.

- Ion exchange can be applied to complex shapes, whereas this is not possible for thermal tempering.
- Relatively thin glasses can be strengthened by ion exchange whereas the limitation is about 2 mm for conventional thermal tempering.
- Most significantly greater surface compressive stresses can be obtained by chemical tempering.
- There is no optical distortion on the surface of the chemically strengthened glass. (Corning, 2016)

The magnitude of compressive stress for chemically strengthened glass varies according to glass composition, exchanging pair of ions, temperature, time. Typically, the compressive stress falls in the range of 100 to 400 MPa for soda-lime-silica glasses and 500 to 700 MPa for lithium aluminosilicate glasses. For lithium aluminosilicate glasses compressive stress values up to 1 GPa have been reported, with Corning Gorilla®3 glass reported as having an average surface compression stress of 1140 MPa and an average layer depth (or case depth) of 9.5µm (Varshneya, 2018). The depth of the compression layer for chemical strengthened glasses is also an important parameter. For ordinary products, the layer (case) depth could be 30-40 µm whereas for the products such as aircraft cockpit windshields it should reach up to 300µm (Varshneya, 2006). Ion-Armor™ (marketed by Saxon Glass Technologies) is reported to have surface compression values near 1 GPa and a near 1 mm case depth (Chisholm et al. 1966; Hammer 1970; LaCourse et al. 1989).

There are numerous patent applications related to chemical tempering treatment. Although soda-lime-silica glass (Beall et al. 1989; Varshneya 2012) has been used in some of the patents, the most studied glass is alkaline aluminosilicate glass, for instance lithium aluminosilicate (Ellison and Gomez, 2010; Varshneya, 2012). Chemical tempering process may involve single or multiple ion exchange processes with salt baths which are used in different compositions as pure or as salt mixtures. Since chemical tempering is a process based on the mutual diffusion of ions, the effects of parameters such as process temperature and duration have been investigated in a large number of studies (Nordberg *et al.*, 1964; Donald, 1989). Although there are various products and patents developed by different glass producers around the world; as the efficiency of the process, temperature, duration, bath composition and concentration vary according to different parameters such as glass composition, it is an important research subject where studies are continued, and new developments are recorded with each passing day.

The composition of glass relates to ion exchange capability of glass. Chemical strengthening is applicable for many alkali-containing glasses, particularly alkali aluminosilicate glasses (Varshneya 2010). Aluminosilicate glasses are reported as having higher ion-exchange rates because they have greater glass transition temperatures, due to reduced numbers of non-bridging oxygens, which enables higher temperature processing and thus more rapid ion exchange which aids the achievement of larger case depths (Ragoen *et al.*, 2017). As the amount of Al_2O_3 increases in the base Na-aluminosilicate glasses, the surface compressive stress and the surface hardness that can be obtained therefore increases (Olcott 1963; Nordberg et al. 1964; Donald 1989; Gy 2008; Varshneya 2010).

Traditionally, ion-exchange treatments have been mostly carried out using a molten salt bath. (Karlson et al. 2010). The salt solution which is attached to the glass surface during the treatment needs to be removed easily after the treatment. Therefore, the salt must have high solubility in water. To enhance the suitable diffusion rates the temperature of the salt or the salt mixture should be close to the glass softening temperature. KNO_3 (potassium nitrate) is one of the main salts used for the exchange of potassium for sodium. K_3PO_4 (tripotassium phosphate) has also been used, however, it causes stains on the glass surfaces (Yunqiu, Duvigneaud and Plumat, 1986). Mixtures of KNO_3 (potassium nitrate) and KCl (potassium chloride) are also reported to be effective (Talimian and Sglavo 2017). The condition of the salt bath also affects the efficiency of ion exchange. Notably, the presence of Ca and Mg in the

molten potassium salt results in blocking of K^+/Na^+ exchange. In particular even a limited calcium content in the salt blocks the Na^+ - K^+ ion exchange process because the exchange between Na in the glass and Ca in the salt is thermodynamically preferred (Sglavo et al. 2014; Hassani and Sglavo 2015; Sglavo 2015). Therefore, the salt composition should be uncontaminated Patschger and Rüssel (2014).

Hassani and Sglavo (2019) investigated the effect of ion exchange treatment of an industrially produced soda–lime–silica and an industrially fabricated sodium aluminosilicate glasses with using different $NaNO_3$ / KNO_3 ratios in their salt bath. After the treatment, they found the ion-exchanged surfaces had higher K^+ contents when the salt mixture was rich in KNO_3. Although they pointed out Na^+- K^+ exchange in less Na-containing salt was more limited than the one in more Na-containing salt potassium rich salt, the particular diffusion coefficients were independent of the potassium concentration on the glass surface.

One of the drawbacks of ion-exchange in a molten salt bath is that the treatment takes a long time. During the treatment, the amount of the potassium inside the salt bath decreases and the concentration of sodium ion increases, respectively. Thus, the effectiveness of ion exchange may be reduced with time. However, (Uhlmann, 1980) found that the efficiency of chemical strengthening remained the same up to 5% $NaNO_3$ being present in the KNO_3 salt bath. The other practical disadvantages of molten salt baths are that the presence of water can cause an explosion and the vapours coming out of the bath are corrosive by Weber (1965). Use of an electric field in the salt bath was first developed (Talimian et al., 2017) to increase the rate of the ion exchange process. Electric field assisted ion-exchange can help to improve the surface compression and the diffusion case depth and also takes less process time than commercial ion-exchange (Watanabe, 1980).

Spraying and dipping are alternative methods to the molten salt bath method for ion exchange (Fabes and Uhlmann 1990; Patschger and Rüssel 2016). Spraying or using salt paste methods require use of mixtures of different salts or addition of another phase such as clays or aluminosilicates into the KNO_3 Karlsson et al. (2015). A study published by Patschger and Rüssel (2016) presents a method in which an aerosol fed through a tube furnace is used to deposit some K^+ ions into the surface of float glass. The performance of commercial ion-exchange process conducted using a molten salt bath was compared by ion-exchange conducted by vapour deposition. Outcomes showed that the latter technique could be an

alternative approach to the industrial ion-exchange process. Nevertheless, further research needs to be done to improve the parameters such as salt adhesion and distribution on the surface, the pressure in the generator, temperature.

Similarly, (Patschger et al., 2016) reported an ion exchange treatment using a potassium salt coating. A mixture of KNO_3 – KCl – K_2SO_4 salts was applied by spraying on the surface of the glass. The single-side ion exchange process is advantageous because it reduces the amount of the salt is used for ion exchange; hence the cost of the overall process decreases. However, as the thickness of the salt layer applied by spraying, was between 2 – 6 μm, the diffusion was relatively slow. Nevertheless, it was found that for both salt bath and the spraying method, the interdiffusion coefficients were similar to each other, meaning that same diffusion depths could achieve by using the spraying method (Wang 2014).

Another method claims that applying an extra layer of a coating such as titanium oxide, helps to fill the microcracks on the surface after the ion exchange process (Kistler 1962; Shaisha and Cooper 1981; Karlsson et al. 2017). However, this method seems not to be practical for mass production, and does not appear to be cost-effective as it involves both ion exchange and a subsequent coating process.

There are also other options of ion exchange by substitution of different monovalent ions. Reported diffusion rates are in the order of $Ag^+ > K^+ > Tl^+ > Rb^+ > Cs^+$ (Hornschuh et al., 2004; Verné et al., 2009; Dimitrova et al., 2016; Guldiren et al., 2016). Hence Ag^+ for Na^+ exchange gives higher interdiffusion coefficients than K^+ for Na^+ exchange. However, the presence of silver leads to the colouration of the glass and thus silver ion-exchange is not usually used for strengthening purposes, instead being mostly used for antimicrobial property enhancement and colouring (Gy 2008).

Since the ion exchange strengthening process is based on the principle of the replacement of smaller ions by larger ions, it is expected that a volume increase will be observed after the treatment. It is stated in the literature Karlson et al. (2010) that the amount of potassium can be calculated by weighing measurements before and after the treatment by assuming that the potassium ions in the surface of the glass are displaced in 1:1 ratio with all the sodium ions on the surface.

Observations of the depth of exchange layer can usually made by SEM-EDS (Scanning Electron Microscopy – Energy Dispersive X-ray Spectroscopy), EPMA (Electron Probe Microanalysis) and also SIMS (Secondary Ion Mass Spectrometry). Morris et al. (2004) argued that the Surface Ablation Cell technique which is a piece of laboratory equipment for determining the surface concentration profiles has been utilised to characterise surface ion exchange processes in float glass gives similar results to SEM-EDS, EPMA and SIMS and yet it is cheaper and easier to use. Accordingly, it could be a competitive method.

2.4.1.1. Mechanical Properties of Ion-Exchanged Glasses

Kese et al. (2004 stated the high surface compressive stress leads a surface hardness enhancement as well as the fracture resistance of ion-exchanged aluminosilicate glasses. Depending on the process variables such as glass composition, bath composition, temperature and time, the amount of compressive stress on the surface is related to the changes in hardness. Jannotti et al. (2012)) and (Garza-Méndez *et al.*, 2007; Jannotti *et al.*, 2011) determined the change in hardness before and after ion exchange using Vickers microhardness and nanoindentation measurements under varying periods and loads. It has been found that during indentation the large compressive stress also suppresses radial crack formation. Changes in the hardness values of the glass samples before and after an ion-exchange treatment have been conducted using Vickers microhardness and nanoindentation measurements under varying periods and loads for different studies. Increase in hardness is explained by the generation of compressive stress on the glass surface and also compositional change at the glass surface by stuffing K^+ ions into the smaller sites of Na^+ ions occupying Koike et al. (2012). (Kese, 2004) reported the difference cracking behaviour of thermally strengthened and chemically strengthened soda-lime-silica glasses by using indentation. After normalisation by the indent size, they found that the size of the residual stress field in the thermally tempered glass was smaller than that in the original glass. Whereas, the size in chemically tempered glass was larger than that in the original glass (Kese and Rowcliffe, 2003). Chemically tempered glass showed higher cracking resistivity, but higher brittle tendency than thermally tempered glass.

Another method to examine the relationship between hardness and compressive stress around a Vickers indentation uses nanoindentation hardness measurements at periodic intervals from the indent towards the edge of the sample. As the tensile stress moved away

from the trace boundary (towards the areas without stress), an increase was observed in hardness (Kese et al., 2006).

For the determination of the compression stress profile, there are also studies on the glass section where Vickers hardness measurements are taken from the surface to the centre at periodic intervals. The decrease in the hardness of the measured values of decreasing compression occurs in the measurements. It is stated that the hardness and increase in the elastic modulus are caused by the fact that the surface has become more resistant to penetration Koike et al., (2012).

Hermansen et al., (2013) found that the crack initiation load during Vickers indentation increases with the surface compressive stress of chemically tempered soda-lime float glass. (Morris et al., 2004; Morozumi et al., 2015) also showed as the amount of compression stress increases, the crack lengths are reduced. In these studies, the limit load where cracks start to propagate is determined by applying gradually increased indentation loads, and mechanical behaviour of the samples subjected to ion exchange treatment under different conditions is compared. Some of the authors also reported the probability of crack initiation measurements (Brzesowsky et al. 1998; Fett et al. 2005; Fett et al. 2007; Wen et al. 2008; Jannotti et al. 2014). They found that the probability of crack formation decreases with increasing compressive stress.

It is known that the compressive stress on the glass surface by chemical tempering creates an increase in the strength of the glasses up to 10 times. In the literature, the strength measurements of the strengthened glass samples have been performed with three or four-point bending, ball impact and ring-on-ring tests (Karlsson 2012; Karlsson et al. 2013; Erdem et al. 2017; Varshneya 2018) with the most commonly used method being four-point bending (Sglavo et al. 2001; Sglavo and Green 2001; Abrams et al. 2003; Sglavo et al. 2004). Ring-on-ring and ball impact tests are biaxial, three- or four-point bending tests are uniaxial. measurement.

2.4.1.2. Other Ion-exchange Processes

A two-step ion exchange, or double ion exchange treatment on silicate glasses has been also used to produce so-called Engineered Stress Profile (ESP) glasses (Shen and Green, 2004). The first treatment is used to induce compressive stresses by conventional ion exchange and then the second ion exchange either reintroduces the first host ion or a new ion. For instance, a

relatively long ion exchange (from 24 to 120 hr) in a KNO_3 bath was applied in the first stage where K^+ ions are exchanged for Na^+ ions followed by a second shorter treatment (30 minutes) where a portion of the K^+ ions are exchanged back for Na^+ ions in a KNO_3 / $NaNO_3$ mixed salt bath Shen and Green (2004). This combination of two-step ion-exchange can provide multiple cracking prior to failure which provide warning of imminent failure.

However, Corning have patented a modified version of this process (Corning, 2012) where the ion exchange order is opposite from (Lee et al., 2012) for alkali aluminosilicate glasses. In this case in the first stage, 2.5 – 10 wt% $NaNO_3$ was added into the KNO_3 bath and the treatment lasted 270 minutes at 412 °C. In the second stage, samples were subjected to ion exchange for 120 minutes at 410 °C in pure KNO_3. After the first stage, it was determined that the compressive stress on the glass surface decreased with the increasing $NaNO_3$ percentage in the salt bath from 710 MPa to 477 MPa. After the second stage, an increase in compressive stresses the range of 750 - 765 MPa was determined. It is emphasised that the obtained values are higher compared to the compression stress values obtained after single step chemical tempering as shown in Figure 2. 14 (Lee, Quintal and Yan, 2012).

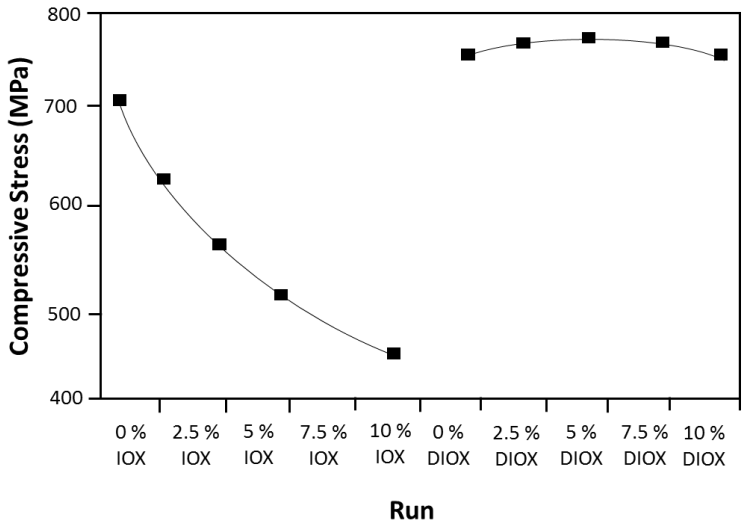

Figure 2. 14 compressive stress versus dilution with $NaNO_3$ of the primary (IOX) and secondary (DIOX) ion exchange salt baths (Beall et al.*, 2016)*

Although glass ceramics are more complicated than glasses due to their polycrystalline structure, they can also be ion exchanged (Kreski, Varshneya and Cormack, 2012; Tandia *et al.*, 2012; Fu and Mauro, 2013; Stavrou *et al.*, 2014a). Ion-exchange generally takes place mostly in one phase, either in the crystalline phase or in residual glass. For example, lithium disilicate

glass ceramics have been reported to be ion exchanged strengthened mainly using Li, Na or K nitrates (Fischer et al. 2008; Łączka et al. 2015). Also, a relatively recent study has used Rb^+ and Cs^+ ions for ion exchange strengthening of lithium disilicate glass ceramics to improve flexural strength and corrosion resistance (Shan et al. 2018).

2.4.1.3. Structural changes on ion exchange

Investigations of the structural changes induced by an ion-exchange process in the literature are limited to the calculations of the change in molar volume from the optically measured stress or to molecular dynamic (MD) simulation calculations (Tandia et al., 2012; Kreski et al., 2012). Molecular dynamics has been used mainly for investigations of Na^+ / K^+ ion-exchanged glasses and the equivalent potassium containing as-melted glasses in terms of changes in the silicon-oxygen coordination and the difference in potassium-oxygen coordination number Tandia et al., (2012).

On the basis of MD (Lee et al., 1997) reported that the strain generated after ion-exchange, which is a key factor in achieving required compressive stress, can be recovered by performing a reverse ion-exchange to reinstate the original alkali ions in the glass. Therefore, they claimed the deformations happens during ion-exchange can be categorised as nonlinear elasticity.

Figure 2. 15 shows the presence of a new band near ~ 950cm^{-1} ion-exchanged glasses which signifies the number of non-bridging oxygens has increased in the surface layer reported by Lee et al. (1997). After K^+ for Na^+ ion exchange of soda-lime-silica glass, a shift to the lower wavenumbers of the structural 1050 cm^{-1} peak was also observed.

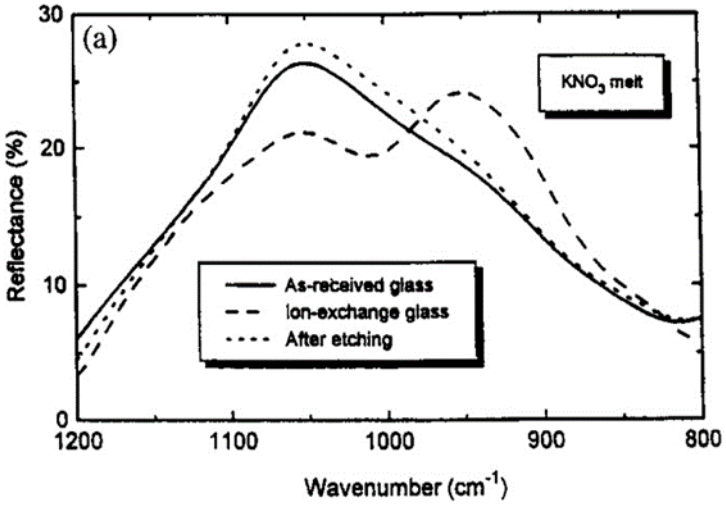

Figure 2. 15: Infrared reflection spectra of soda-lime glass ion-exchanged at 600°C for 3 h in molten KNO_3 (Stavrou et al.*, 2014a)*

(Stavrou *et al.*, 2014a) reported structural changes due to ion exchange of both K^+ for Na^+ and Ag^+ for Na^+ in aluminoborosilicate glasses by using infrared spectroscopy. They found that the replacement of Na^+ by K^+ led to a shift to the right on $Q^2 + Q^4 \Leftrightarrow 2Q^3$ equilibrium determined by Fourier Transform Infrared spectroscopy (FTIR) as shown in Figure 2. 16. However, the replacement of Ag^+ for Na^+ showed an opposite shift.

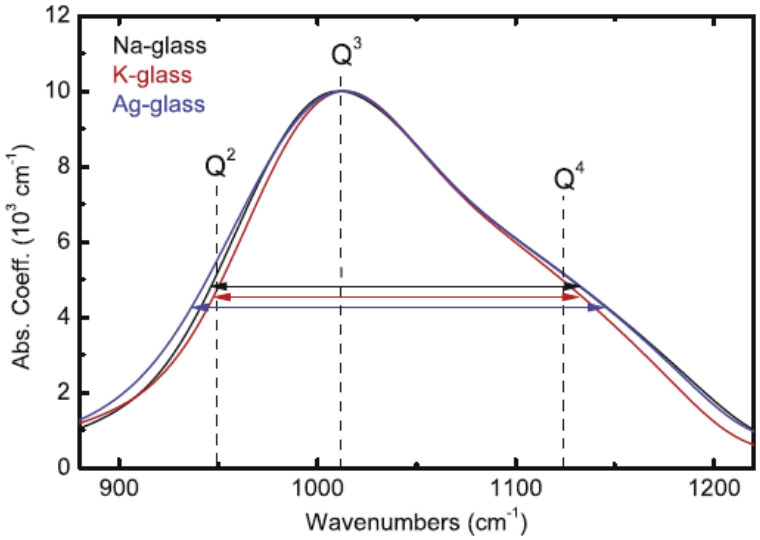

Figure 2. 16: Infrared range in 850 – 1250 cm^{-1} due to Si-O stretching vibrations of ion-exchanged aluminoborosilicate glasses (Donald 1989; Varshneya 2010; Macrelli 2017)

2.4.1.4 Ion Exchange Kinetics

The ion exchange process is based on diffusion. Hence heat treatment temperatures and times can be predicted by using the mathematics of diffusion and suitable diffusion constants. Chemical strengthening (Garfinkel, 1968; Varshneya, 2006) and optical waveguide production (Gy 2008; Varshneya 2010) are the most examined ion exchange processes. According to ion-exchange kinetics, the transport coefficient is controlled by different manufacturing parameters, such as the composition of the salt and/or bath, the composition of the substrate glass, the size and the charge of exchanging ions, temperature, time. Hence the performance of the final product is influenced by those parameters,

Diffusion is a transport phenomenon where molecules or atoms from a high concentration region to a low concentration region. The diffusion coefficient follows an Arrhenius equation:

$$D = D_0\, exp(-E/RT) \qquad \textit{Equation 2. 25}$$

where D=the diffusion coefficient, D_0=a temperature independent pre-exponential, E=activation energy for diffusion, R=gas constant, T=absolute temperature.

Fick's first law is used to relate the diffusion flux to the concentration:

$$J = -D\frac{\partial C}{\partial x} \qquad \textit{Equation 2. 26}$$

where J = diffusion flux, c = concentration, x = distance of a point in the interior of the sample from the surface, D = diffusion coefficient, i.e., an expression representing area required to permit diffusion of unit volume (or mass) in a unit of time at temperature, t(T).

With the assumption that D is independent of the concentration and is a constant, the general form of the diffusion equation (Fick's second law) is obtained.

$$\frac{\partial C}{\partial t} = \frac{\partial}{\partial x}\left(D\frac{\partial C}{\partial x}\right), \frac{\partial C}{\partial t} = D\frac{\partial^2 C}{\partial x^2} \qquad \textit{Equation 2. 27}$$

The equilibrium for ion exchange is represented by

$$A_{glass} + B_{salt} \rightleftarrows B_{glass} + A_{salt} \qquad \textit{Equation 2. 28}$$

where A represents host mobile ion and B represents mobile ion in the molten salt. A ions diffuse out of the glass sample and B ions diffuse into the glass from the molten salt. (Cooper and Krohn 1969; Sane and Cooper 1987)

The effective diffusion coefficient is calculated using

$$D = \frac{D_A D_B}{D_A C_A + D_B C_B} \qquad \textit{Equation 2. 29}$$

where C_i is the fractional concentration of alkali ion i, and D_i is its self-diffusion coefficient in mixed-alkali glass compositions.

The driving force of diffusion is the difference in concentration between the diffusion pair of ions. Thus, the more significant the difference in concentration, the higher the rate of mutual diffusion will be in theory. During the ion exchange process with soda-lime-silica glass, the sodium ions on the surface of the glass pass into the salt bath where they replace the potassium ions. This leads to a reduction in the potassium concentration difference between the bath and the glass surface which has a decelerating effect. At the same time, since the accumulation of potassium ions in the cavities in the surface glass structure will obstruct new

potassium ions that are trying to diffuse into the glass surface, the diffusion of the mobile ions that are decreasing in mobility towards the centre of the glass will slow down. For this reason, it is expected that a profile that reduces from the glass surface towards the centre is observed in the ion concentration that is added to the structure (Shaisha and Cooper 1981).

The ion concentration that is added to the structure is

$$C_K(x,t) = C_{sK} + (C_O - C_{sK}) . erf\left(\frac{x}{2.\sqrt{D_{AB}.t}}\right) \quad \textit{Equation 2. 30}$$

Where C_o is the initial concentration of occupying ions in the glass and C_{sK} is the equilibrium surface concentration of occupying ions during the ion-exchange process. C_{sNa} is the surface concentration of un-exchanged ions.

That $c_O = 0$, reduces to:

$$C_K(x,t) = C_{sK} . erfc\left(\frac{x}{2.\sqrt{D_{AB}.t}}\right) \quad \textit{Equation 2. 31}$$

Where the exchange ratio "r" is important to define the condition of maximum of surface concentration of occupying ions. For instance, if C_{sNa}=0, r=1.

$$r = \frac{C_{sK} - C_O}{C_{sK} + C_{sNa} - C_O} \quad \textit{Equation 2. 32}$$

2.4.1.4.1 Stress Generation by Ion Exchange

Stress generation by ion-exchange is associated with the difference in the size of exchanging pair of atoms and the kinetics of diffusion. The relative volume ($\Delta V/V$) increases due to the replacement of smaller ions by larger ones. Thus, stress is generated as expansion is limited by the constraint arising from the underling substrate (Hale, 1968). The chemical expansion that occurs in the glass body due to a larger alkali ion occupying an alkali site shaped by a smaller host alkali ion is similar to thermal expansion, and it is referred to as linear network dilatation coefficient (LNDC) (Gy 2008).

LNDC can be calculated by using

$$B(z) = \frac{1}{3}\frac{\partial lnV(z)}{\partial C(z)} \quad \textit{Equation 2. 33}$$

where B (z) represents LNDC, V (z) is molar volume, and C (z) is the concentration of the new, larger ion. The stresses resulting from ion exchange as a function of z (the thickness direction) are given by,

$$\sigma_{zz}\,(z) = 0$$

$$\sigma_{xx}\,(z) = \sigma_{yy}\,(z)\frac{-EB(z)C(z)}{(1-v)} + \frac{E}{H(1-v)}\int_0^H B(z)C(z)dz \qquad \textit{Equation 2. 34}$$

where stress is a function in the z-direction, E is Young's Modulus H is the thickness of the substrate in the direction of diffusion and v is Poisson's ratio. (Bradshaw, 1979a)

The stress profile can be estimated using birefringence which is based on the photoelastic principle (Abrams et al., 2004). There are some destructive methods established by etching away the surface layer and measuring the subsequent tensile stress change in the centre of the glass using scattered light (Sglavo et al., 2005), using transmission photoelasticity (Kishii, 1983) or by measuring the surface curvature change Hödemann et al. (2016). Non-destructive methods for stress profile measurements are done by differential surface refractometry using guided waves (Sane and Cooper 1987; Tyagi and Varshneya 1998; Gy 2008), and a gradient scattered light method which provides to determine the depth profile of compressive stress is proposed by (Varshneya, 2018). As noted above measured stress values (100MPa to 1GPa) and ion-exchange case depths (20 to 1000μm) have been reported (Varshneya *et al.*, 2015). Stress profile induced by ion-exchange can also be calculated theoretically using simulations which supports measurements of complex-shaped glasses. (Varshneya, 2010c).

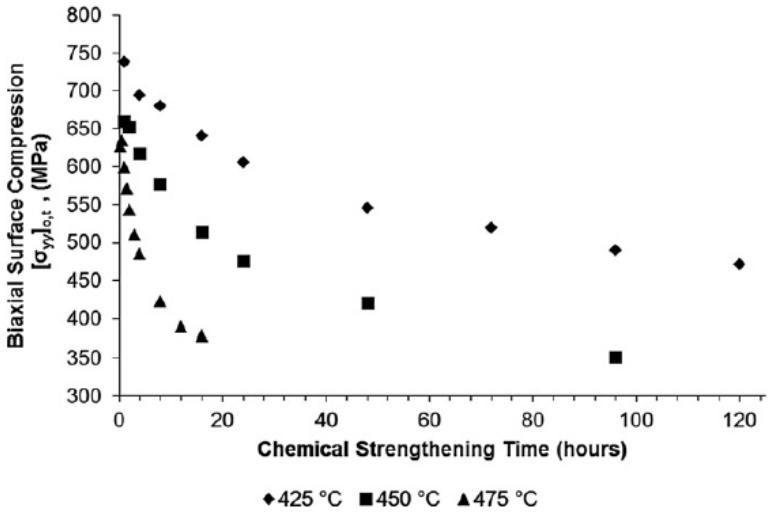

Figure 2. 17: Biaxial surface compression $[\sigma_{yy}]o,t$ measured at room temperature as a function of time and ion exchange temperature of $15Na_2O{\cdot}10CaO{\cdot}75SiO_2$ (mol%) glass Nordberg et al. (1964); Varshneya (1975); Sane and Cooper (1987); and Shen et al. 2003)

2.4.1.4.2 Stress Relaxation

At temperatures approaching the glass transition temperature viscoelastic or structural relaxation may occur on the glass surface. On glass surfaces subject to relaxation, the concentration profile is unchanged, while the maximum tensile stress moves to a point below the surface, depending on the amount of relaxation in the glass (Tyagi and Varshneya 1998). For this reason, it is essential to determine the ion exchange parameters that differ in the different types and composition of the glass in the chemical tempering process.

Stress relaxation in ion exchange has been investigated by Ragoen et al. (2018). They found that after the introduction of the larger ions into the glass; the network restructures to create new sites for the upcoming larger ions. Stress relaxation affects both the stress profile and the final strength of ion-exchanged glasses. As the ion exchange time increases the depth of the compressive layer will increase, however the final stress will be reduced (Ragoen *et al.*, 2018). Kilinc (2016) reported about the effect of network-modifying cations in the stress relaxation process. They claimed that despite the stress relaxation process, the potassium ion environment in the ion-exchanged glass is not the same as the one in sodium potassium as melted glass (Varshneya 2010).

2.5. Summary of Literature

Glass is transparent, reasonably rigid, despite providing strength it is brittle too. Glass breaks under tension, not in compression. Surface flaws limit the strength of glasses. Different techniques have been used to increase the strength as summarized in Table 2. 1. Chemical tempering or ion-exchange strengthening is based on exchanging a small ion for larger ion in the surface of a glass, therefore introducing surface compression. The efficiency of the ion-exchange process depends on different parameters such as duration, temperature, salt bath composition and concentration, glass composition. Therefore, the research related to ion-exchange strengthening is still popular, new developments needs to be done.

The literature provides different aspects of ion exchange strengthening mostly focused on potassium – sodium and sodium – lithium exchange. There are not any data of ion exchange strengthening focused on caesium – potassium exchange. There are a few studies including both K^+ - Na^+ ion-exchanged and as melted sodium – potassium silicate glasses which were done mostly using MD simulations. However, those studies are mostly done on aluminosilicate glasses.

During the literature investigations, no source was found that includes and compares these characterisation steps all at the same time, as done in this thesis. Therefore, the comparative interpretation of the mechanical and structural properties examined from various perspectives as a result of the experiments is thought to be a study with a unique value in the literature.

Chapter 3. Methodology

3.1 Introduction

In the following, first the processes of glass melting for as-melted glass specimens are explained. Secondly, the ion exchange procedure is explained. Then the background information and the methods of measurement techniques are given. Structural property measurements were undertaken using Raman Spectroscopy and Fourier Transform Infrared Spectroscopy. Other measurement techniques used include density measurements, compositional analysis by X-Ray fluorescence and Scanning Electron Microscopy (SEM) and Energy Dispersive X-Ray Spectroscopy (EDS). Finally, measurement techniques of mechanical properties such as hardness, toughness, and moduli were also undertaken.

3.2. Glass Compositions

The nominal glass composition was $72SiO_2 \cdot 13.5Na_2O.10CaO \cdot 3MgO \cdot 1.5Al_2O_3$ (mol %). This is the same as the base composition studied by (Nunzio et al. 2004; Gy 2008). In addition soda potassia-soda–lime–silica glasses with compositions $72SiO_2 \cdot (13.5–z)Na_2O \cdot zK_2O.10CaO \cdot 3MgO \cdot 1.5Al_2O_3$ (mol %) where z = 0, 2.7, 5.4, 8.1, 10.8 and 13.5 were also prepared for comparison with ion-exchanged samples. Lithia-soda-lime-silica glasses were also produced based on the same initial soda-lime-silica glass composition $72SiO_2 \cdot (13.5 – z)Na_2O \cdot zLi_2O.10CaO \cdot 3MgO \cdot 1.5Al_2O_3$ (mol %) where z = 0, 2.7, 5.4, 8.1, 9.0. If z exceeded 9mol%, it was found that the lithium glasses started to crystallize.

SiO_2 (99.5%), Na_2CO_3 (99.1%), $CaCO_3$ (99.3%), K_2CO_3 (99.5%), Li_2CO_3 (99.4%) (all from Glassworks Services), Na_2SO_4 (sodium sulphate, ≥ 99.0%) (from Acros Organics), $4MgCO_3 \cdot Mg(OH)_2 \cdot 5H_2O$ (≥ 99.0%) and $Al(OH)_3$ (≥ 99.0%) (both from Fisher Scientific) were mixed to produce the glass batches. Batches to produce 300 g of glass were melted in platinum crucibles at a temperature 1450°C. The first hour of the melting process was to allow batch reactions to go to completion. For the following four hours the melt was stirred by a platinum stirrer. After melting and fining, the glasses were cast into a block shape using preheated steel moulds. All the blocks annealed for one hour, at around 500°C to 560°C depending on the glass transition temperature and then cooled down to room temperature by 1°C/min.

Pieces were sectioned into square shape slides approximately 2mm×35mm×35mm using Secotom-50 tabletop cut-off machine with a water-cooled diamond blade for further analysis.

All the broad faces of the square slide were successively ground using SiC 400/600/800/1200 grits under running water and then polished by 6 µm, 3 µm and 1µm diamond suspensions to obtain a mirror-like finish. All polished samples cleaned with isopropanol on both sides and dried by compressed air. Subsequently these samples were re-annealed by heating to the annealing temperature at 1°C/min, holding for one hour and then cooling down to room temperature at a rate of 1°C/min to remove any residual stresses arising from the cutting, grinding and polishing. A polariscope was used to check that the residual stresses had been removed by the re-annealing.

3.3. Ion Exchange Procedure

As mentioned in the literature review, ion exchange is typically conducted by using a molten salt bath containing the alkali cations. The methods using coatings or pastes are less popular for mechanical applications. Coatings or pastes are usually used in optical modifications by ion exchange (Patschger, Marek; Rüssel, 2016). However, in this study ion exchange treatments only taken by applying the salt paste on the glass specimen developed by heat treatment below the glass transition.

For initial ion exchange experiments, soda-lime-silica microscope slides 0.7 mm× 35 mm×7.5 mm in size (Academy Science Limited) with the nominal composition shown in Table 3.1 were used.

Glass code	SiO_2	Na_2O	K_2O	CaO	MgO	Al_2O_3	SO_3
microscope slide	72.69 (73)	14.87 (14)	0.36 (0)	5.93 (7)	4.42 (4)	1.56 (2)	0.15(0)

Table 3. 1: Analysed glass compositions (mol %); XRF data normalised to 100 mol%

Samples were sectioned using a water-cooled diamond blade on a Secotom-50 cutting machine. The laboratory made glasses were cut into 1.8 to 2.5 mm thick specimens. All specimens were cleaned using isopropanol and wiped before the ion exchange process to minimize contamination on the glass surface. A certain amount of salt or salt mixture mixed with enough distilled water to obtain a paste was applied to the surface of the glass. Approximately, 0.75 – 1 g of the salt or salt mixture (depending on the exchanging pair of ions) was applied per cm^2 of the glass piece. After placing the coated glass samples into a stainless-steel beaker, they were treated at temperatures between 480°C to 520°C for 4 to 16

hours. After the treatment, remaining salt on the glass surface was washed off using water. Later, they were cleaned with isopropanol on both sides and dried by compressed air.

Since the atomic weight of potassium is higher than that of sodium, an increase in sample weight was expected after the ion exchange process; weight change has been reported to quite notable after K^+ - Na^+ ion-exchange (Karlsson, 2012). A digital balance of 10^{-4} precision was used for the weight measurements of the ultrasonically cleaned samples before and after the ion exchange process. The amount of potassium ions added to the glass structure was the calculated using

$$K \text{ in the glass} = [(wt_{before} - wt_{after}) / (aw^K - aw^{Na})]. aw^K \qquad \text{Equation 3. 1}$$

where the weights before and after the wt_{before} and wt_{after} ion exchange process, aw^K and aw^{Na} are the atomic weights of potassium and sodium, respectively.

3.3.1. Ion Exchange Treatment

3.4.1.1. Na/K exchange

Sodium and potassium ions are widely used alkali metal ions for ion exchange strengthening. Mixture of potassium nitrate and potassium chloride salts are used. Potassium nitrate and potassium chloride are chosen to bind the paste on to surface and remove it easily after the ion exchange process (Kistler, 1962). 1 to 2 and 2 to 1 by mass salt mixtures prepared and applied by following the paste application procedure as explained previously. The melting temperature of KNO_3 is 334°C, the melting temperature of KCl is 770°C; and the eutectic temperature for KNO_3:KCl is 320°C(Ferraro 2002; Cornel et al. 2012). The ion-exchange treatment is conducted at 420°C, 450°C and 480°C at various times from 1 hour to 12 hours.

3.4.1.2. Li/Na exchange

Na^+ (ionic radius 0.98 Å) for Li^+ (ionic radius 0.68 Å) ion exchange was expected to be more efficient than exchanging K^+ (ionic radius 1.33 Å) for Na^+ (ionic radius 0.98 Å) as mentioned already in the literature review (Colomban, 2003; Wang *et al.*, 2011). As the diameter difference between the exchanging pair of ions becomes smaller, the displacement movement is also facilitated. Since the lithium-sodium mutual diffusion coefficient is greater than the coefficient of the standed potassium, a greater diffusion layer depth can be obtained at lower temperatures and shorter times during the chemical strengthening of lithium-containing glasses with sodium. In this way, the risk of viscoelastic or structural relaxation is minimized.

8.1 % lithium containing soda-lime-silica glass is used for Li/Na ion exchange. The treatment is conducted at 400°C and 450°C for 12 hours.

3.4.1.3. K/Cs exchange

Due to the larger size of Cs^+ (ionic radius 1.67 Å) the diffusion is relatively slow and takes longer time so exchanging of Cs^+ for K^+ is relatively harder than Na/K exchange. The K/Cs ion-exchange treatment is conducted at 450°C and 480°C for 12 hours.

3.1.4.4. Na/Cs exchange

Again, the exchange of larger size Cs^+ the diffusion is expected to be slow. However, Na/Cs ion exchanged still conducted at 480°C for 12 and 24 hours.

3.1.4.5. Ca/Ba exchange

KNO_3 and $Ba(NO_3)_2$ mixture is applied as a salt paste expecting both Na/K and Ca/Ba exchange at the same time. The treatment is done at 520°C for 8 hours.

3.5. Structural Property Measurements

3.5.1. Raman Spectroscopy

Raman spectroscopy is a technique which utilises the inelastic scattering the incident light. When a light quantum or a photon hits a molecule, light can either be scattered elastically or inelastically, the latter giving rise to a frequency shift. The vibrational energy transitions that can arise and which give rise to fundamental modes of vibrations are shown in Figure 3. 1. Rayleigh scattering accounts for the majority of interactions that occur, however, there is a small amount of light that undergoes Raman scattering and is transferred from the excitation frequency (laser) to the vibrations of the bonds in the sample (Colomban, 2003; Wang *et al.*, 2011) resulting in scattering of quanta with energy $v_0 - v_{vib}$ or $v_0 + v_{vib}$, (Stokes and anti-Stokes scattering, respectively).

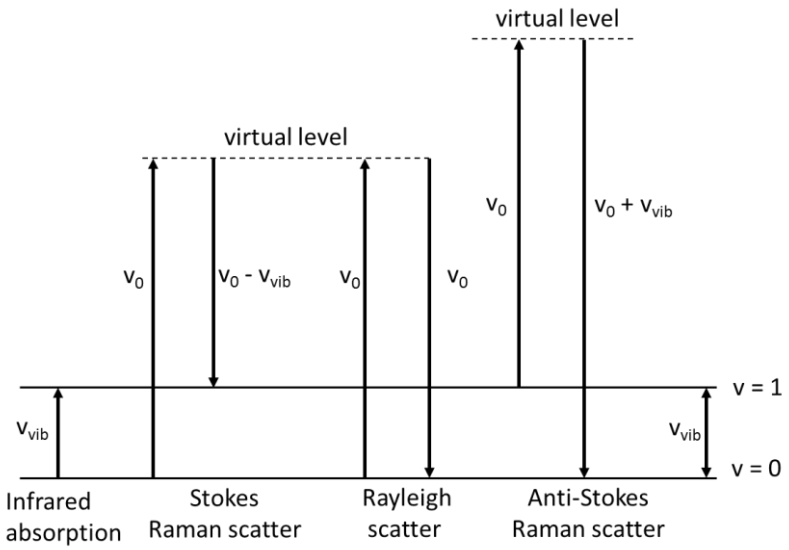

Figure 3. 1: An energy level diagram showing transitions equivalent to IR absorption, Raman, and Rayleigh scattering

Raman Spectroscopy is a useful technique to gain insight into the structure of glass. It is a complementary technique to infrared spectroscopy. Raman spectra of silicate glasses generally contain bands in 10 - 1500 cm^{-1} region. There are four main regions: the boson region (10 – 250 cm^{-1}), the low-frequency region (250 – 700 cm^{-1}), the medium frequency region (700 -850 cm^{-1}) and the high-frequency region (850 – 1300 cm^{-1}) (Wang *et al.*, 2011). The 850 – 1300 cm^{-1} high-frequency region is assigned to the Si–O stretching vibrations of [SiO_4] structural units with different Q^n units giving rise to different frequency shifts (see table 3.1).

Wavenumber (cm^{-1})	**Vibration Modes**	**Reference**
580	Si–O^0 rocking motions in fully polymerized SiO_2 (Q^4) units, isolated SiO_4	(Wang *et al.*, 2011)
600	Si–O–Si bending vibration in depolymerized structural units	(Wang *et al.*, 2011)
700-850	Si–O–Si symmetric stretching of bridging oxygen between tetrahedra	(Colomban, 2003; Wang *et al.*, 2011) (Eckert, 2015)
850-1300	Si–O^0 and Si–O^- stretching vibration of Q^n with different n (n=0,1,2,3,4)	

Table 3. 1. Band frequencies and corresponding vibration modes of Raman spectra of silicate glass (Gervais et al. 1987)

In this study, Raman spectroscopy is used to determine the effect of ion exchange on structural modifications and to observe structural differences on the equivalent potassium and lithium-containing as-melted glasses. Taking advantage of the relationship between the Si-O bond length, Si-O-Si bond angle, and Raman shifts. Raman spectroscopy was performed

on bulk samples, using a Renishaw inVia Raman Spectrometer scanned by a green laser (514.5 nm, 20 mW) from 0 to 1500 cm^{-1} by 10 accumulations. Calibration was undertaken using a silicon wafer, beforehand for each measurement. The raw Raman data were analysed using OriginPro and Fityk. First, the raw data were smoothed via Wire 3.4 software and deconvoluted, then compared to each other.

3.5.2. Fourier Transform Infrared Spectroscopy (FTIR)

FTIR (Fourier transform infrared spectroscopy) is a non-destructive technique that can be used to obtain chemical information about the materials especially chemical bonding. The system is shown in Figure 3. 2. There are mirrors; one of them is fixed, the other moves on the axis perpendicular to its plane constantly. Between the mirrors, there is a beamsplitter which partially transmits and reflects the incoming beam. IR radiation goes through the sample, and some of the infrared radiation is absorbed by the sample; some of it is passed through resulting in a wavelength spectrum. Fourier transform instrument is capable of measuring all wavelengths at once, and a transmittance or absorbance spectrum can be produced. (Agarwal and Tomozawa 1995)

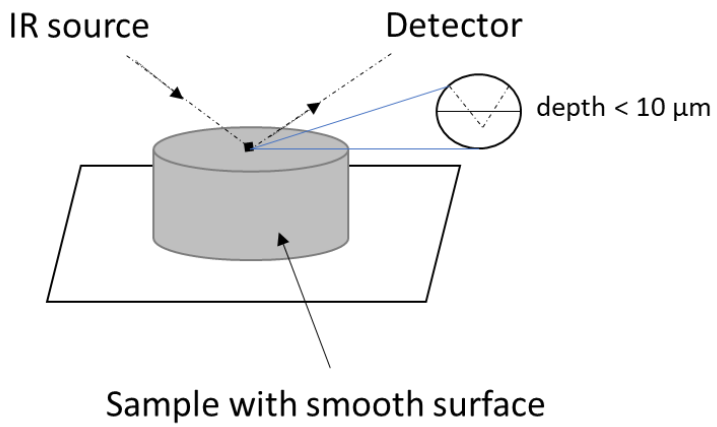

Figure 3. 2: Schematic of the essential features of a Reflectance Fourier transform infrared spectrometer

Fourier transform infrared spectroscopy (FTIR) is sensitive to the local structure of silicate glasses, which helps to define how the Si-O-Si vibrational mode changes and thus details about the structure of glass can be inferred from the resultant infrared spectroscopy data. The fundamental silica and silicate structural bands appear from 1500 to 400 cm^{-1} regions of the IR reflection spectra. The infrared spectra of silica and silica glasses generally contain three characteristic bands which are localized at around 450, 750 and 1000 cm^{-1}. The 450 cm^{-1} and 1000 cm^{-1} bands correspond to stretching and bending modes, respectively. Whereas

750 cm^{-1} includes bending mode of bridging oxygen perpendicular to Si-Si axis and within Si-O-Si plane (Agarwal and Tomozawa, 1995). The structural band near 1100 cm^{-1} which represents Si – O – Si bridged stretching is usually dominant. The band at 950 cm^{-1} represents Si – O non-bridging stretching for soda-lime-silica glasses (Agarwal and Tomozawa, 1995).

Overall due to their different selection rules, FTIR and Raman Spectroscopies are complementary techniques.

Type of Glass	Bond locations of the vibrational bands (cm^{-1})				Reference
As-received soda-lime silicate glass	1056	_	765	460	(Simon and McMahon 1952)
As-polished soda-lime silicate glass	1122	_	785	477	(X. Zhou et al. 1990)
Vitreous Silica	1100	_	_	_	(X. Zhou et al. 1990)
Vitreous Silica	1271	1125	_	_	(Varma, Kothari and Tewari, 2009)
Sodium Calcium Silicate Glass	1211	1071	_	_	(Ferraro and Manghnani, 1972)
Soda Lime Glass	1080	952	_	_	(Domine & Piriou 1983)
Fused Silica	1087	_	815	475	(Macdonald *et al.*, 2000)
Na_2O – 1.41 SiO_2 Glass	1040	925	_	_	(Macdonald *et al.*, 2000)
20%Na_2O – 80%SiO_2	1100	1000	780	480	(Sharaf, Condrate and Ahmed, 1991)
20%Li_2O – 80%SiO_2	1100	950	780	480	(Sharaf, Condrate and Ahmed, 1991)
Sodium Calcium Silicate Glass	1201	1069	763	473	(Park, J.W. ; Chen, 1980)
Ag^+ - Na^+ ion-exchanged glass	1194	1057	762	466	(Park, J.W. ; Chen, 1980)

Table 3. 2: Summary of FTIR bond locations of the vibrational bands of different types of glasses

Wavenumber (cm^{-1})	Assignment	Vibration	Reference
1050	Si-O-Si	Stretching mode involving bridged oxygens	(Husung and Doremus, 1990)
950	$Si-O^-$	Stretching mode of non-bridging oxygens	(Husung and Doremus, 1990)
1065	Si-O-Si	Antisymmetric stretching of bridging oxygens within the tetrahedra	(Husung and Doremus, 1990)
970	$Si-O^-$	Stretching mode of non-bridging oxygens	(Husung and Doremus, 1990)
770	Si-O-Si	Symmetric stretching of bridging oxygens between tetrahedra	(Sharaf, Condrate and Ahmed, 1991)
460		Bending modes	

950	Si-O-Si and	Stretching modes involving nonbridging	
	O-Si-O	Oxygens	(Sharaf, Condrate and Ahmed, 1991)
470	$Si-O^-$		
1070		Bending modes	(Sharaf, Condrate and Ahmed, 1991)
760	O-Si-O	Stretching mode involving bridged oxygens	
450	$Si-O^-$	Stretching mode that involve bridging oxygens	
980	$Si-O^-$	Bending	(Sharaf, Condrate and Ahmed, 1991)
1060	Si-O-Si	Stretching modes of Si atoms	
	$Si-O^-$	Stretching modes of Si atoms	(Burns, Brack and Risen, 1991)
	$Si-O^-$		(Burns, Brack and Risen, 1991)
			(Burns, Brack and Risen, 1991)
			Evans and Charles (1976)
			Ponton and Rawlings (1989)

Table 3. 3: Summary of FTIR peak assignments of silicate glasses

In this study, FTIR spectroscopy is used to determine the effect of ion exchange on the glass structure and to observe structural differences in the equivalent potassium and lithium-containing as-melted glasses. FTIR spectroscopy was performed on bulk samples, the range 400 to 4000 cm^{-1} using a Perkin Elmer Frontier Fourier transform infrared spectrometer instrument. Prior to measurement background scanning was undertaken collecting data of on IR reference material. The acquisition was performed with 4 scans, and a resolution of 4 cm^{-1} was performed. Transmittance data were collected after which peaks assigned different bonds were using data in the literature. FTIR bond locations of the vibrational bands of different types of glasses and peak assignments of silicate glasses are summarised in Table 3. 2 and Table 3. 3, respectively.

3.6. Chemical and Physical Measurements

3.6.1. Density

The density of fabricated glasses was measured with an electronic densimeter based on Archimedes' principle using deionised water as the immersion medium. The mass of a glass specimen in air and in deionised water was weighed as m_1 and m_2, respectively. Thus, V_A is the volume of glass, which is equal to the volume change of deionised water ΔV_W when the glass is completely immersed is obtained by Equation 3.2.

$$V_A = \Delta V_W = \Delta m_W/\rho_W = (m_1 - m_2)/\rho_W \qquad \textit{Equation 3. 2}$$

where ρ_W is the density of deionised water which is known at a given temperature. Therefore, the density of glass (ρ) can be calculated by Equation 3.3.

$$\rho = m_1/V_A = \rho_W m_1/(m_1 - m_2) \qquad \textit{Equation 3. 3}$$

Density measurements were assessed as being accurate to 0.001 g/cm^{-3}. Each glass sample was measured for five times; error bars were determined using standard deviation from five times repeated measurements.

3.6.2. Differential Thermal Analysis (DSC – TGA)

The glass transition temperatures (T_g) measurement of the produced glasses was obtained using differential thermal analysis (Perkin Elmer STA 8000). As a reference material alumina was used to determine the difference in temperature (ΔT) at a constant heating rate. Particle size of the powder samples were < 75 µm. Powder samples were heated up to 1000°C at a heating rate of 10°C/min, then cooled down to room temperature at the same rate, followed by another heating again up to 1000°C at 10°C/min. The glass transition temperatures were obtained from the second heating curve using in-built Pyris software on DTA instrument as shown in Figure 3. 3.

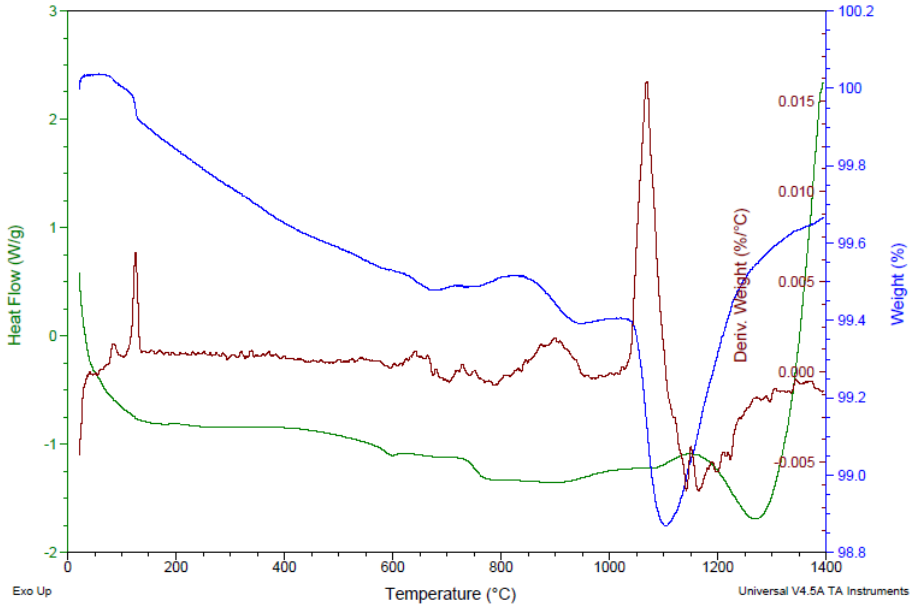

Figure 3. 3: DSG -TGA analysis of 72SiO_2·13.5Na_2O.10CaO·3MgO·1.5Al_2O_3 glass

3.6.3. Compositional Analysis by X-Ray Fluorescence

The compositional analysis of the as-melted glasses was measured by XRF (X-ray fluorescence). Polished bulk samples were undertaken using PanAnalytical Zetium XRF instrument. The analysis was run in a vacuum with each sample being cleaned using isopropanol to prevent any contamination. As a reference a certified soda lime silica glass is used. Results were taken from XRF compositional analysis were semi-quantitative and can be used only as a guide to compositions. Estimated experimental errors are ±1 wt. % for SiO_2; ±0.5 wt. % for major oxides which may range between 1.5 - 15 wt. %; and ±0.3 wt. % for minor oxides where the content of each was less than 1.5 wt. %. XRF is incapable of detecting any elements lighter than boron; hence lithium content was not measured directly.

3.6.4. Scanning Electron Microscopy (SEM) and Energy Dispersive X-Ray Spectroscopy (EDS)

EDS is a relatively efficient method regarding geometry and analytics of the detector. However, sometimes the energy resolution of the peaks is poor. Sample preparation for SEM especially for glass samples needs care. Cold mounted glass samples need to get gentle grinding and polishing. Since glass is a non-conductive material carbon coating and silver paste were essential for SEM imaging to prevent any charging. The analysis was examined using an XL – 30S FEG scanning electron microscope (SEM) with and Energy Dispersive X-Ray (EDS) capability. The chemical compositions of selected ion-exchanged strengthened glasses and as-melted glasses were analysed using line EDS during SEM examination. The analysis was carried out semi-quantitatively.

3.7. Mechanical Property Measurements

3.7.1. Vickers Hardness

Hardness measurements of bulk glasses were assessed using Vickers indentation. The polished glass surfaces with a standard load of 9.81 N for 15 seconds using a Durascan Micro Hardness Measurement Instrument. The number of indentations made on each specimen was ~10. The hardness was calculated using

$$H_v = 1.8555 \frac{P}{d^2} \qquad \text{Equation 3. 4}$$

where *P* is indentation load in kg, and *d* is the average diagonal length of the indents. The hardness values were calculated from averages of the 10 readings.

Vickers indentation was also used to measure the crack resistance of ion-exchange strengthened glasses. The glass specimens were indented by a Vickers diamond indenter with a 15 s loading time and the radial cracks which were appeared on the corners of the indented shape were counted. At least twenty indentations were made for each applied load, and the following range of loads (2.94, 4.9, 9.8, 24.5 and 49 N) was used. The probability of crack initiation was obtained by a fraction of the number of corners with the cracks to the total number of the corners of indentations accordingly to Figure 3. 4. As the applied load increases, the percentage of crack initiation increases from 0% (no crack appears at any of the indent corners) to 100% (cracks appear at all of the indent corners).

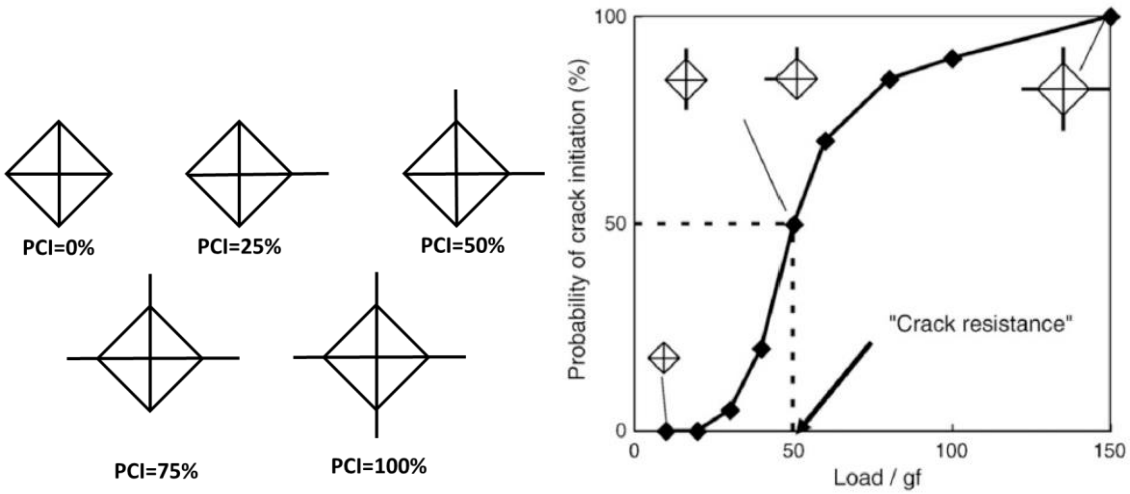

Figure 3. 4: Probability of crack initiation (Simultaneous chemical vapour deposition and thermal strengthening of glass – Sundberg et al) Effect of densification on crack initiation under Vickers indentation test, 2010

3.7.2. Indentation Toughness

The indentation fracture toughness measurement of as-melted glasses was measured directly after Vickers indentations made five different loads (2.94, 4.9, 9.8, 24.5 and 49 N). After each indent, the length of the median-radial cracks originating from the corners was measured. Then indentation fracture toughness assessed using

$$K_{Ic} = \frac{0.0824P}{c^{3/2}} \qquad \textit{Equation 3. 5}$$

where P is the load in (N) and c is the half crack length, and the constant 0.0824 was proposed by (Kilinc, 2016)and supported by Karlsson et al. (2010).

3.7.3. Nanoindentation

Nanoindentation measurements were carried out to understand how the ion exchange strengthening affects the near surface hardness and elastic modulus of the surfaces under study.

Nanoindentation is a type of indentation method in which the penetration depth is measured in nanometres (10^{-9} m) instead of microns (10^{-6} m) or millimetres (10^{-3} m). Besides the scale of the measurement, nanoindentation does not produce a direct measurement of the contact area between the specimen and the indenter, unlike conventional indentation techniques. Since measuring the area of contact is not convenient for nanoindentation tests, it based on obtaining elastic modulus and hardness of a calibration material from load and displacement measurements to determine how the shape of the tip varies with depth. Spherical Indenter, Vickers indenter, Berkovich indenter, cube corner indenter are the indenter types used for nanoindentation testing. A three sided Berkovich indenter is used for brittle materials such as glass and ceramics. The tip radius of a typical Berkovich indenter is 50-100 nm which increases up to 200 nm by use (Fischer-Cripps, 2011).

The most widely used method is Oliver and Pharr's method which was first introduced in 1992 to determine hardness and elastic modulus from load-displacement data. In 2003 the method improved and extended to be used for wider applications (Oliver and Pharr, 1992; Oliver and Pharr, 2004).

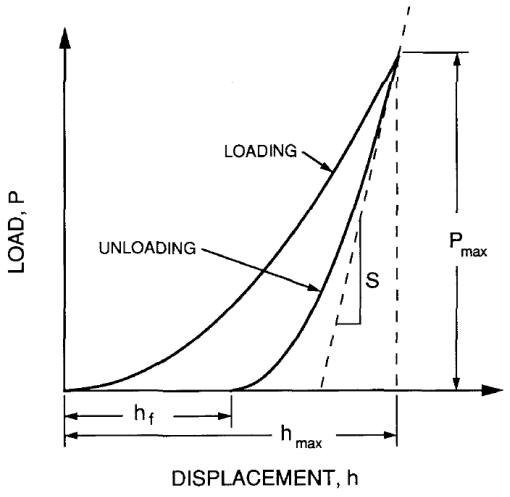

Figure 3. 5: A schematic representation of load versus indenter displacement data for an indentation experiment. (Oliver and Pharr, 1992)

Force and depth of penetration are recorded during the load which is applied for 5 seconds from zero to maximum, 5 seconds dwell and 5 seconds from maximum back to zero. As the emphasis was to obtain data in the indentation depth range of 0 to 100 nm, low depth calibration was carried out before doing nanoindentation on samples. The basic analysis followed the method of Oliver and Pharr (1992), but the calibration function was obtained as an equivalent radius, r_c, following the procedure suggested by Tadjiev et al., (2010) which was designed for shallow depth calibration. Using this procedure calibration runs on fused silica were undertaken, which involved producing multiple arrays of 10×10 indents with a standard loading scheme. Hardness was evaluated from the load-displacement data by using Equation 3.6.

$$H = \frac{P_{max}}{A_{max}} = \frac{P_{max}}{\pi r_c^2} \qquad \textit{Equation 3. 6}$$

P_{max} = the maximum load during an indentation and A_{max} = the corresponding tip contact area.

The unloading stiffness, S, determined by the Oliver and Pharr method and was used to calculate the reduced modulus of the samples using

$$E_r = \frac{S}{2.1\ r_c} \qquad \text{Equation 3. 7}$$

3.7.4. Strength Measurements

Strength measurements consist of applying increasing the stress on a definitely shaped sample until failure occurs. Conveniently, strength is measured by using a 3-point bending test, or preferably, 4-point bending test as shown in Figure 3. 6. Strengths measured using these tests also which are adjustable to several temperatures and environmental conditions. These can also be called as modulus known modulus of rupture (MOR) (Varshneya, 2006).

For the 4-point bending test,

$$\sigma = \frac{(F/2)\ [(L_1 - L_2)/2]h/2}{b\ h^3/12} \qquad \textit{Equation 3. 8}$$

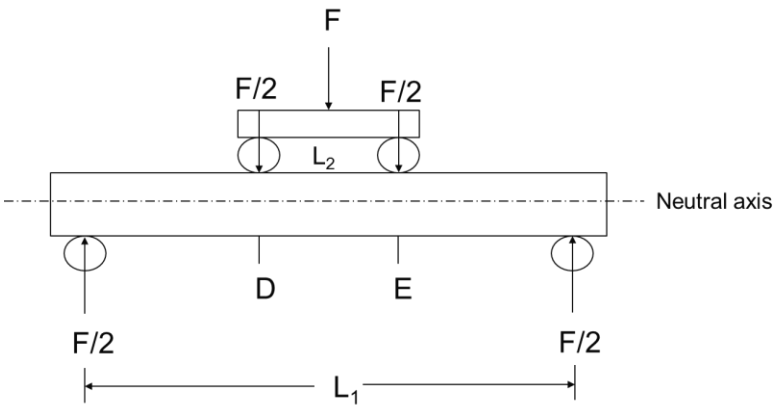

Figure 3. 6: Schematic diagram of four-point bending

3.7.5. Fracture Toughness

Fracture toughness measurements of lab-made glasses were made using the SCF method with controlled defect introduced via Knoop indentation according to the BS-EN ISO-18756: 2005 standard. The Knoop indentation load to introduce a controlled crack on the surface was 19.61 N which is a maximum value on Durascan Micro Hardness Measurement Instrument. The samples were cut into rectangular bars of approximately 3.5 × 4.0 × 46 mm cut from bulk glass specimen and ground to 600-grit finish. In order to prevent possible notch tip blunting, samples were annealed, prior to introducing the Knoop indentation at the centre of the 46 × 4.0 mm face. The semi-elliptical crack formation was acceptable for all series of glasses by the defect introduced using 19.61 N Knoop indentation load Karlsson et al., (2015). A four-point bend fixture was mounted on a CSIC small tensometer was used. The articulating rollers of the four-point bend fixture was used with the inner and the outer span set to 20 mm and 40 mm. In order to minimize environmental effects during testing, the pre-crack was filled with silicone oil. The characterization of various types of cracks for different fracture toughness measurements obtained from Nikon Eclipse LV150 microscope. An example of a semi-elliptical crack formed after bending an 'as-indented' glass specimen as shown in Figure 3. 7.

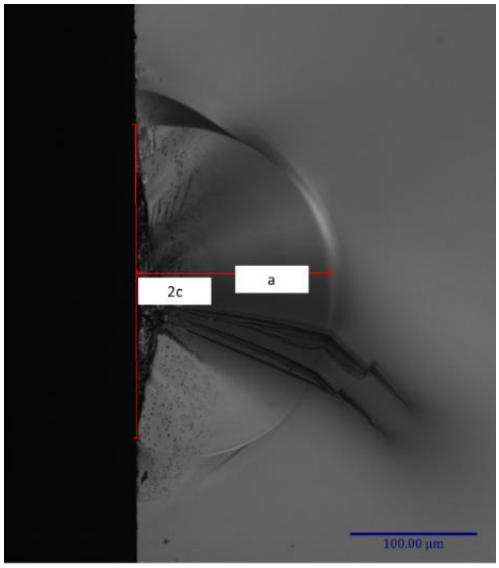

Figure 3. 7: Example of semi-elliptical crack formed after bending an 'as-indented' glass specimen (Images obtained from Nikon Eclipse LV150 microscope)

3.7.5. Elastic Moduli

Elastic moduli of as-melted glass specimens were measured using an Olympus Epoch 6000, ultrasonic pulse echo instrument. The longitudinal (V_L) and the transverse (V_T) velocities were measured using 20 MHz and 5 MHz transducers, respectively. Glycerol and a shear coupling gel were used as appropriate to obtain a proper contact between the surface and the transducers.

The wave velocity (V) of the material under test can be calculated as follows.

$$V = \frac{2l}{t} \qquad \textit{Equation 3. 9}$$

where l is the thickness of testing material.

The Shear modulus, *G*, was obtained using

$$G = \rho {V_T}^2 \qquad \textit{Equation 3. 10}$$

where ρ is density, and V_T is longitudinal velocity. The Young's modulus, E, was obtained using

$$E = \rho {V_T}^2 \frac{(3{V_L}^2 - 4{V_T}^2)}{({V_L}^2 - {V_T}^2)} \qquad \textit{Equation 3. 11}$$

To minimise the cumulative error, Poisson's ratio (v) and bulk modulus (K) were also obtained from the wave velocities using

$$v = \frac{({V_L}^2 - 2{V_T}^2)}{2({V_L}^2 - {V_T}^2)}$$ *Equation 3. 12*

And

$$K = \rho \frac{3{V_L}^2 - 4{V_T}^2}{3}$$ *Equation 3. 13*

Chapter 4. Results and Discussion

4.1. Introduction

This chapter has three main subsections apart from this introduction. Section 4.2 covers the experimental results obtained on the K^+ for Na^+, Na^+ for Li^+ and Cs^+ for K^+ ion-exchanged glasses. Section 4.3 includes the results obtained on the equivalent potassium containing glasses. Finally, section 4.4 covers the experimental results obtained on the lithium-containing glasses. This chapter also discusses the mechanical and structural properties of ion-exchanged glasses produced in this work. Relevant literature on soda-lime-silica- glasses and ion-exchanged glasses are used in the discussion for comparison of the results of this study.

4.2. Ion-Exchanged Glasses

4.2.1. Na/K exchange in soda-lime-silica glasses

It is essential to understand the structural changes that led to developed mechanical properties of ion-exchanged glasses. First of all, there was no visible change in the surface the ion-exchanged soda-lime-silica glass slides. Thus, the glass slides were still transparent after the ion exchange treatment, and no colour change was observed, as expected.

The depth profile characterised by line EDX on SEM. Annealing causes the K^+ ions to diffuse further into the bulk glass, as shown in Figure 4. 1 which shows the atomic percentages of Na^+ and K^+ ions as a function of cross-sectional depth. Black and red dots indicate the sodium concentration in the ion-exchanged glass and reannealed ion-exchanged glass, respectively. Blue and green dots indicate the potassium concentration in the ion-exchanged glass and reannealed ion-exchanged glass, respectively. Purple dots show the potassium amount in the original glass composition according to the XRF results (see Table 3. 1). However, the EDS results in Figure 4. 1 indicates that the potassium amount is above 1 %. This issue is most probably related to the EDS calibration. Overall, it can be seen that K^+ concentration is decreasing from near surface to bulk, while Na^+ concentration is increasing from near surface to bulk. On annealing the rate of decrease in K^+ concentration with depth is slightly smaller than for the ion exchanged glass, indicating increased potassium diffusion to greater depths.

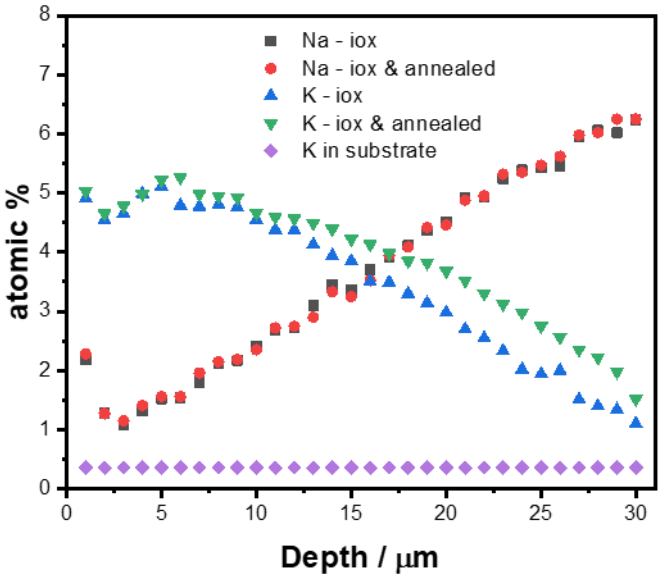

Figure 4. 1: EDS measured Na and K contents of soda-lime-silica glass ion exchanged at 480°C for 12 hrs in a 2:1 KNO_3: KCl mixture and ion-exchanged at 480°C for 12 hrs in a 2:1 KNO_3: KCl mixture and then reannealed

It is known that the penetration depth is affected by the temperature, process time and the concentration dependent interdiffusion coefficient of the alkali ions (Gy 2008). The potassium ion diffusion depth is greater than 15-20 µm according to the SEM/EDS results. Patschger and Rüssel (2016) using Atomic Absorption Spectroscopy, and a Surface Ablation Cell reported an approximately 40 µm diffusion depth for K^+ after heat treatment at 500°C for 10 h using single side ion exchange. Guldiren et al., (2016) also reported 40 µm diffusion depth for K^+ for ion exchange in a molten salt at 425°C for 16h. Thus, the data here is in line with reported penetration depths for single-side ion exchange.

Other approaches to potassium ion-exchange have reported similar diffusion depths. For instance, (Sharaf et al. 1991; Agarwal and Tomozawa 1995; Lee et al. 1997; Varma et al. 2009) found up to a 10 µm penetration depth of K_2O on ion-exchanged soda lime silica glasses treated at 450±60°C and 2 to 6 hr by using in-line vapour deposition method. (Agarwal, Davis and Tomozawa, 1995; Varma, Kothari and Tewari, 2009) reported up to a 28 µm diffusion depth of potassium following a spray-technique producing 6 µm thick salt layer and up to 30 hours of treatment time. Thus, the penetration depth is dependent on the composition of the glass, ion exchange time, temperature and the properties of the salt. Therefore, the comparison should be made considering all parameters.

Both Raman spectroscopy and FTIR showed that replacement of alkali ions induces structural changes in the glass network. Infrared reflection spectra from ion-exchanged samples produced by using different weight percentage mixtures of potassium nitrate and potassium chloride salts are shown in Figure 4. 2 The ion-exchanged samples all exhibit a new peak near ~ 950 cm^{-1}. This new peak is assigned to the Si – O stretching modes involving nonbridging oxygens and suggests that there is an increase in the number of nonbridging oxygen concentration in the surface layer, as reported by several authors (Park and Chen, 1980; Agarwal and Tomozawa, 1995; Varma et al., 2009).

To investigate this further the ion-exchanged specimens were also reannealed at 540°C for 1 hour to observe whether the new peak near ~ 950cm^{-1} is a consequence of the compositional change or relates to the stresses in the material itself. Figure 4. 3 shows the reflectance spectra of an ion-exchanged specimen produced using a 1:2 KNO_3: KCl mixed salt paste at 480°C for 12 hrs and a reannealed specimen of the same ion-exchanged glass. Similarly, Figure 4. 4 shows the reflectance spectra of an ion-exchanged specimen produced using a 2:1 KNO_3: KCl mixed salt paste at 480°C for 12 hrs and reannealed specimen of the same ion-exchanged glass. Both figures show that after reannealing the new peak near ~950 cm^{-1} remains, however the intensity declines. Hence, it is concluded that this structural peak is linked to the K^+ for Na^+ ion-exchange process. Furthermore, there are some changes in the peak at ~470 cm^{-1} which shifts to lower wavenumbers on ion exchange; the shift is the same for different weight percentage mixtures of potassium nitrate and potassium chloride salts. The band ~470cm^{-1} is associated with O-Si-O bending modes. Agarwal and Tomozawa (1997) After reannealing the position of this peak remains the same for the different weight percentage mixtures of potassium nitrate and potassium chloride salts. However, the intensity declines similar to the peak near ~950cm^{-1}. The peak ~760$cm^{-1,}$ which is associated with Si – O stretching modes that involve bridging oxygens, also shifts to lower wavenumbers.

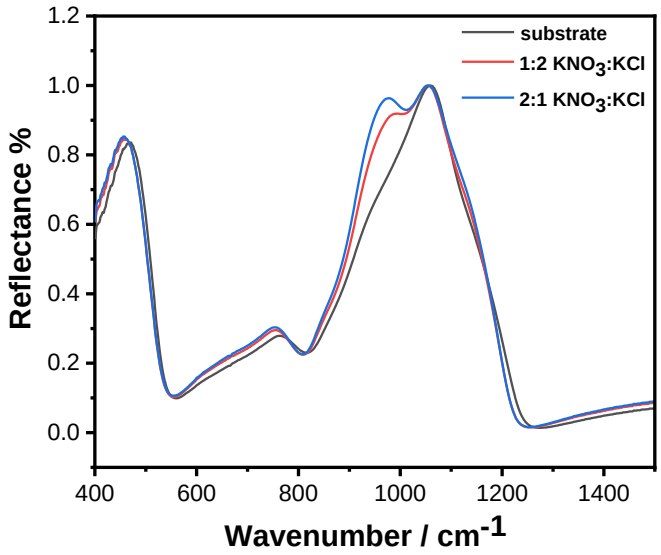

Figure 4. 2: Infrared reflection spectra of K^+ for Na^+ ion-exchanged soda-lime-silica glass at 480°C for 12 hrs in 1:2 KNO_3: KCl, 2:1 KNO_3: KCl mixtures

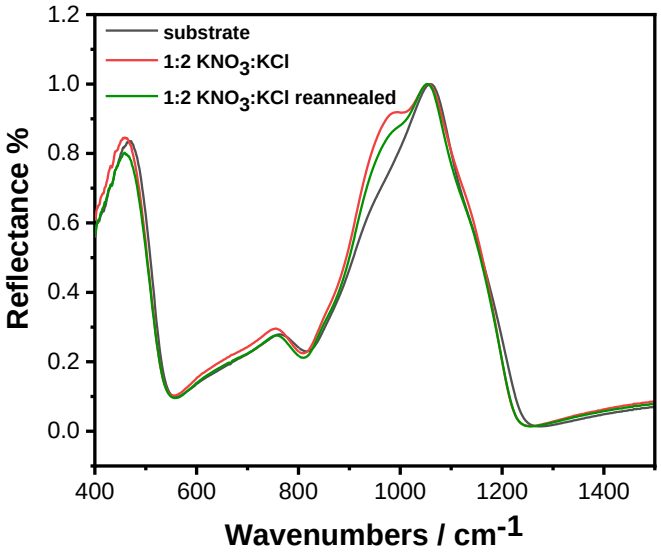

Figure 4. 3: Infrared reflection spectra of K^+ for Na^+ ion-exchanged soda-lime-silica glass at 480°C for 12 hrs in 1:2 KNO_3: KCl mixtures and reannealed 1:2 KNO_3: KCl ion-exchanged specimens

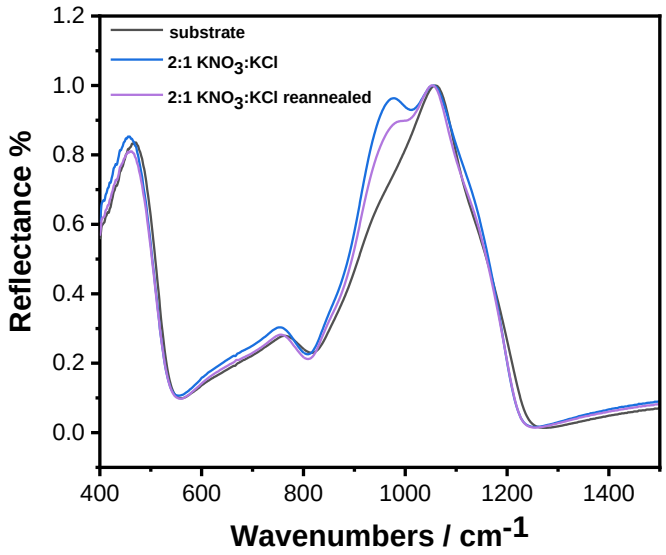

Figure 4. 4: Infrared reflection spectra of K^+ for Na^+ ion-exchanged soda-lime-silica glass at 480°C for 12 hrs in 2:1 KNO_3: KCl mixtures and reannealed 2:1 KNO_3: KCl ion-exchanged specimens

Furthermore, after K^+ for Na^+ ion exchange of soda-lime-silica glass there is a shift to lower wavenumbers of the 1050 cm^{-1} peak which is assigned to the symmetrical stretching modes of Si – O – Si i.e. modes involving bridging oxygens (Sharaf et al., 1991; Wang, 1997). According to (Sharaf et al., 1991), the structural changes in silica glass which are measurable by infrared spectroscopy by observing a structural shift in Si – O stretching band depend on the fictive temperature and the hydrostatic compressive stress. They reported a shift towards to lower frequencies on the IR reflection band position of ion-implanted and irradiated silica fibre glasses compared to same silica fibre samples heat-treated in the temperature range of 950 to 1400°C.

The overall experimentally observed band locations of the vibrational bands present are summarised in Table 4. 1.

Type of Glass	**Bond locations of the vibrational bands (cm^{-1})**			
Untreated glass	1059		762	471
Ion exchanged glass (2:1 KNO_3:KCl mix)	1055	**979**	751	463
Ion exchanged glass (2:1 KNO_3:KCl mix) reannealed	1051	**980**	754	463
Ion exchanged glass (1:2 KNO_3:KCl mix)	1055	**992**	755	463

Ion exchanged glass (1:2 KNO_3:KCl mix) reannealed	1052	**990**	757	463

Table 4. 1: Experimentally observed bond locations of the vibrational bands (cm^{-1}) (errors are equal to ±1 for each value)

Karlsson (2012) suggested mixing salts in his thesis, where he reported on a single side in-line ion exchange method using vapour deposition. Considering the melting temperature of KCl (770°C) is notably higher than the melting temperature of KNO_3 (334°C), KCl helps the salt paste to remain on the surface of the glass for longer during the process, as the mixture remains solids at high temperatures hence the KNO_3 rich paste mixture (2:1 KNO_3: KCl) gives a sharper peak around 950 cm^{-1} than the KCl rich paste mixture (1:2 KNO_3: KCl). In the literature, annealing after ion exchange has been used to obtain silver nanoclusters to produce waveguides in the silver ion-exchanged glasses Özdemir Yanık et al. (2018). Ag^+ - Na^+ ion-exchanged glasses are reported to have noticeable structural band shifts towards to lower wavenumbers in reflectance spectra, but, the structural bands shift to higher wavenumbers for the same glasses after heat treatment Leboeuf et al. (2013). However, in the current study infrared reflectance spectra for reannealed K^+ - Na^+ ion-exchanged glasses presented band shifts still in the same direction to those observed for the K^+ - Na^+ ion-exchanged glasses. This disagreement might be because annealing tends to be at lower temperatures than those used for heat treatment to form nanocrystals. Also, the exchanging pair of ions is different and after heat treatment silver ions form nanoparticles. Furthermore, the covalent character of the Ag - O bond is greater than that of the Na - O bond which causes the force constant for Si - O to be lower for Ag – Si – O (NBO) than for Na – Si – O (NBO). (Gy 2008) also suggested a structural change after Ag^+ for Na^+ ion-exchange showing that the structural peak shifted in the direction of the lower wavenumbers for the experimentally obtained FTIR reflectance data.

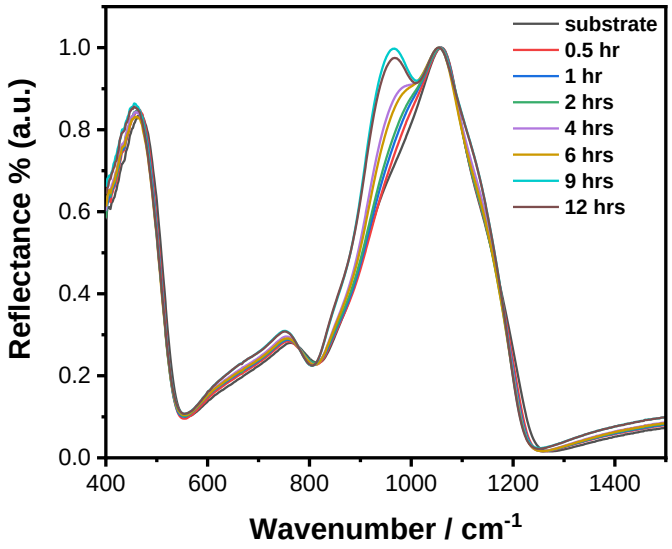

Figure 4. 5: Infrared reflection spectra of K^+ for Na^+ ion-exchanged soda-lime-silica glass at 480°C for 0.5 hr to 12 hrs in 2:1 KNO_3: KCl mixture

Infrared reflection spectra with increasing K^+ for Na^+ ion-exchange times are shown in Figure 4. 5. The effect of occupying K^+ ions on the glass structure is visible on 9 and 12 hrs at 480°C. Most clearly, K^+ by Na^+ ion-exchanged soda-lime-silica glasses exhibit a structural band shift as well as resulting in a new peak near ~ 950cm^{-1}. (Quaranta *et al.*, 2012; Stavrou *et al.*, 2014a; Calahoo, Zwanziger and Butler, 2016) reported on FTIR reflectance spectra of Na^+ - K^+ ion-exchanged glasses, showing an increase of glass rigidity by polymerisation and an expansion around 1000 cm^{-1} which increases with the ion-exchange time. As the ion exchange process time increases, Q^4 units decreases while Q^3 and Q^2 units increase. These changes are correlated to the structural modification of the glass strengthened by the ion-exchange process. Additionally, the infrared reflection peak shift of K^+ by Na^+ ion-exchanged soda-lime-silica glass at 480°C for 0.5 hr to 12 hrs is shown in Figure 4. 6. It can be seen that 6 hrs, 9 hrs, and 12 hrs ion exchange times result in an equal maximum shift. It is known that the penetration depth is affected by the temperature, process time and the self-diffusion coefficient of the alkali metal (Terakado et al. 2016; Calahoo et al. 2016).

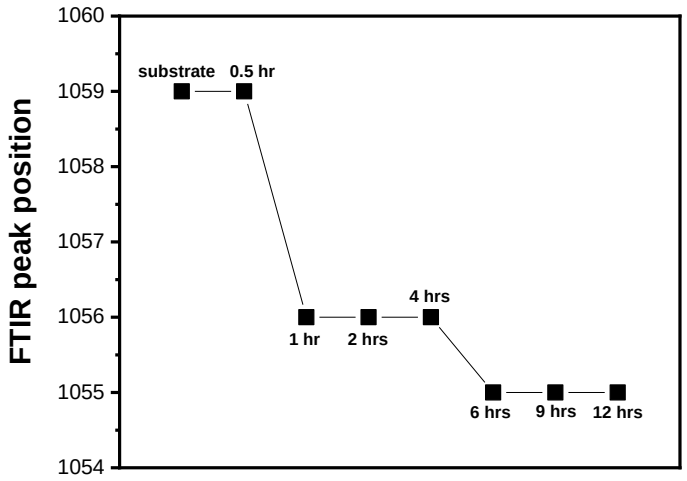

Figure 4. 6: Infrared reflection peak shift of K^+ by Na^+ ion-exchanged soda-lime-silica glass at 480°C for 0.5 hr to 12 hrs in 2:1 KNO_3: KCl mixture (errors ~ ±1 for each value)

Since the atomic weight of potassium ion is greater than that of the sodium ion, it is expected to increase the sample weight after the ion-exchange process. Figure 4. 7 shows the effect of increasing process temperature and time on the mass increase in the samples. As expected, both an increased temperature and a constant temperature with increased ion exchange time increases sample weight.

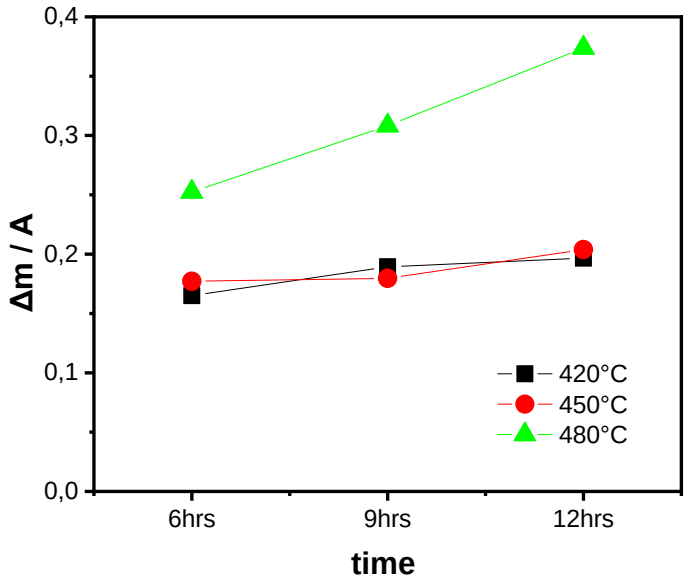

Figure 4. 7: Calculated potassium content divided by area for different temperature and times of ion-exchanged samples (errors ~ ±0.01 for each value)

Raman spectroscopy has been used for the investigations of ion-exchanged glasses to observe the change in the topological structure (Furukawa et al. 1981; P. McMillan, 1984). Depth profile analysis of ion-exchanged layers can also be studied by Raman Spectroscopy (Wojdyr, 2010). Raman spectra collected at increasing time from K^+ by Na^+ ion-exchanged soda-lime-silica glass surfaces are shown in Figure 4. 8. The spectra have been normalized to the intensity of the high-frequency band, for instance the relative height of the low-frequency band to the high-frequency band is changing. In Figure 4. 9 the high-frequency region of the spectra is shown to indicate how the shifts differ with changing ion exchange time. Increase in potassia concentration with the loss of sodium results in some notable changes in the low-frequency region of the Raman spectra. The total intensity of the main single low-frequency band increases as the Na^+ - K^+ ion exchange time increased. There are also changes in band shape between 200 cm^{-1} and 400 cm^{-1} can be seen in the difference spectra shown in

Figure 4. 10. Modification in the low-frequency band indicates changes in Q^n species as the band is assigned to vibrations of the Si-O-Si bridging oxygens (P. McMillan, 1984).

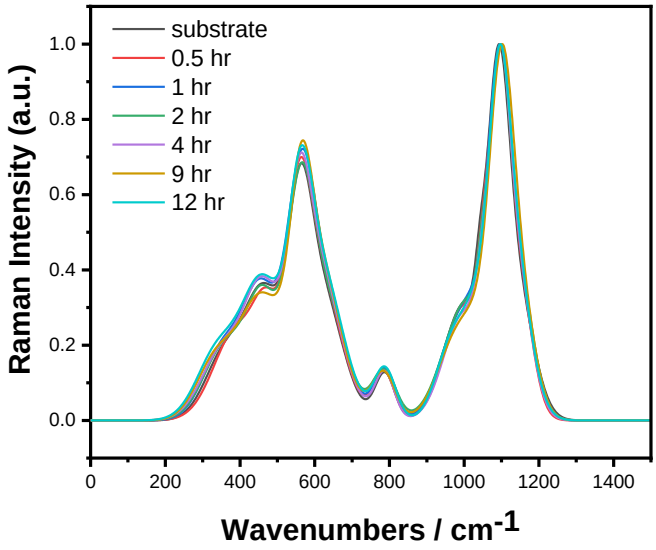

Figure 4. 8: Raman intensity full spectra of K^+ by Na^+ ion-exchanged soda-lime-silica glass at 480°C for 0.5 hr to 12 hrs in 2:1 KNO_3: KCl mixture

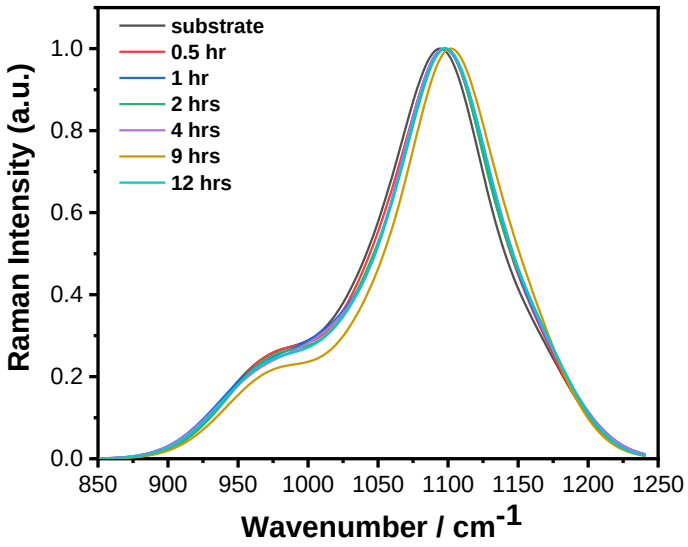

Figure 4. 9: High-Frequency region of Raman spectra of K^+ by Na^+ ion-exchanged soda-lime-silica glass at 480°C for 0.5 hr to 12 hrs in 2:1 KNO_3: KCl mixture

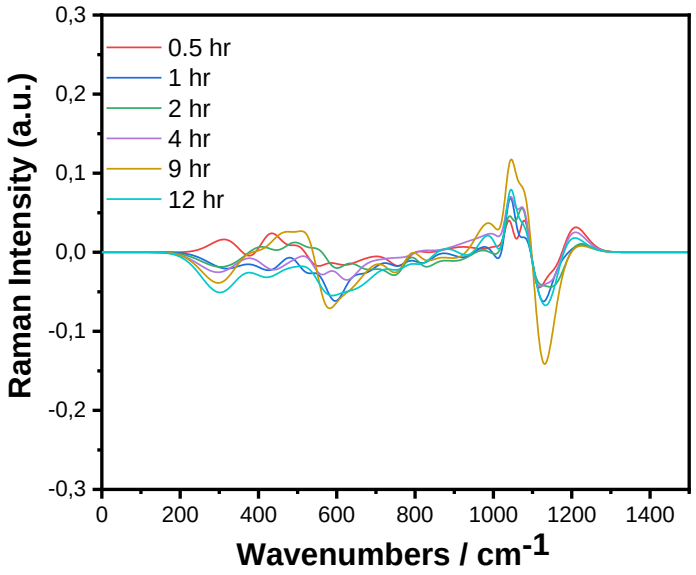

Figure 4. 10: Differences in Raman Intensity (substrate – ion exchanged glasses by different times)

The Raman spectra plots also display a shift of the ~1100 cm^{-1} band to higher wavenumbers as the ion-exchange temperature increases. The Raman spectra were fitted with a number of Gaussian peaks using Fityk software((Stavrou *et al.*, 2014a) . Figure 4. 11 and Figure 4. 12 show the deconvolution of reference glass and ion-exchanged glass, respectively. Ion-exchange treatment was conducted at 480°C for 12 hrs. For the non-ion-exchanged soda-lime-silica glass in the low-frequency region (250 – 700 cm^{-1}) the four peaks at 350, 459, 555 and 591 cm^{-1} have been allocated to Si-O-Si stretching and bending of Q^4, Q^3, Q^2 and $Q^{2'}$ units (Stavrou

et al., 2014b; Calahoo, 2016a), respectively. In the medium frequency region (700 – 850 cm^{-1}) the single peak between 790 – 800 cm^{-1} is assigned to antisymmetric Si motion in a cage or identified as highly depolarized (Brawer and White, 1975; Matson et al. 1983; McMillan, 1984). In the high-frequency region (850 – 1200 cm^{-1}) the four peaks at 964, 1039, 1093 and 1146 cm^{-1} have been assigned to Si – O- stretches of Q^2, Q^4, Q^3 and $Q^{3'}$ (that is, Q^3 with two different second-neighbour environments) units, respectively (Calahoo 2016).

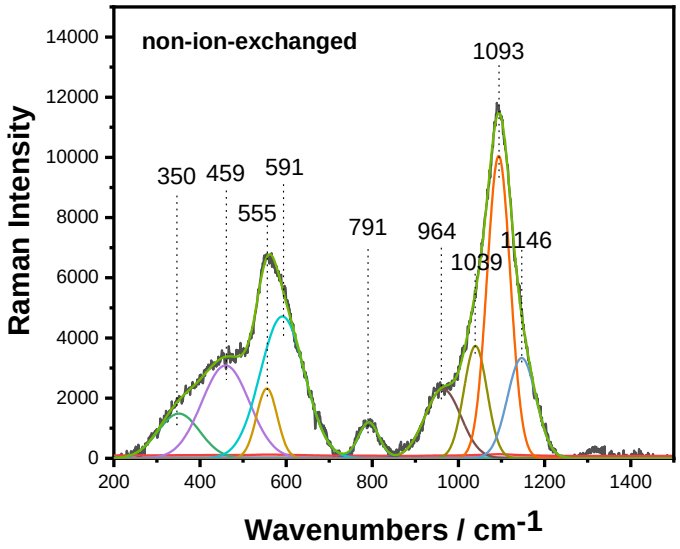

Figure 4. 11: Deconvolution of the Raman spectra of non-ion exchanged soda lime silica glass

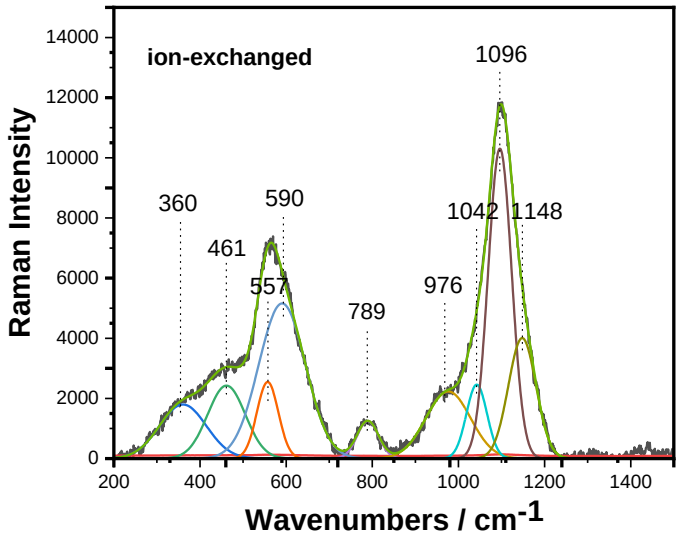

Figure 4. 12: Deconvolution of the Raman spectra of ion exchanged soda lime silica glass

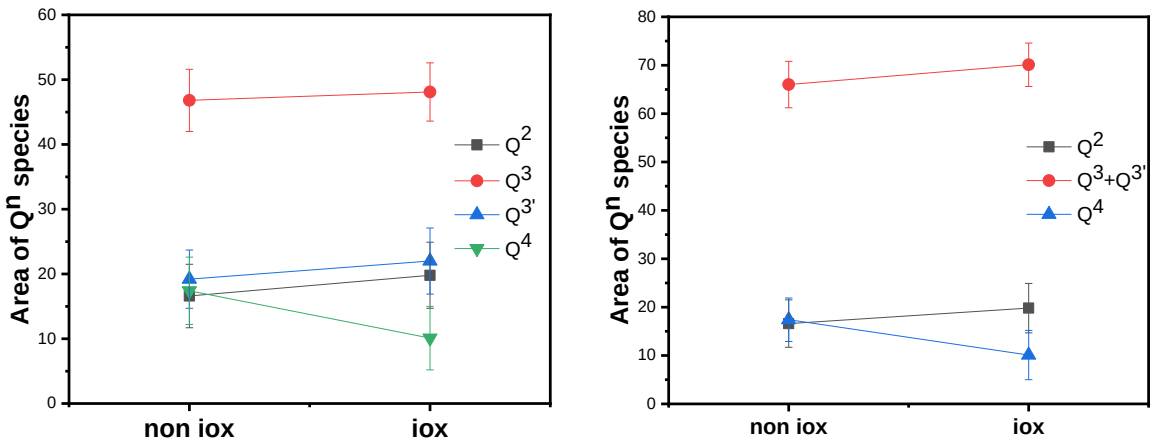

Figure 4. 13: Area of Q^n species of ion-exchanged and non-ion-exchanged glass specimens

Figure 4. 13 shows the fraction of Q^n species. Q^4 is slightly reduced, Q^2 slightly increased, to observe the change in Q^3 and $Q^{3'}$ the data plotted together on the right-hand side which shows a slight increase on the overall Q^3. Therefore, reduction in connectivity is observed as a direct consequence of ion exchange treatment. Also, the equilibrium of $Q^2 + Q^4 \Leftrightarrow 2Q^3$ shifts to the right after ion exchange treatment. This also agrees with the study published by (Varshneya, 2010b) whereas they worked on ion-exchange of sodium aluminosilicate glasses.

For the high-frequency bands, the Raman shift is a function of internal Si-O bond length, a higher wavenumber relates to a shorter Si-O bond. It has been seen to shift to lower wavenumber with increased alkali content (Varshneya, 2010b).

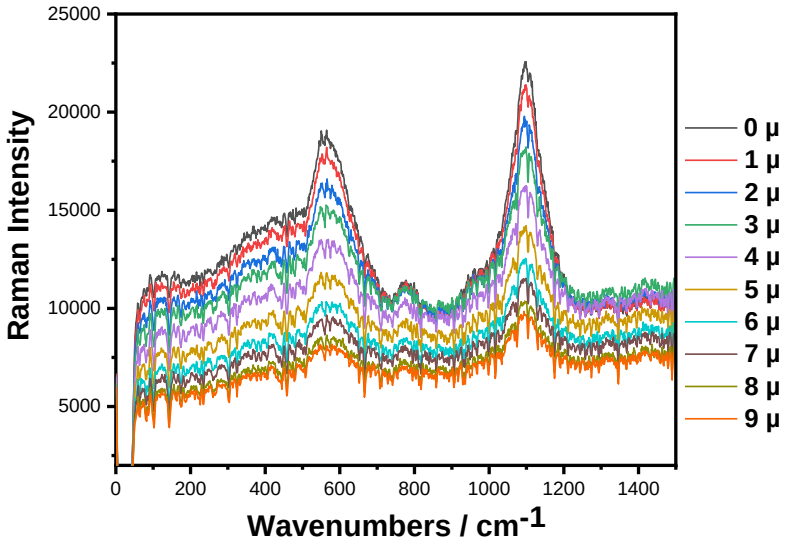

Figure 4. 14: Full Raman depth profile spectra of K^+ by Na^+ ion-exchanged soda-lime-silica glass at 480°C for 12 hrs in 2:1 KNO_3: KCl mixture

Some additional analysis was done to get more information on the changes with increasing diffusion depth. The Raman spectra collected at increasing depths from Na^+ - K^+ ion-exchanged glass surface is shown in Figure 4. 14. These spectra are increasingly noisy the further into the sample the laser spot is focussed. It can be seen that the high-frequency peak position shifts slightly to the lower wavenumbers with increasing depth. This is in a good agreement with the literature showing that high-frequency peak positions move to higher wavenumbers with a decreasing depth into a bulk glass for the chemically strengthened Corning Gorilla Glass 3 (Terakado *et al.* 2016).

Flexural strengths measured using a 4-point bending test for the 2:1 KNO_3: KCl paste and 1:2 KNO_3: KCl paste is shown in Figure 4. 15. The ion-exchange conducted on microscope slides at 480°C for 12 hours. The KNO_3 rich paste resulted in higher strengths than the KCl rich paste. This reflects a greater degree of ion exchange which is in line with the growth observed in the peak at 1050cm^{-1} in the FTIR results as well as the 1100cm^{-1} shift to the higher wavenumbers in the Raman Spectra.

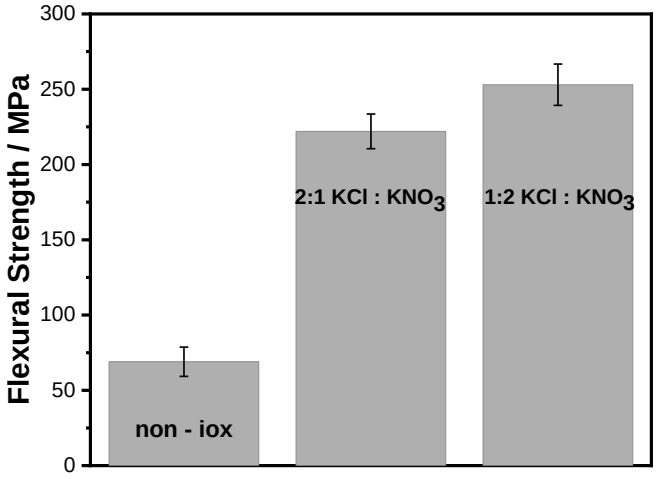

Figure 4. 15: Flexural Strength of non-ion-exchanged soda-lime glass, ion-exchanged at 480°C for 12 hrs using the 2:1 KNO_3: KCl and the 1:2 KNO_3: KCl pastes

Thus, for these ion exchanged soda-lime-silica glass specimens an increase in strength of 3.2 to 3.8 times was observed; larger strength values have been obtained commercially by ion exchange using a salt bath, and it has been stated that the strength of soda-lime-silica glass can be increased by 3 to 4 times by ion-exchange (Varshneya, 2001; Gy, 2008a), especially for ion exchange times of up to 16 hours (Gervais et al.1987). However, the current results are higher than the results which were reported by Patschger and Rüssel (2016) for spray ion-exchanged samples, when an increase of 2.8 times was obtained. They are also larger than the results obtained in the single-side ion exchange strengthening study published by Karlsson et al. (2013) in which ring-on-ring flexural strength measurements showed an increase between 1.85 to 2.15 times.

Because of the sample preparation requirements of the 4 – point bending test, the tests could not run on the ion-exchanged as melted specimens. However, nanoindentation experiments took place for as melted soda-lime-silica glass and the same glass used as a substrate for K^+ by Na^+ ion – exchange performed at 480°C for 12 hours by using 1:2 KNO_3: KCl mixture paste. It is shown that the values of hardness improved by 10 percent, whereas the reduced modulus only slightly increased, as seen in Figure 4. 16.

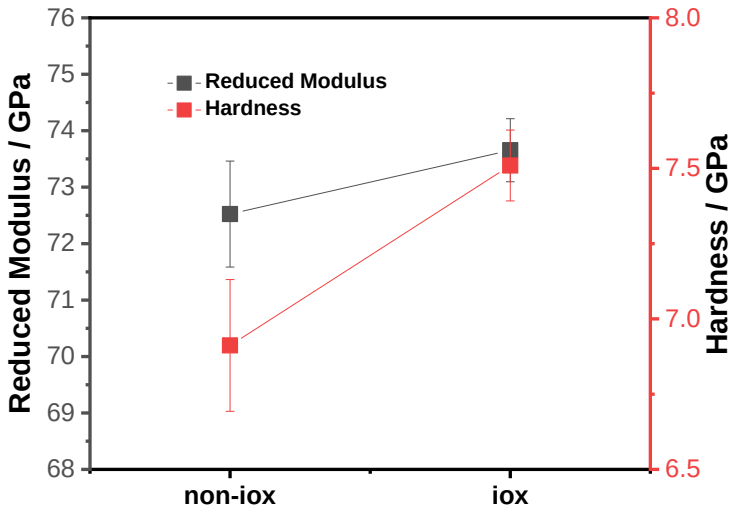

Figure 4. 16: Experimentally obtained Reduced Modulus and Hardness plot of an as melted soda-lime-silica glass and the same soda-lime-silica glass ion-exchanged at 480°C for 12 hrs in a 2:1 KNO_3: KCl mixture

The experimental results indicate that the K^+ - Na^+ ion-exchange resulted in both strengthening and structural changes. As diffusion becomes more rapid with increasing temperature, the structural relaxation in the glass also increases and this will relieve some of the stresses that are induced with ion-exchange (Varshneya 2010a). The increase in hardness at different temperatures can be explained by the compression of the network structure by placing the potassium ions in the surface structure into the relatively small regions of the sodium ions in the glass structure as indicated in the literature (Macdonald *et al.*, 2000). The resulting compressive compression creates stress and increases the resistance of the surface to indentation (Kese and Rowcliffe 2003; Garza-Méndez *et al.,* 2007; Jannotti *et al.,* 2011; Jannotti *et al.,* 2012; Karlsson 2012; Shim *et al.,* 2015).

4.2.2. Li/Na exchange in lithia-lime-silica glasses

Na^+ for Li^+ ion-exchanged lithia-lime-silica glasses also exhibited no visible change on the glass surface with the glass specimens still being transparent after the ion exchange treatment. In this case no new bands are seen in the infrared reflectance spectra on ion exchange (see figure 4.15), however there is a small shift in the band at ~1100 cm^{-1} to lower wavenumbers with increasing ion exchange temperature (see figure 4.16). Hence the same type of shift is seen when smaller alkali ions are replaced by larger ones both when K^+ replaces Na^+ and when Na^+ replaces Li^+.

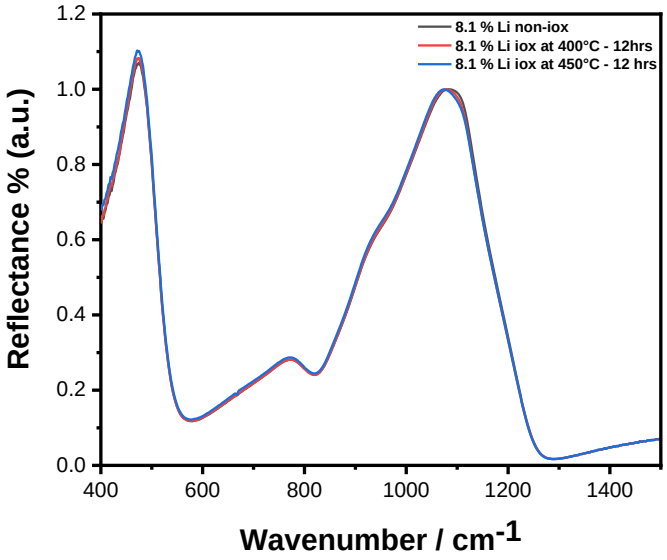

Figure 4. 17: Infrared reflection spectra of Na^+ for Li^+ ion-exchanged lithium-lime silica glass

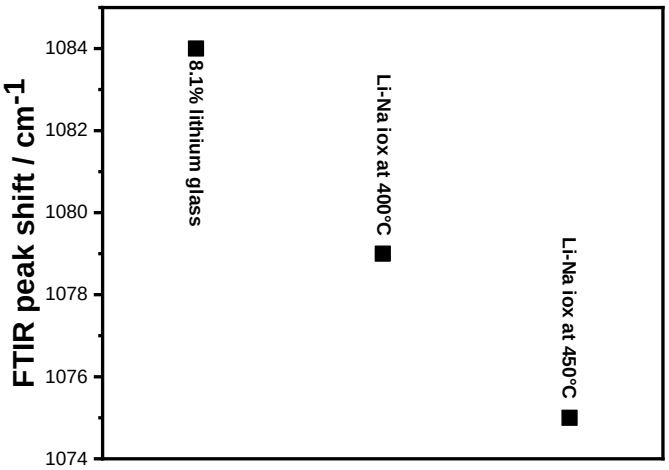

Figure 4. 18: Infrared reflection peak shift for Na^+ for Li^+ ion-exchanged lithium-lime silica glass

4.2.3. K/Cs exchange in potassium silica glasses

Ion exchange of K^+ by Cs^+ was conducted on as melted potassia-lime-silica glasses. Unfortunately, the process resulted in severe cracks in the ion-exchanged specimens. Thus, no further mechanical characterisation of these specimens could be undertaken. The infrared

reflectance spectra of these specimens as seen in Figure 4. 19 and a new peak at around 950cm^{-1} is also observed from Cs^+ - K^+ ion-exchange at 480°C for 12 hours. Also, the main peak at around 1050cm^{-1} is also shifted slightly to the higher wavenumbers similar to observations made on Na^+- K^+ ion-exchanged glasses.

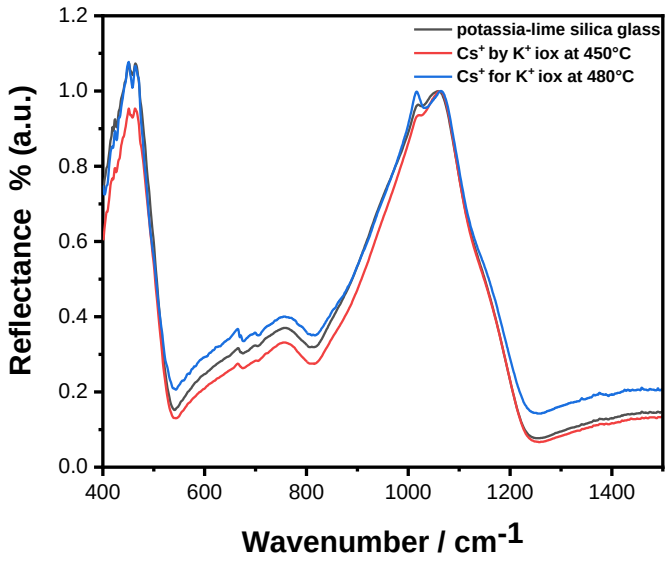

Figure 4. 19: Infrared reflection spectra of Cs^+ for K^+ ion-exchanged potassium-lime silica glass

4.2.4. Na/Cs exchange in soda-lime-silica glasses

Cs^+ ion-exchange was also conducted on as melted soda-lime-silica glass. Again, severe cracking of the ion-exchanged samples was observed, so no further mechanical characterisation was conducted. The infrared reflectance spectra of Cs^+ for Na^+ ion-exchanged specimens at 480°C for 12 and 24 hours in comparison to the spectra for soda-lime-silica glass are shown in Figure 4. 20. After 12 hours of ion-exchange treatment nothing was observed in the infrared reflectance spectra. The main peak at around 1060cm^{-1} is also shifted slightly to lower wavenumbers as shown in Figure 4. 21 which is the opposite direction to that observed on Na^+- K^+ ion-exchanged glasses. Also, a new peak at around 950cm^{-1} is also observed for Cs^+ - Na^+ ion-exchange at 480°C for 24 hours. However, this peak is not observed for Cs^+ - Na^+ ion-exchange at 480°C for 12 hours.

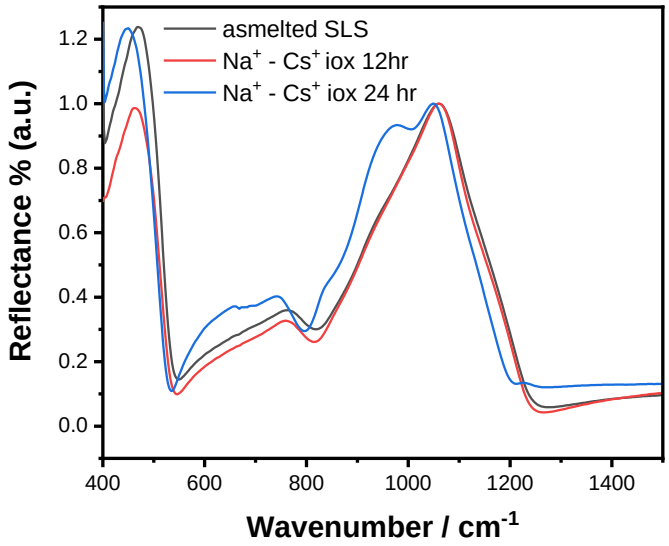

Figure 4. 20: Infrared reflection spectra of Cs^+ for Na^+ ion-exchanged soda-lime silica glass

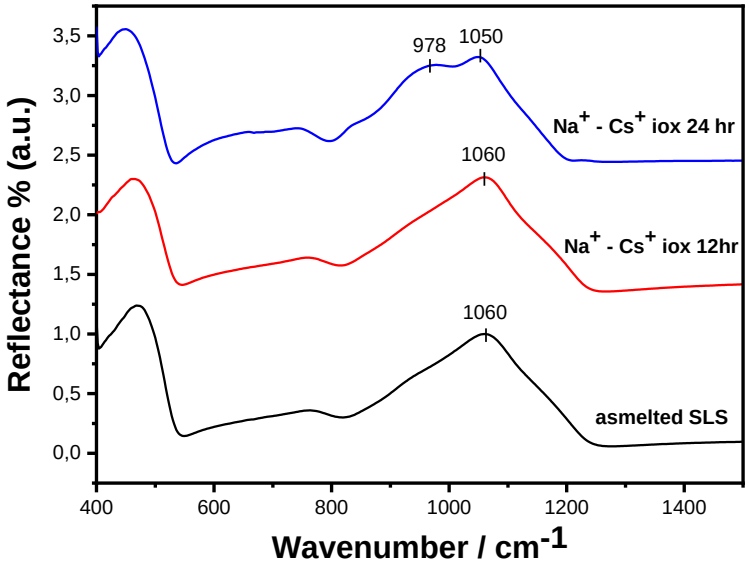

Figure 4. 21: Infrared reflection spectra of Cs^+ for Na^+ ion-exchanged soda-lime silica glass

4.2.5. Ca/Ba exchange in soda-lime-silica glasses

Severe cracking observed and no change was observed on FTIR reflectance and Raman Spectroscopy, so no results could be reported and no further mechanical characterization was conducted.

4.2.6. Summary of Ion-Exchange Strengthening Results

The results of experimental work discovered that compared to non-ion-exchanged reference soda-lime-silica glass samples, Na^+ - K^+ ion exchanged glasses provide increased surface microhardness / nanohardness, and strength. It can be suggested that the ion – exchange process involving the use salt paste was most successfully achieved on Na^+ - K^+ exchanged ones by using 1:2 KCl: KNO_3 salt mixture at 480°C for 12 hours ion exchange treatment. Alterations in the in the Na^+ - K^+ ion – exchanged glasses are observed to be associated with structural band changes in the silica network structure. Structural alteration occurred near the surface as a result of ion-exchange investigated by infrared reflectance spectra is shown in

Figure 4. 22 for different ions. Although, some shifts observed on the exchanges of Na^+, K^+, Cs^+ ions the most noticeable ones, the most changing glass was Na – K ion exchanged glass.

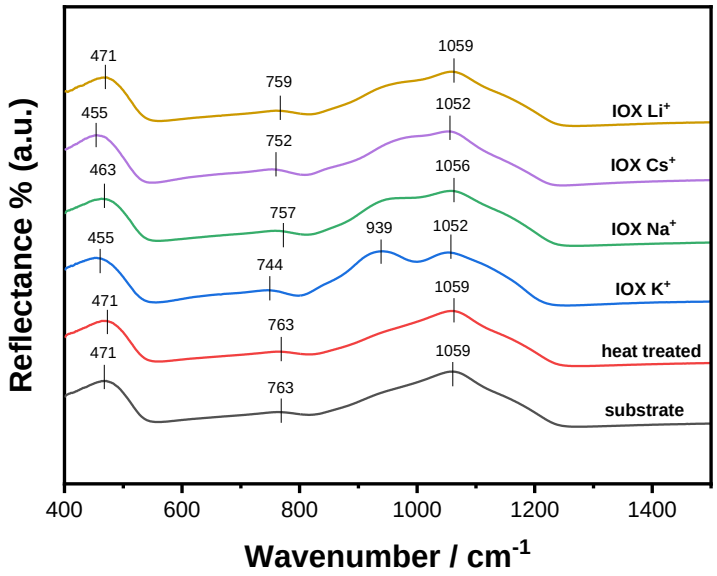

Figure 4. 22: Infrared spectra of İon-exchanged glasses

SEM/EDX results suggest that potassium ion diffusion depth profile is higher than 15-20 µm for samples treated at 480°C for 12 hours using 1:2 KCl: KNO_3 salt mixture.

Raman spectra is also shown structural changes accordingly. Raman Spectra of the Na^+ - K^+ ion – exchanged glasses is shown a shift of the ~1100 cm^{-1} band to higher wavenumbers as the ion-exchange temperature increases.

4.3. Potassium Containing Glasses

XRD of the as melted soda-lime-silica glass which is a typical spectrum proves that no crystallisation occurred (see Figure 4. 23).

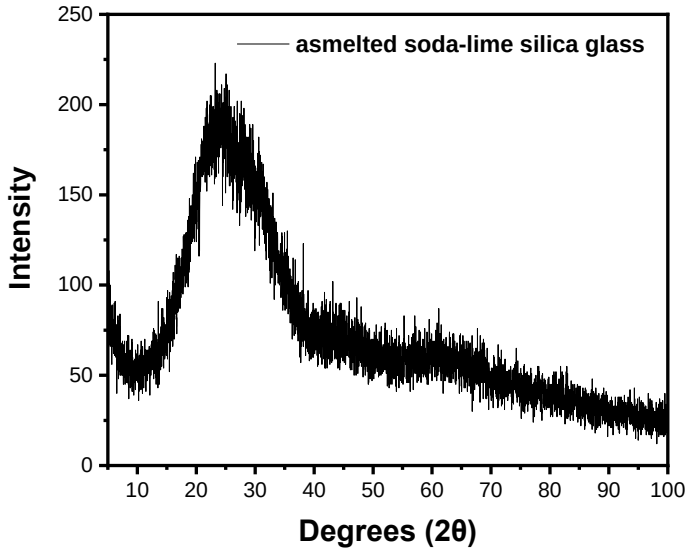

Figure 4. 23: XRD pattern of as melted soda-lime-silica glass

The glass compositions analysed by XRF are given in Table 4. 1. Experimentally, there is no problem with using XRF to confirm the chemical composition of the $72SiO_2 \cdot (13.5– z)$ $Na_2O \cdot zK_2O.10CaO \cdot 3MgO \cdot 1.5Al_2O_3$ (mol %) glass series. However, the presence of Li_2O in the $72SiO_2 \cdot (13.5 – z)Na_2O \cdot zLi_2O.10CaO \cdot 3MgO \cdot 1.5Al_2O_3$ (mol %) glasses lead to significant uncertainties as XRF is not capable of detecting elements lighter than boron. So, only the chemical composition of the potassium glass series is given in Table 4. 1.

Glass code	SiO_2	Na_2O	K_2O	CaO	MgO	Al_2O_3	SO_3
1	72.95 (72)	**14.18 (13.5)**	**0 (0)**	9.24 (10)	2.20 (3)	1.42 (1.5)	0 (0)
2	73.08 (72)	**11.59 (10.8)**	**2.35 (2.7)**	9.40 (10)	2.10 (3)	1.46 (1.5)	0 (0)
3	73.60 (72)	**8.91 (8.1)**	**4.61 (5.4)**	9.11 (10)	2.07 (3)	1.42 (1.5)	0.27 (0)
4	74.64 (72)	**5.57 (5.4)**	**6.98 (8.1)**	8.99 (10)	2.10 (3)	1.46 (1.5)	0.25 (0)
5	74.05 (72)	**3.12 (2.7)**	**9.46 (10.8)**	9.56 (10)	2.12 (3)	1.29 (1.5)	0.23 (0)
6	75.32 (72)	**0.19 (0)**	**11.76 (13.5)**	9.09 (10)	2.12 (3)	1.51 (1.5)	0 (0)

Table 4. 1: Analysed glass compositions (mol %); XRF data normalised to 100 mol%. Batched compositions were $72SiO_2 \cdot (13.5– z) Na_2O \cdot zK_2O.10CaO \cdot 3MgO \cdot 1.5Al_2O_3$ (mol %) where z = 0, 2.7, 5.4, 8.1, 10.8 for the potassium series.

The infrared reflectance spectra of the 5 potassium containing glasses is shown in Figure 4. 24 and show a slight shift of the band at ~1100 cm^{-1} towards lower frequencies which corresponds to the localized vibration of sodium and potassium cations (Hanna and Su, 1964). This suggests the addition of alkali metal ions in the glass leads new vibrational modes which represent Si – O – [alkali] bending and stretching modes (Park and Chen 1980; Agarwal and Tomozawa 1995; Varma et al. 2009). Three reflection bands were observed near 460, 760 and 1060 cm^{-1} for all six glasses.

It is reported that the presence of sodium leads an expansion at low frequency and a division of the Si – O stretching mode into two sections which arises for a particular range of compositions. This division assigned to the vibration of SiO_4 tetrahedra that contain non-bridging oxygens linked to sodium or potassium (Furukawa et al. 1981; McMillan, 1984). The low frequency infrared band at around 460 cm^{-1} which corresponds to stretching modes shows a shift towards to lower wavenumbers with increasing potassium content. The high frequency band at around 1060 cm^{-1} which corresponds bending modes also shifts towards to lower wavenumbers. The size of the shift is shown in more detail in Figure 4. 25 represents a shift to the lower wavenumbers of the 1050 cm^{-1} peak which assigned symmetrical stretching modes of Si-O-Si, bridging oxygens (Calahoo, 2016b).

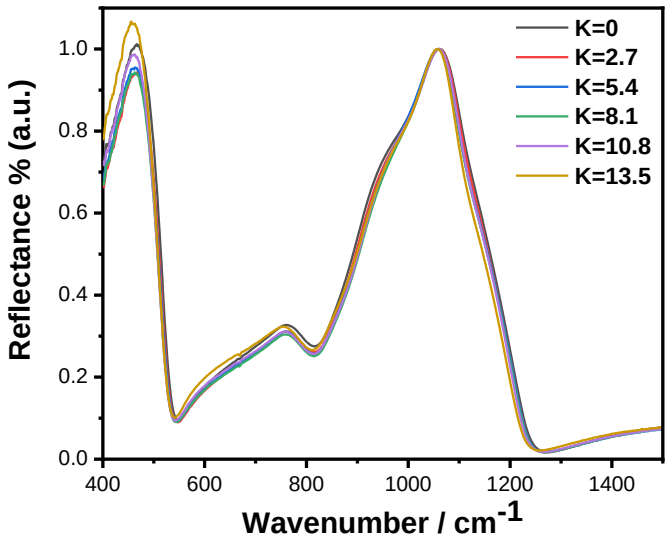

Figure 4. 24: Infrared reflection spectra of the potassium containing glass series

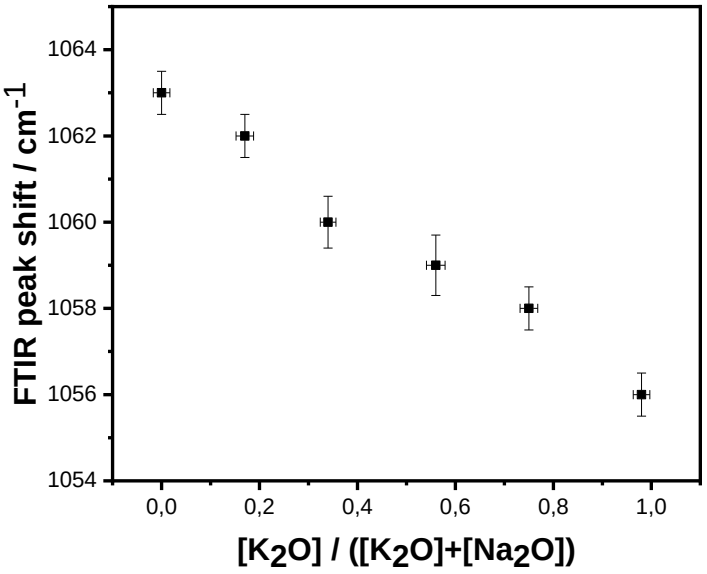

Figure 4. 25: Infrared reflection peak position as a function of relative alkali ratio

Raman spectra collected on the as melted potassia-soda-lime-silica glass surfaces are smoothed and shown in Figure 4. 26. Increasing potassia concentration and reducing soda content resulted in significant changes in the low frequency region of the Raman spectra. For spectra normalised by the height of the band at ~1100 cm^{-1} the relative intensity of the main single low frequency band increased as the potassium / sodium molar ratios increased. Modification in the low frequency band indicates vibrations of the Si-O-Si bridging oxygens in Q^n species gives rise to the band in this region (Tandia et al., 2012). Addition of potassia also results in substantial changes in the high frequency region. In Figure 4. 27 the high-frequency region spectra are smoothed to show the shifts more clearly. In Figure 4. 28 the high-frequency region of the spectra is shown to more clearly indicate how the shifts differ with changing composition. Clearly as the amount of potassium in the bulk glass increases the high-frequency band shifts to higher wavenumbers. This is in agreement with the Raman spectra obtained on the ion-exchanged glasses. Hence both potassium containing soda-lime-silica glasses and potassium containing ion-exchanged glasses exhibit the same type of Raman shifts. In the case of the high-frequency band shifts this consists of a shift to higher wavenumbers which corresponds to a shorter Si-O bond (Fluegel *et al.*, 2008). The average coordination of oxygen around potassium is expected to be larger than the average coordination of oxygen around sodium Fluegel et al. (2008).

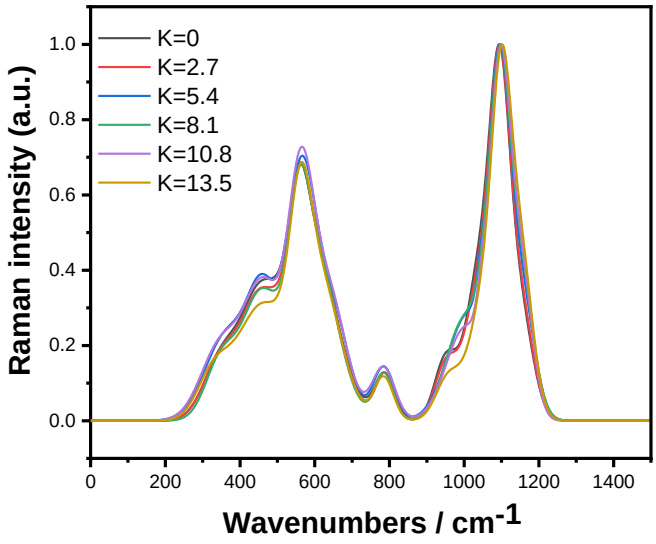

Figure 4. 26: Raman spectra of the potassium containing glass series

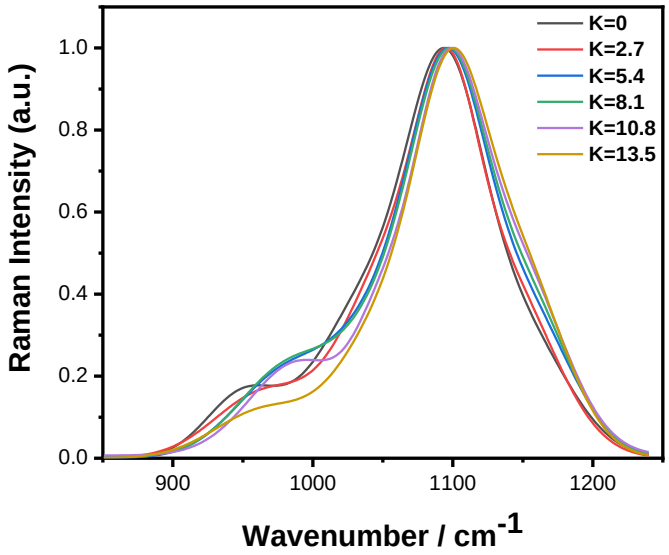

Figure 4. 27 : High Frequency band of Raman spectra of the potassium containing glass series

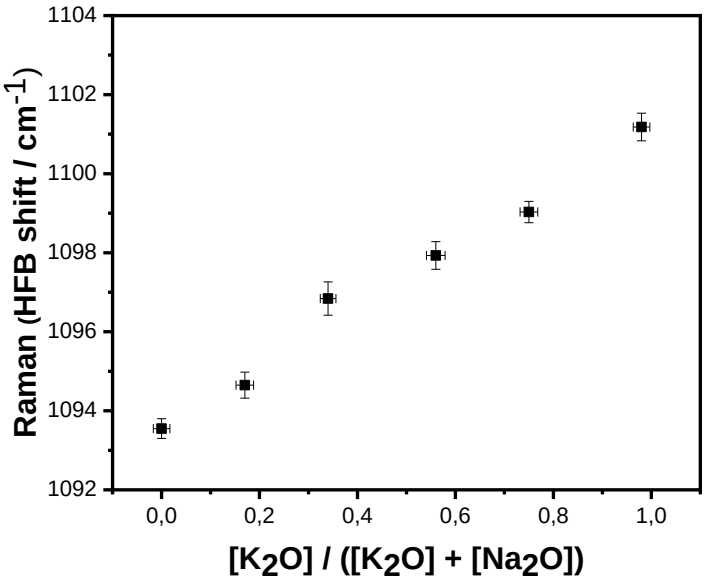

Figure 4. 28: Raman Spectroscopy High-Frequency Band Shift as a function of relative alkali ratio

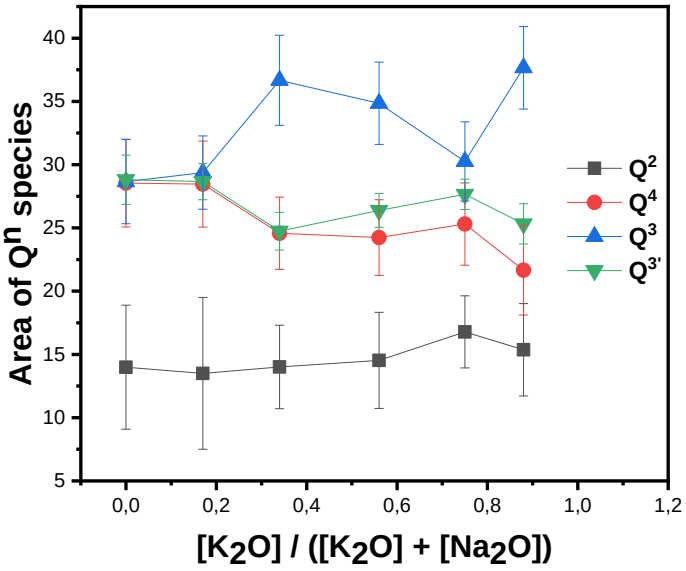

Figure 4. 29: Area of Q^n species of $72SiO_2$· (13.5– z) Na_2O·zK_2O.10CaO·3MgO·1.5Al_2O_3 (mol %) glasses as a function of relative K_2O ratio for the high-frequency peaks which corresponds to Si-O bond lengths

Deconvolution carried out to observe Q^n species for the high-frequency peaks as a function of potassium oxide ratio presented in Figure 4. 29. Based on the literature the fitted peaks are assigned as follows: Q^2 (around 960 cm^{-1}), Q^4 (around 1040 cm^{-1}), Q^3 (around 1080 cm^{-1}) and $Q^{3'}$ (around 1120 cm^{-1}). Despite discrepancies as the amount of K_2O increases in the glass composition the numbers of Q^2 units does not change within the error band, and Q^1 units do

not show big changes. The shifts both slightly increase as the potassium oxide amount increases, which represents a decrease in connectivity.

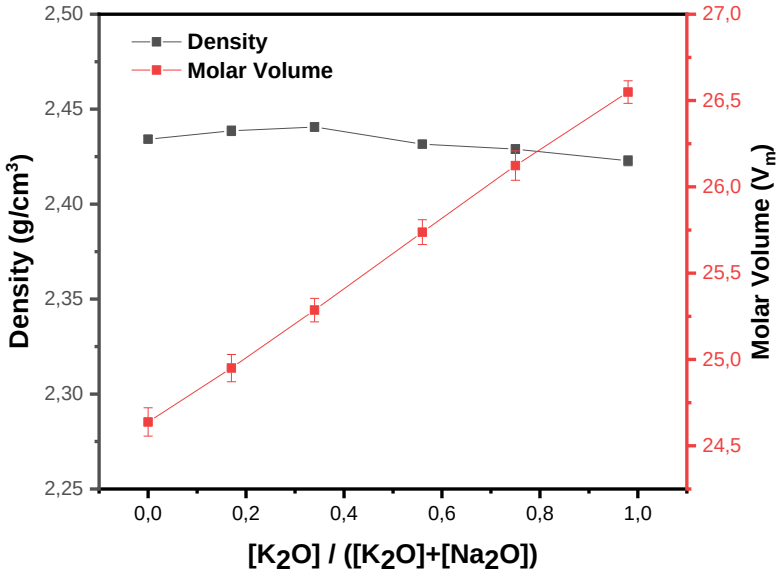

Figure 4. 30: Experimentally obtained density and molar volume plot as a function of relative alkali ratio

Figure 4. 30 presents the experimentally obtained density versus molar volume data as a function of the amount of potassium oxide in the glass composition. A similar plot is shown in Figure 4. 31 where the density is calculated using a model proposed by Fluegel Charles (1966). Despite the inconsistency at the lowest soda content between the experimentally measured density and the density obtained from the Tandia et al., (2012) the molar volume data agree with molar volume increasing with increasing potassium content. Whereas the density decreases with the increase the amount of potassium oxide in the glass. Tandia et al., (2012 reported that in binary alkali-silicate glasses the replacement of SiO_2 by K_2O increased molar volume of the glass whereas replacement of SiO_2 by Na_2O decreases the molar volume. Compositional dependence of molar volume of as melted glasses and ion-exchanged glasses in the $xNa_2O.(20\text{-}x)K_2O.80SiO_2$ (mol%) system is reported by (Fluegel *et al.*, 2008). (Sehgal and Ito, 1998, 1999; Kingston and Hand, 2000a; Dériano *et al.*, 2004; Hand and Tadjiev, 2010; Kilinc and Hand, 2015)) suggested that the molar volume of as melted glasses decreases as the Na_2O increases in the glass composition. Also, the molar volume of the ion-exchanged glasses is reported to be dependent on the initial glass composition and the molar volume value is less

than as-melted potassium glass due to the LNDC. (see 2.4.1.4.1 Stress Generation by Ion Exchange)

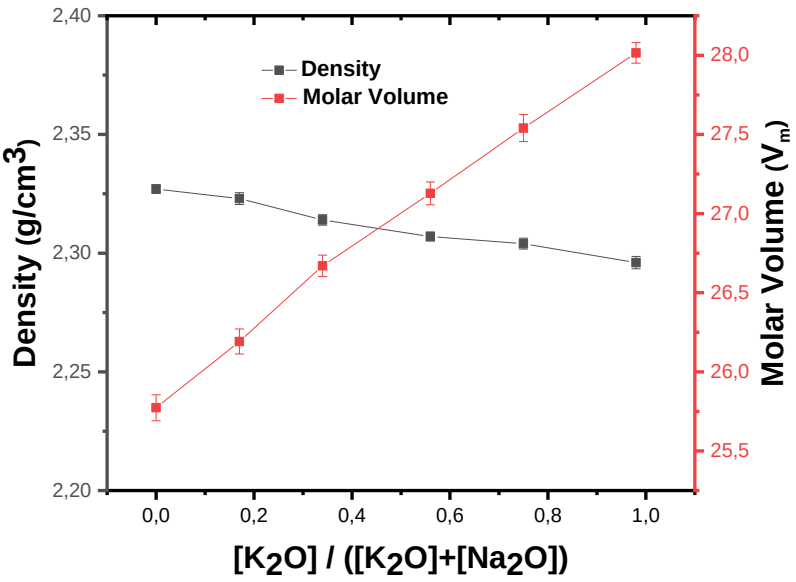

Figure 4. 31: density and molar volume plot as a function of relative alkali ratio obtained from the model by Kingston and Hand (2000)

Figure 4. 32 represents the Vickers hardness and the indentation fracture toughness of the potassium glass series as a function of relative K_2O ratio. Both the Vickers hardness and the fracture toughness values are in the same trend according to relative potassium oxide ratio. The Vickers hardness and fracture toughness values reduce with increasing potassium content. However, within error there is a little actual variation apart from the middle datapoint indentation fracture tends to go up with increasing K_2O.

Variation of mechanical properties of soda-lime-silica glasses with composition are reported by several authors Sehgal and Ito (1998). (Lakin, 1991) reported mixed alkali effect on the strength and fracture toughness of soda-potassia-silicate glasses. They found the strength of the of soda-potassia-silicate glasses is higher than the more complex soda–potassia–calcia–glasses. (Ray, 1974) proposed a less brittle soda-lime-silica glasses based on a replacement of some of the soda with potassia, some of the calcium with magnesia and some of the silica with alumina. They reported the substitution of potash for soda and magnesia for calcium effected on the decrease in brittleness, because potash containing glasses have a larger molar

volume than the glasses with soda (Fluegel *et al.*, 2008) suggests a decrease of brittleness due to a higher molar volume motivates the deformation.

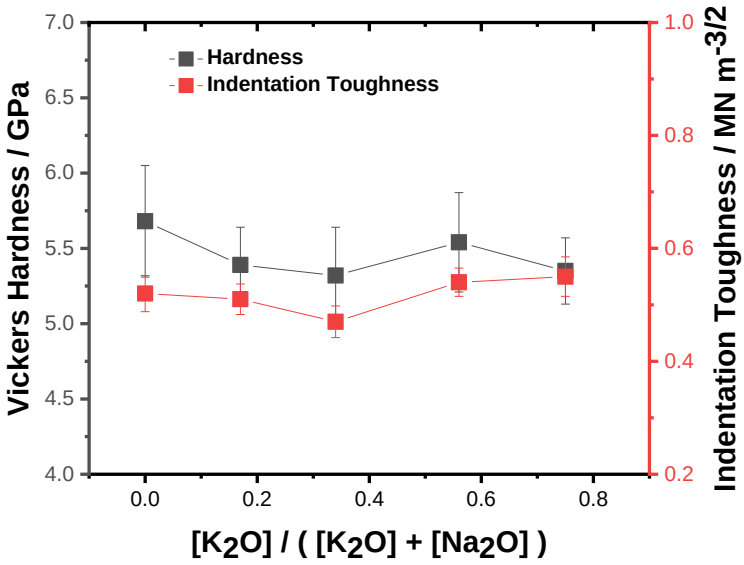

Figure 4. 32: Vickers hardness (HV) and fracture toughness (K_{IC}) of the series as a function of relative alkali ratio

Figure 4. 33 represents Reduced Modulus and the hardness of the potassium glass series, which obtained on Nanoindentation, as a function of relative K_2O ratio. Both Reduced Modulus and hardness are in same trend according to potassium oxide ratio. The hardness and Reduced Modulus values reduce with increasing potassium content, except the composition $72SiO_2{\cdot}5.4Na_2O{\cdot}8.1K_2O.10CaO{\cdot}3MgO{\cdot}1.5Al_2O_3$ (mol %).

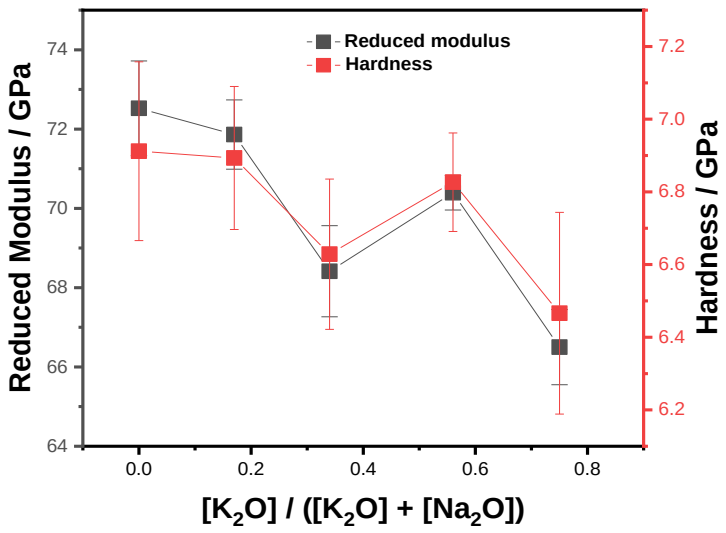

Figure 4. 33: Experimentally obtained Reduced Modulus and Hardness plot of as melted soda-lime-silica glass the series as a function of relative alkali ratio

The relationship between fracture toughness measured by the SCF method with increasing of relative potassium oxide ratio is shown in Figure 4. 34. The fracture toughness increases with increasing potassium content in the glass composition. Due to the considerable bubble content of the highest potassia containing glass, the fracture toughness measurement could not run. Melting for longer hours may help to reduce the bubbles.

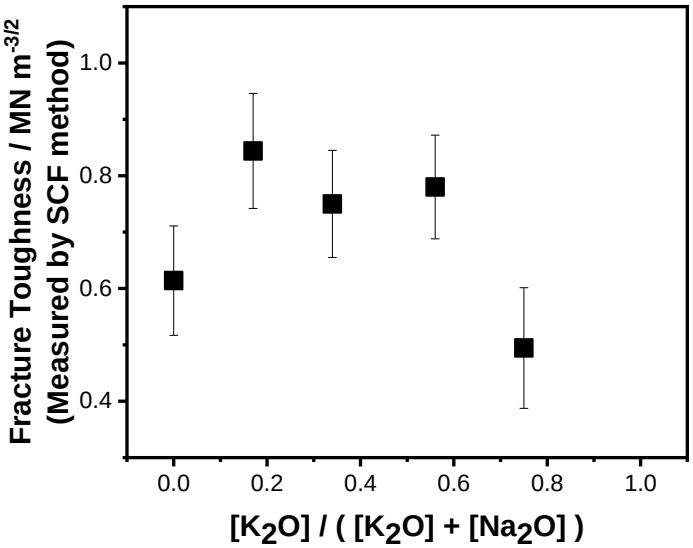

Figure 4. 34: Fracture toughness (K_{IC}) of the series as a function of relative alkali ratio

Young's Modulus of soda-lime-silica glasses decreases with increasing potassium content as seen in Figure 4. 35. Large cations such as potassium expand the network, however larger ions form comparatively weaker bonds which lower the modulus. Small cations such as aluminium and magnesium increase the packing density and therefore increase the modulus (Ray, 1974).

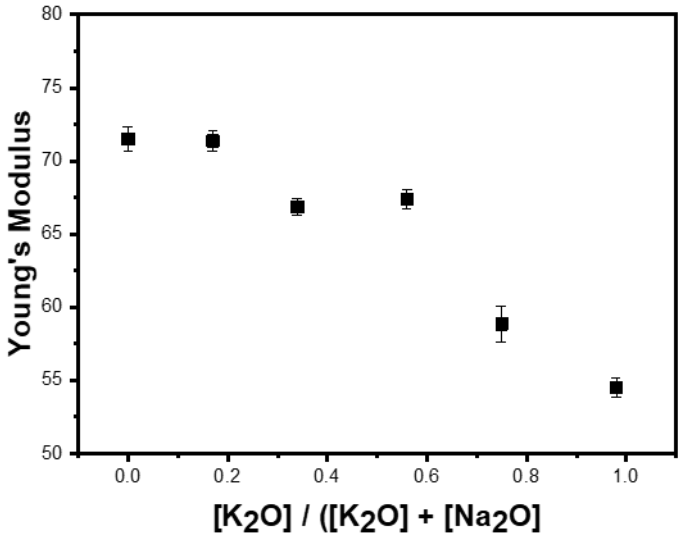

Figure 4. 35: Young's Modulus of the series as a function of relative alkali ratio

Whereas, Bulk Modulus of soda-lime-silica glasses decreases with increasing potassium content as seen in Figure 4. 36.

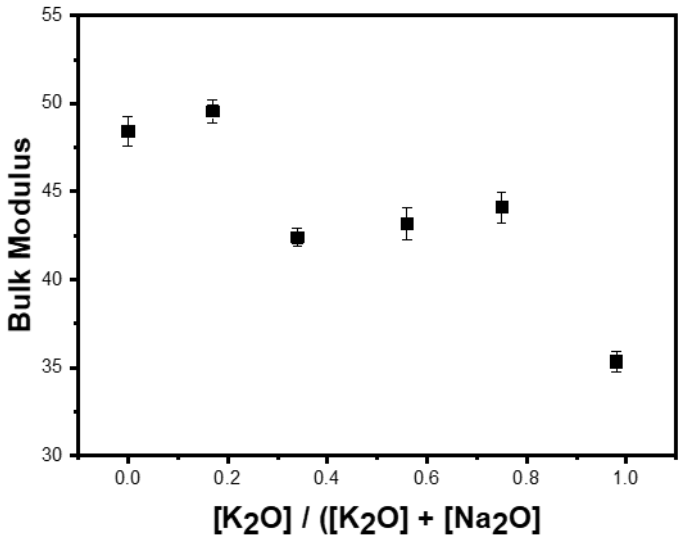

Figure 4. 36: Bulk Modulus of the series as a function of relative alkali ratio

Shear Modulus also decreases with increasing potassium content for soda-lime-silica glass series as seen in Figure 4. 37.

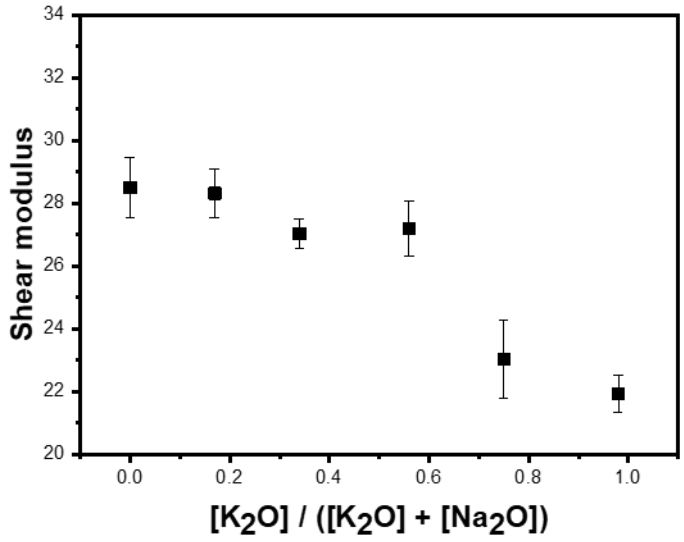

Figure 4. 37: Shear Modulus of the series as a function of relative alkali ratio

4.4. Lithium-Containing Glasses

Structural property assessments of lithium containing series were also conducted. Figure 4. 38 presents the full infrared reflection spectra of lithium-soda-lime-silica glasses. The spectra clearly show difference between different amounts of lithium containing glasses. Three reflection bands were observed near 460, 760 and 1060 cm^{-1} for all five series of glasses.

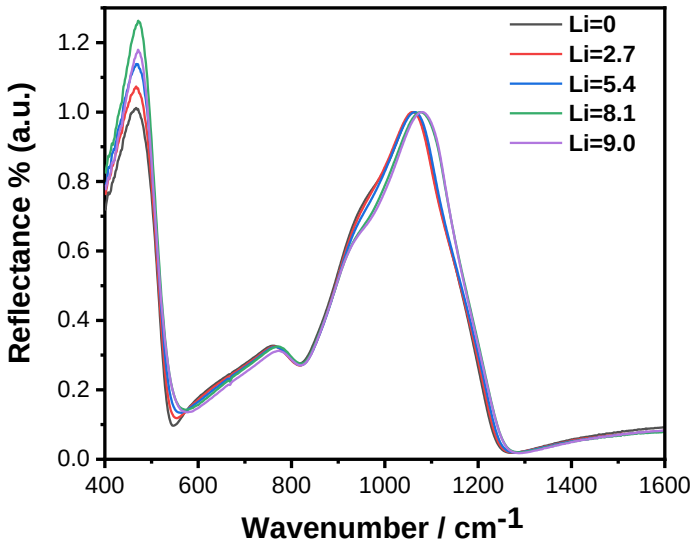

Figure 4. 38: Infrared reflection spectra of the lithium-containing glass series

The structural peak position is at around 1050 cm^{-1} which is assigned to symmetrical stretching modes of Si-O-Si, bridging oxygens shifts to the higher wavenumbers. For clarification the reflection peak shift as a function of relative alkali content plotted according to Na_2O which is shown Figure 4. 39. As the amount of sodium oxide increases in the glass composition the structural peak shifts to the lower wavenumbers. This structural band shift on symmetrical stretching modes of Si-O-Si shows similar trend as melted potassium containing glass series. As the size of the relatively larger sized alkali ion amount increases in the glass symmetrical stretching modes of Si-O-Si, shifts to lower wavenumbers.

Low frequency infrared band at around 460 cm^{-1} which corresponds stretching shows a shift towards to lower wavenumbers with increasing potassium content. The high frequency band at around 1060 cm^{-1} which corresponds to bending modes also shifts towards lower wavenumbers.

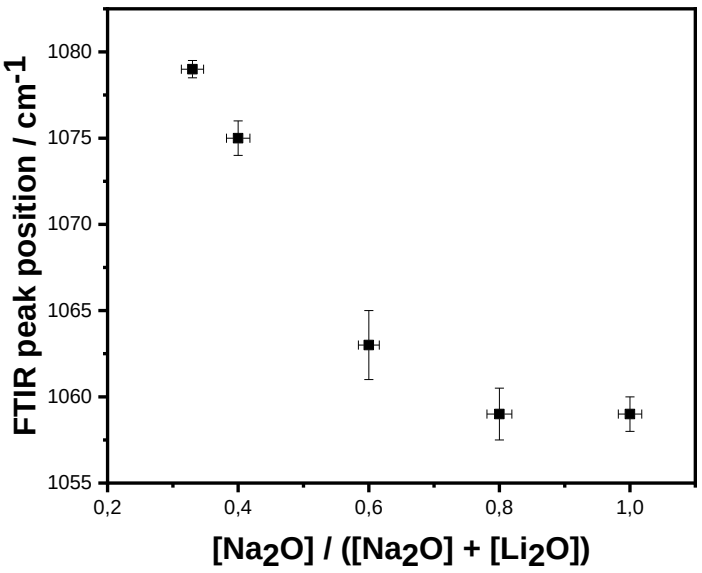

Figure 4. 39: Infrared reflection peak position as a function of relative alkali ratio

The Raman intensity spectra of lithium containing glass series are presented in Figure 4. 40. As the amount of lithium in the bulk glass increases the high-frequency band shifts to lower wavenumbers. The high frequency band shift is presented as a function of $[Na_2O]/([Na_2O] + [Li_2O])$ ratio in Figure 4. 41 to make it comparable to the data shown previously for the potassium containing glasses. As the amount of relatively larger ions increases in the bulk glass, the high frequency band shift to the higher wavenumbers.

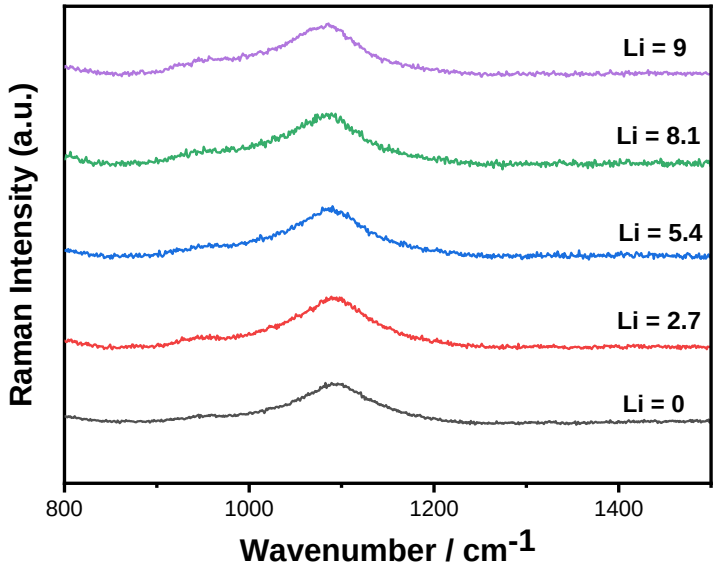

Figure 4. 40: Raman Intensity spectra of the lithium-containing glass series

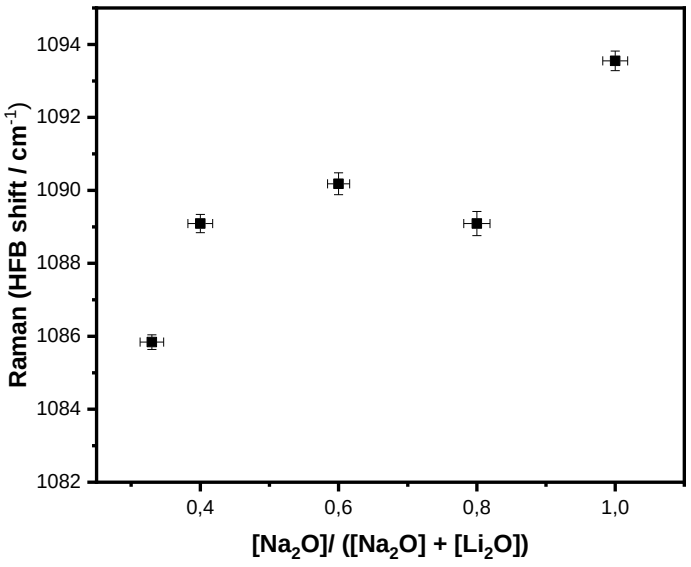

Figure 4. 41: Raman Spectroscopy High-Frequency Band Shift as a function of relative alkali ratio

The molar volume of the all potassium and lithium series of glasses presented in Figure 4. 42. As the amount of the larger size relative alkali ion increase in the bulk glass the molar volume increases. Due to the limitations of the XRF method the lithia series are based on batched compositions whereas the potassia series were based on measured compositions.

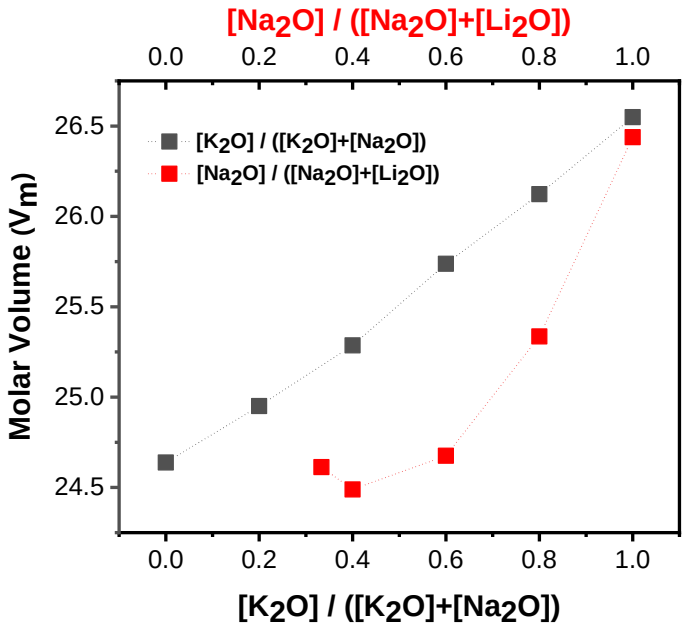

Figure 4. 42: molar volume of the series as a function of relative alkali ratio

The experimentally obtained density versus molar volume data as a function of the amount of sodium oxide in the glass composition is presented in Figure 4. 43. A similar plot is shown in Figure 4. 44 where the density is calculated using a model proposed by Fluegel (Kreski et al., 2012; Tandia et al., 2012). The data which was experimentally obtained and the data processed according to the model are not in agreement since the trend as such density and molar volume increase with increasing relative alkali ratio (Na). This could be related to mixed-alkali effect.

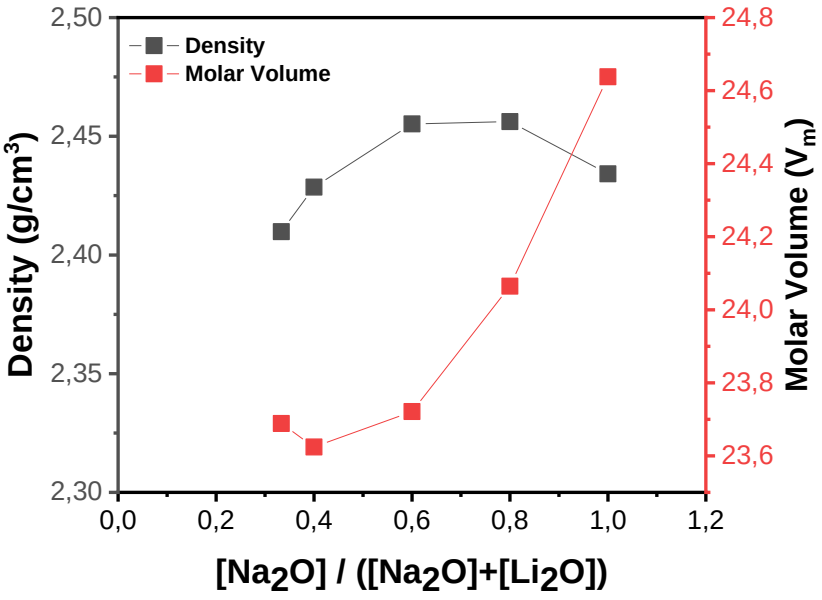

Figure 4. 43: experimentally obtained density and molar volume plot as a function of relative alkali ratio

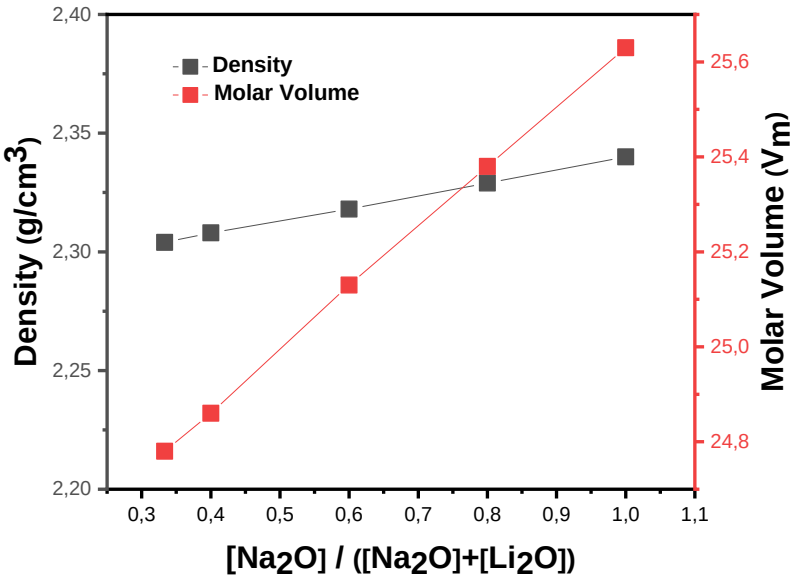

Figure 4. 44: density and molar volume plot as a function of relative alkali ratio obtained from the model

Figure 4. 45 represents the Vickers hardness and indentation fracture toughness of the lithium glass series as a function of relative Na_2O ratio. Both the Vickers hardness and the indentation fracture toughness values are in the same trend except the lowest lithia contents according to relative sodium oxide ratio. The Vickers hardness and fracture toughness values reduce with increasing sodium content.

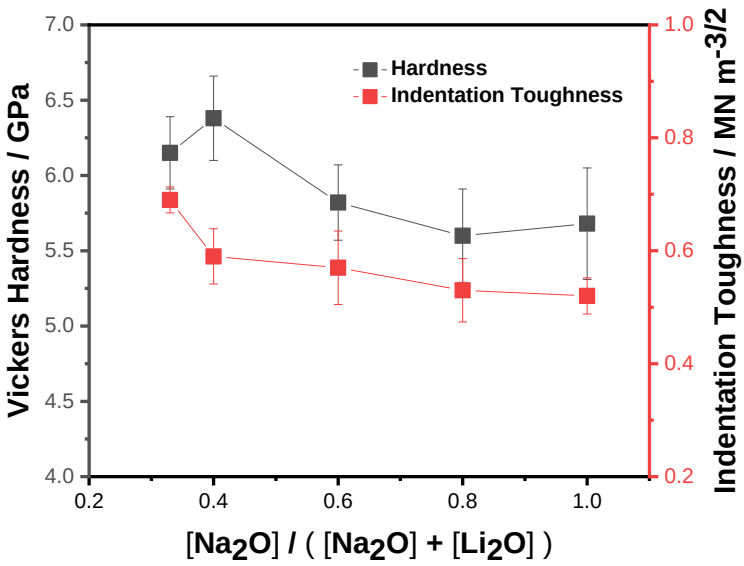

Figure 4. 45: Vickers hardness (HV) and indentation fracture toughness (K_{Ic}) of the series as a function of relative alkali ratio

Indentation fracture toughness of as melted lithium glass series is presented in Figure 4. 46, with increasing sodium content indentation fracture toughness decreases, accordingly.

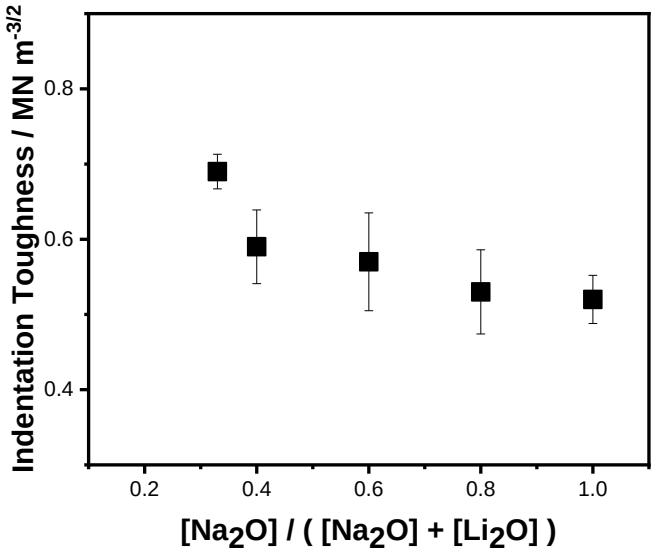

Figure 4. 46: Indentation fracture toughness (K_{IC}) of the series as a function of relative alkali ratio

The relationship between fracture toughness with an increase of relative sodium oxide ratio is shown in Figure 4. 47. The trend shows that fracture toughness decreases with increasing sodium content. The correlation between indentation fracture toughness and SCF fracture toughness is actually quite reasonable for these glasses.

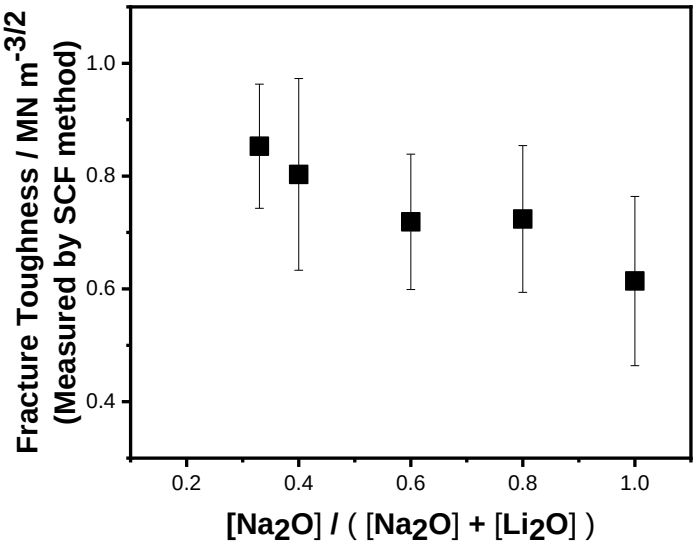

Figure 4. 47: fracture toughness (K_{IC}) of the series as a function of relative alkali ratio

Figure 4. 48 presents the Vickers hardness plotted as a function of relative sodium oxide ratio.

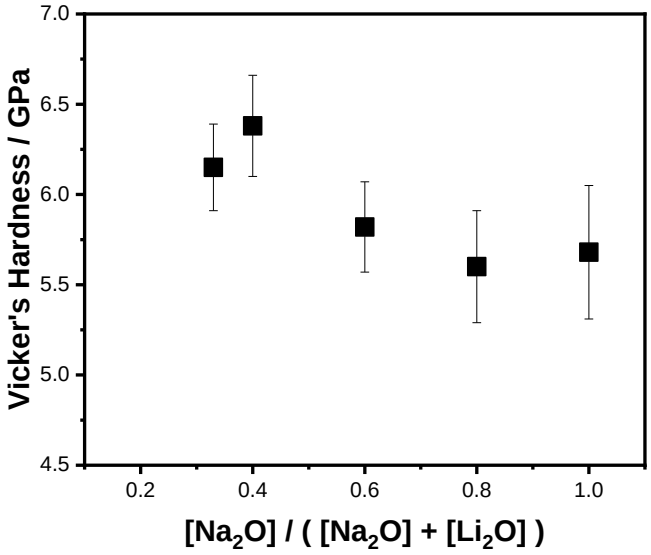

Figure 4. 48: Vicker's Indentation Hardness of the series as a function of relative alkali ratio

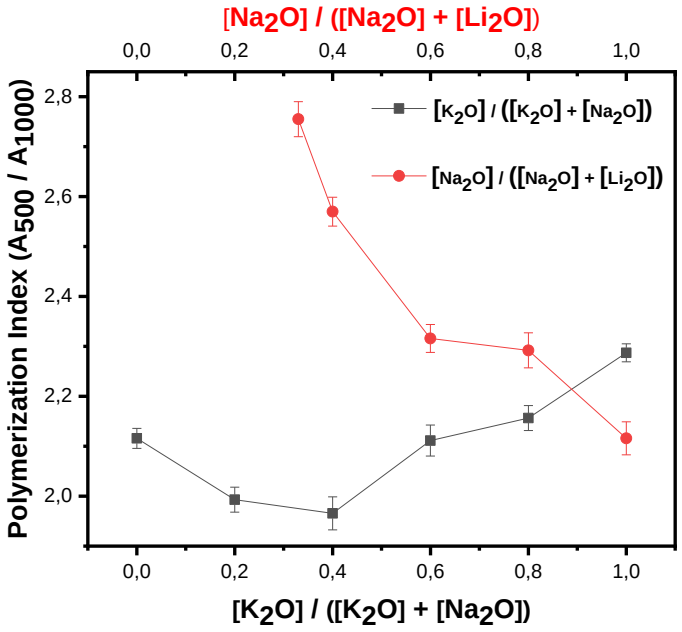

Figure 4. 49: Raman Polymerization Index of the series as a function of relative alkali ratio

Raman analysis of the microstructure of the glass series pointed out that Raman polymerization index decreases and then increases with increasing potassia content in the soda-potassia series and decreases with increasing soda content in the soda-lithia series as seen in Figure 4. 49.

Young's Modulus of the lithium glass series decreases with increasing sodium content as seen in Figure 4. 50. As mentioned previously in part 4.3 large cations such as potassium expand the network however, larger ions yield comparatively weaker bonds which lowers the modulus (Quaranta *et al.*, 2012; Stavrou *et al.*, 2014a). Therefore, as the amount of lithium increases in the bulk glass the modulus tends to increase.

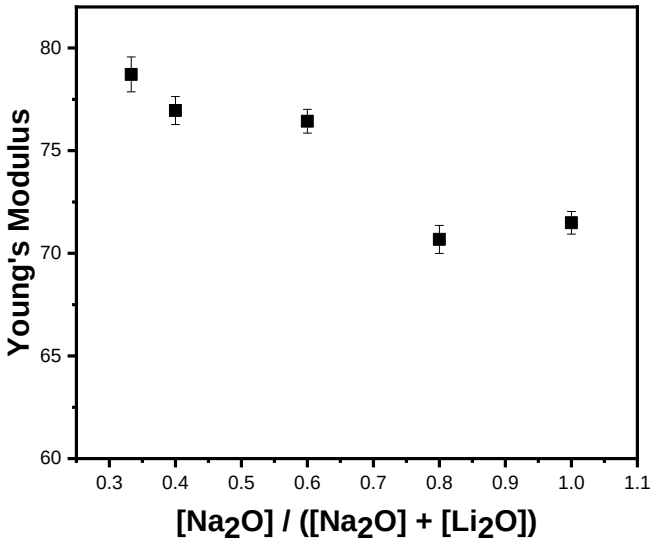

Figure 4. 50: Young's Modulus of the series as a function of relative alkali ratio

The bulk moduli of the lithium series glasses are presented in Figure 4. 51. As with the Young's modulus the bulk modulus tends to decrease with increasing soda content.

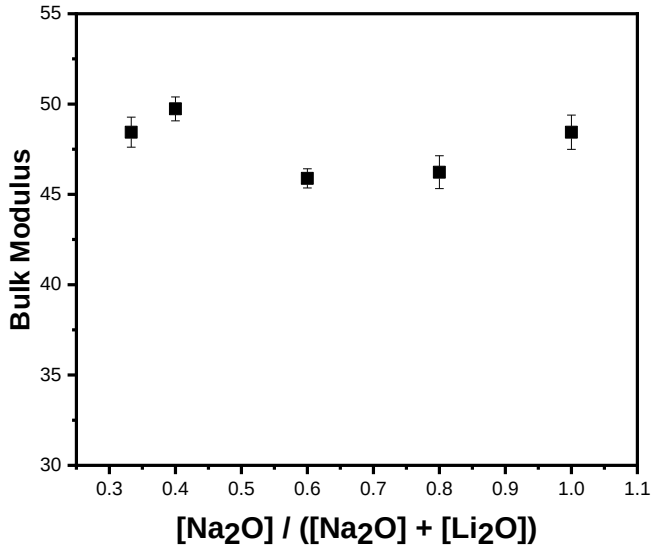

Figure 4. 51: Bulk Modulus of the series as a function of relative alkali ratio

Figure 4. 52 presents Shear Modulus of lithium glass also decreases with increasing sodium content.

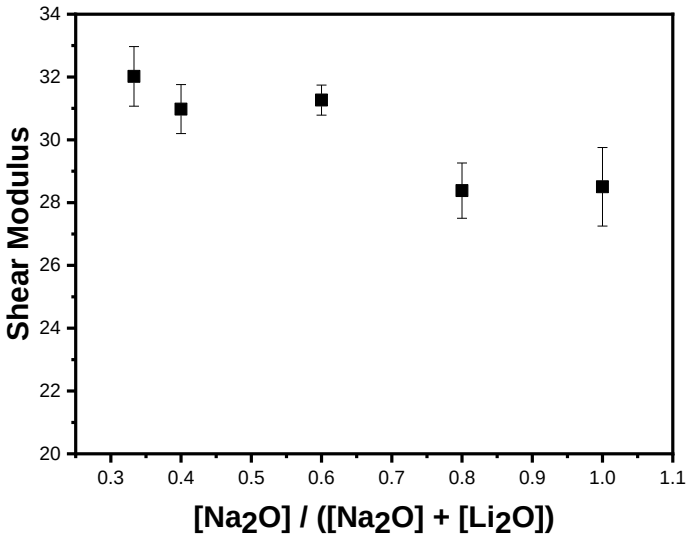

Figure 4. 52: Shear Modulus of the series as a function of relative alkali ratio

4.5. Structural Comparison of ion-exchanged and non-ion exchanged glasses

Some computational studies have suggested the glass network connectivity of ion-exchanged glasses and as-melted bulk glasses are similar. (Park and Chen, 1980; Agarwal and Tomozawa, 1995; Varma et al., 2009), whereas others have observed by Raman spectroscopy that the topological structure of the glass is modified by the ion-exchange process Ragoen et al. (2018). According to the Raman and FTIR data collected during the current study similar features have been observed in both ion exchange glasses and the as-melted glasses. The Raman Spectroscopy and FTIR reflectance spectra also suggest that Q^n network changes based on ion-exchange temperature and time. In the current study, investigations are done to see if there is any significant relationship between the chemical structure of the ion-exchanged surface and the chemical structure of potassium-containing glasses. As the FTIR Reflectance spectra of both potassium ion-exchanged and potassium-containing as melted glasses suggests, a shift to lower wavenumbers of the 1050 cm^{-1} peak observed which can be explained by the change in symmetric stretching modes of Si – O – Si, bridging oxygens (Sundberg *et al.*, 2019). This change could be due to the coordination differences between Si – O – K bonding and Si – O – Na bonding. Due to the ionic size of the potassium ion being bigger than the sodium ion, after ion-exchange potassium ions squeeze into sodium ion sites which causes compressive stress. As the FTIR Reflectance analysis suggests the observed features ~950cm^{-1} could be a direct consequence of ion exchange. As shown in Figure 4. 4 after reannealing of the ion-exchanged glass specimens same features still remains which cannot

be simply due to bigger ions being squeezed into a site previously occupied by smaller ions. (Jannotti *et al.*, 2012) reported an increase in the bond distance of K – O in the ion-exchanged glasses. Even though some stress relaxation occurs, the K^+ environment in the ion-exchanged glass claimed not to be the same in as-melted Na, K – silica glasses because K^+ ions occupy smaller sites which is not possible to achieve by melting glass with the same amount of potassium.

Difference from Raman spectra for the potassium series glasses are replotted by difference is shown in Figure 4. 53. Changes are observed both in the low frequency region and the high frequency region. Also, as the amount of potassium increases in the glass the difference increases, especially in high frequency region. Changes in the both FTIR and Raman spectra with composition and with the ion exchange are showing similar trends.

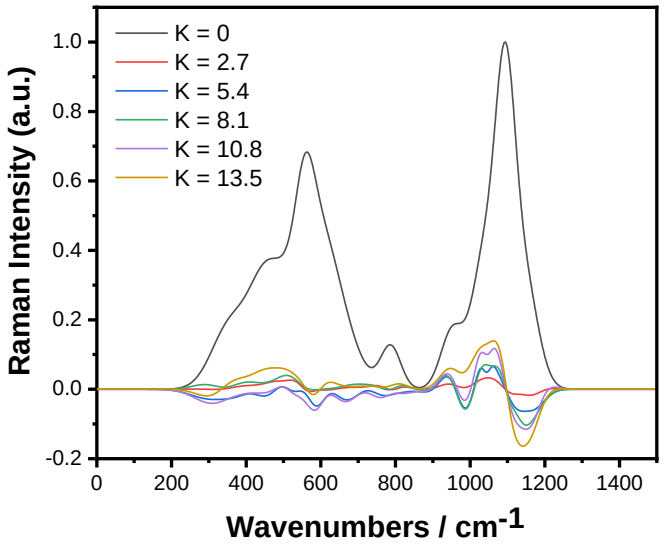

Figure 4. 53: Raman Intensity (soda lime silica glass – potassium series of glasses)

Raman intensity spectra of potassium ion-exchanged glasses in different times is also replotted by difference to the reference substrate is shown in Figure 4. 54. Changes observed both in low frequency region and high frequency region. As the duration of ion-exchange process increases the difference increases the most especially in high frequency region.

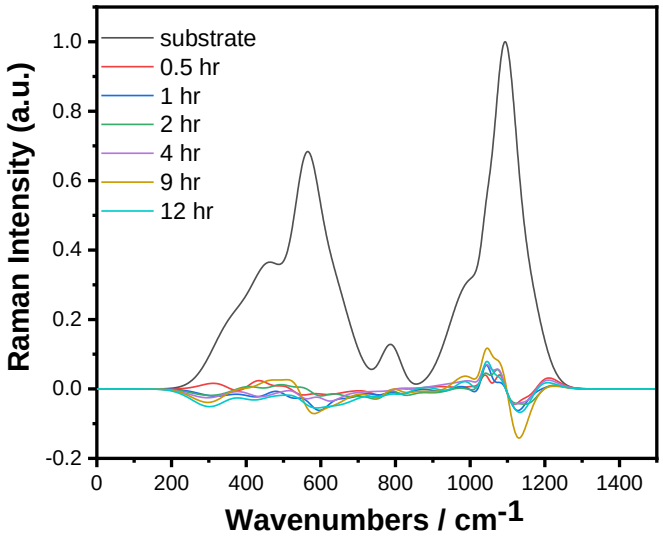

Figure 4. 54: Raman Intensity (substrate – ion exchanged glasses by different times)

FTIR Reflectance spectra of potassium glass series is replotted by difference to the reference soda-lime silica glass(K=0) and is shown in Figure 4. 55. More changes are observed as the amount of potassium increases in the glass.

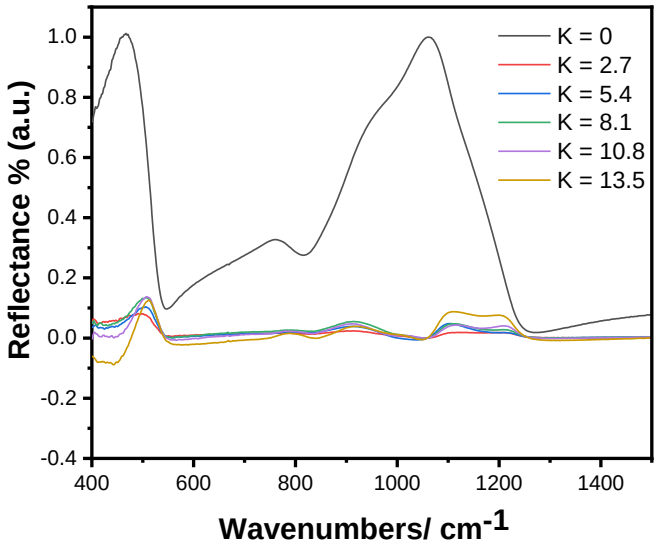

Figure 4. 55: FTIR reflectance spectra (soda lime silica glass – potassium series of glasses)

FTIR Reflectance spectra of potassium ion-exchanged glasses at different times is also replotted by difference to the reference substrate is shown in Figure 4. 56. More changes are observed as the duration of the ion-exchange process increases.

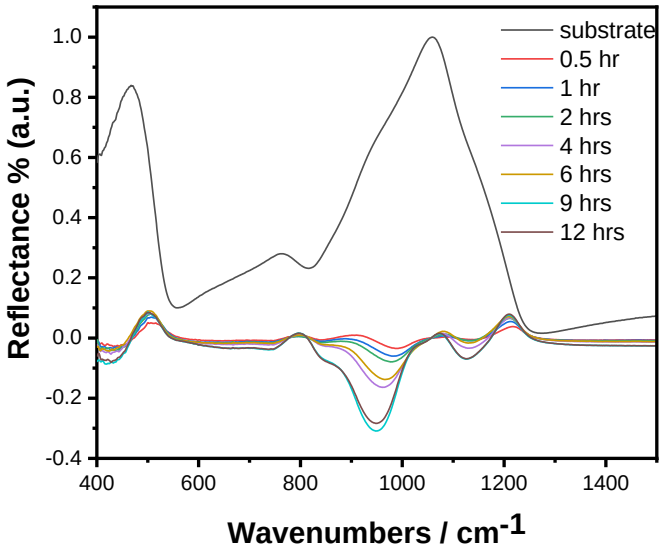

Figure 4. 56: FTIR reflectance spectra (substrate – ion exchanged glasses by different times)

Following figures; Figure 4. 56, Figure 4. 57, Figure 4. 58, Figure 4. 59, Figure 4. 60, Figure 4. 61, Figure 4. 62, Figure 4. 63, Figure 4. 64 have been plotted to show similar features observed on the laboratory-made glasses which was treated by ion-exchange. On the Reflectance spectra, all the structural shifts and the new feature near 950 cm^{-1} observed after ion exchange are also observed on ion-exchanged laboratory-made glasses. Raman spectra also suggest that the same shift to the higher wavenumbers occurs in ion-exchanged laboratory-made glasses.

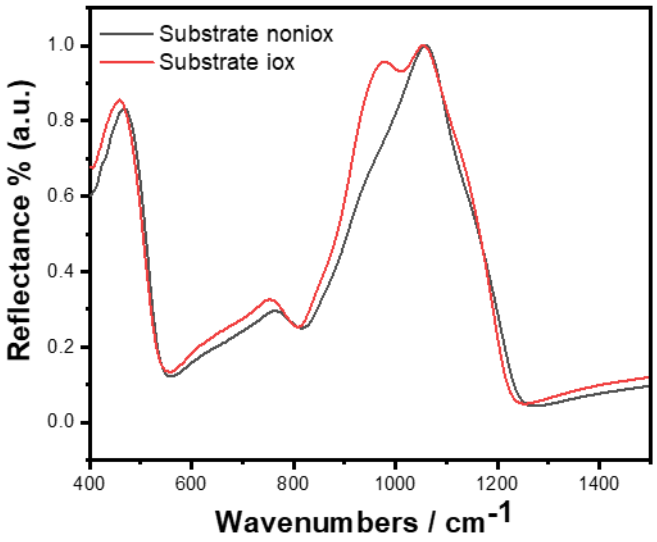

Figure 4. 57: FTIR Reflectance Spectra of substrate and potassium ion-exchanged substrate

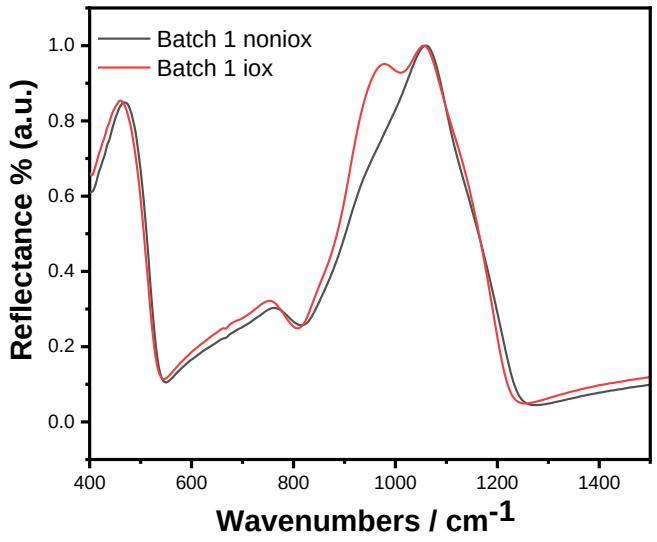

Figure 4. 58: FTIR Reflectance Spectra of batch $72SiO_2 \cdot 13.5Na_2O.10CaO \cdot 3MgO \cdot 1.5Al_2O_3$ (mol %) and potassium ion exchanged batch $72SiO_2 \cdot 13.5Na_2O.10CaO \cdot 3MgO \cdot 1.5Al_2O_3$ (mol %)

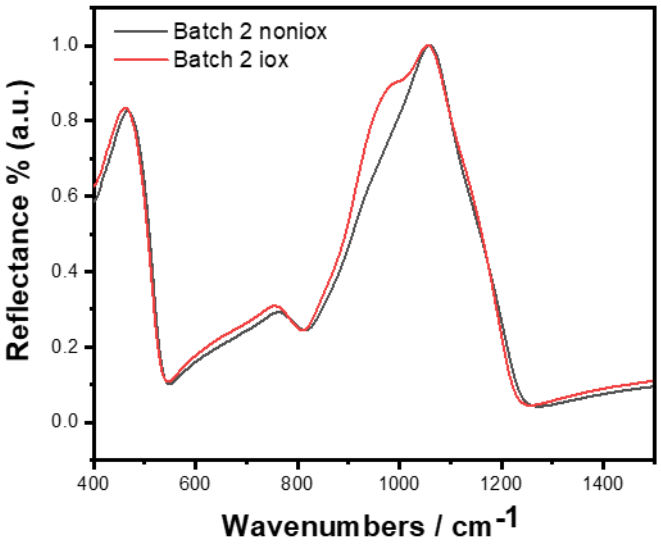

Figure 4. 59: Infrared Reflectance Spectra of batch $72SiO_2$· 10.8 Na_2O·2.7K_2O.10CaO·3MgO·1.5Al_2O_3 (mol %) and potassium ion-exchanged batch $72SiO_2$· 10.8 Na_2O·2.7K_2O.10CaO·3MgO·1.5Al_2O_3 (mol %)

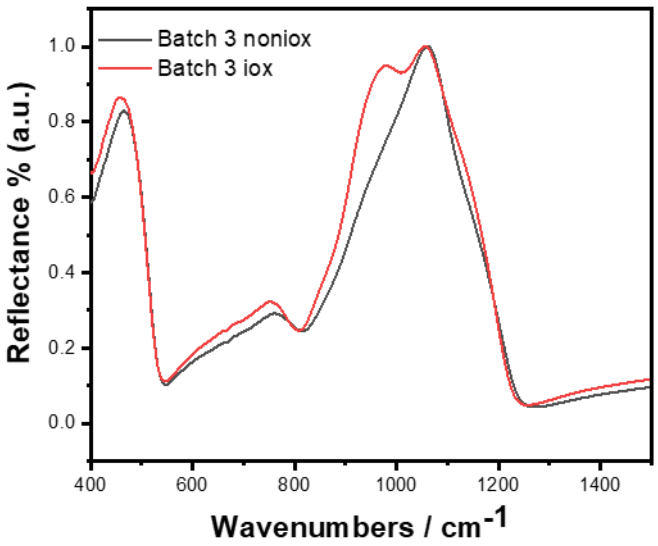

Figure 4. 60: Infrared Reflectance Spectra of batch$72SiO_2$· 8.1Na_2O·5.4K_2O.10CaO·3MgO·1.5Al_2O_3 (mol %) and potassium ion-exchanged batch $72SiO_2$· 8.1 Na_2O.5.4K_2O.10CaO·3MgO·1.5Al_2O_3 (mol %)

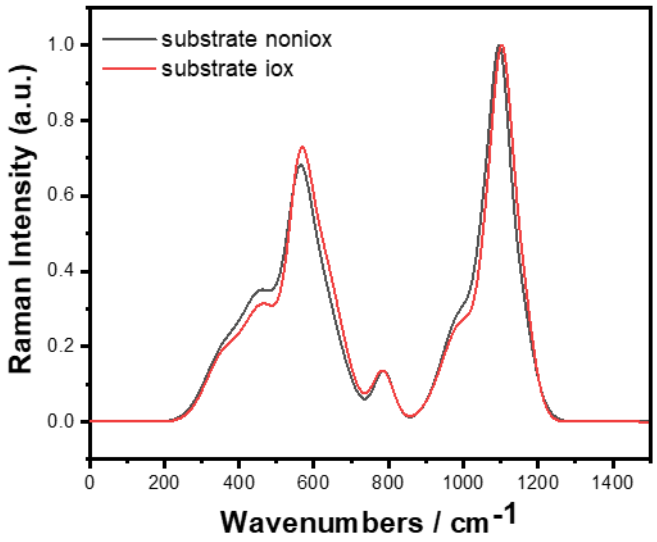

Figure 4. 61: Raman Intensity of substrate and potassium ion-exchanged substrate

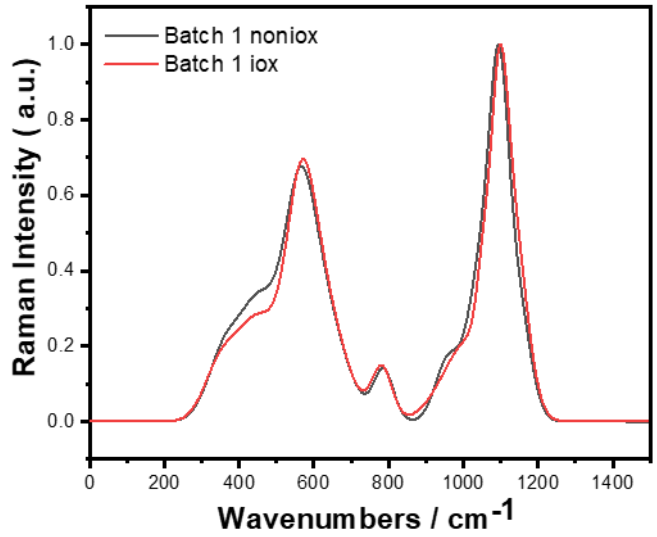

Figure 4. 62: Raman Intensity of batch $72SiO_2 \cdot 13.5Na_2O.10CaO \cdot 3MgO \cdot 1.5Al_2O_3$ (mol %) and potassium ion-exchanged batch $72SiO_2 \cdot 13.5Na_2O.10CaO \cdot 3MgO \cdot 1.5Al_2O_3$ (mol %)

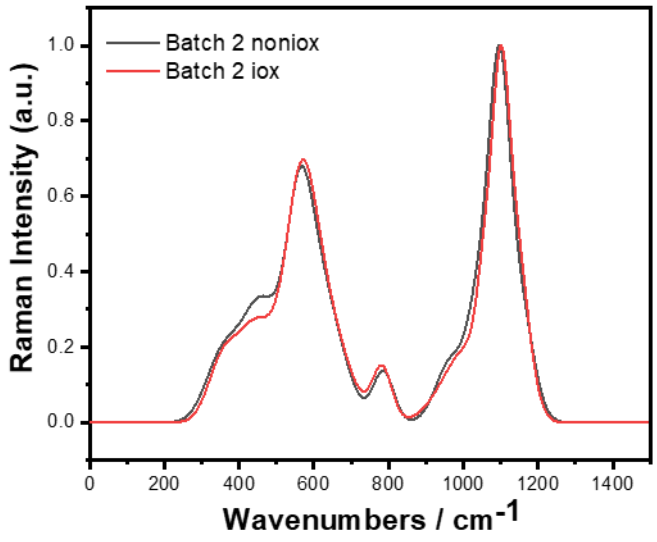

Figure 4. 63: Raman intensity of batch 72SiO_2· 10.8 Na_2O·2.7K_2O.10CaO·3MgO·1.5Al_2O_3 (mol %) and potassium ion exchanged batch 72SiO_2· 10.8 Na_2O·2.7K_2O.10CaO·3MgO·1.5Al_2O_3 (mol %)

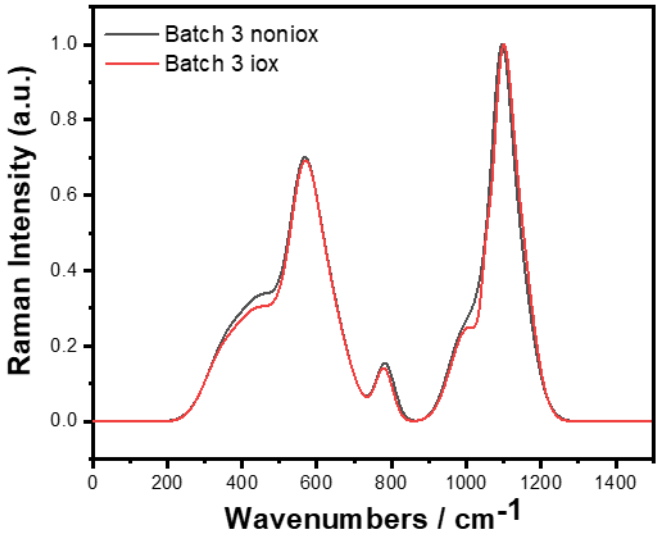

Figure 4. 64: Raman Intensity of batch 72SiO_2· 8.1Na_2O·5.4K_2O.10CaO·3MgO·1.5Al_2O_3 (mol %) and potassium ion exchanged batch 72SiO_2· 8.1 Na_2O.5.4K_2O.10CaO·3MgO·1.5Al_2O_3 (mol %)

4.6. Mechanical Property Comparison of ion-exchanged and non-ion exchanged glasses

As shown in the literature survey mechanical properties especially strength varies according to the surface properties of glasses and the statistical distribution of flaws on the glass (Garza-Méndez et al., 2007; Guldiren et al., 2016). Figure 4. 65 shows the percentage of crack initiation probability of untreated soda lime silica glass and for exchanged soda lime silica glass (K^+ replacing Na^+). The crack resistance of untreated soda lime silica glass is 1.7 whereas the ion

exchange glass has a crack growth resistance of 2.6 which means approximately a 53 % increase.

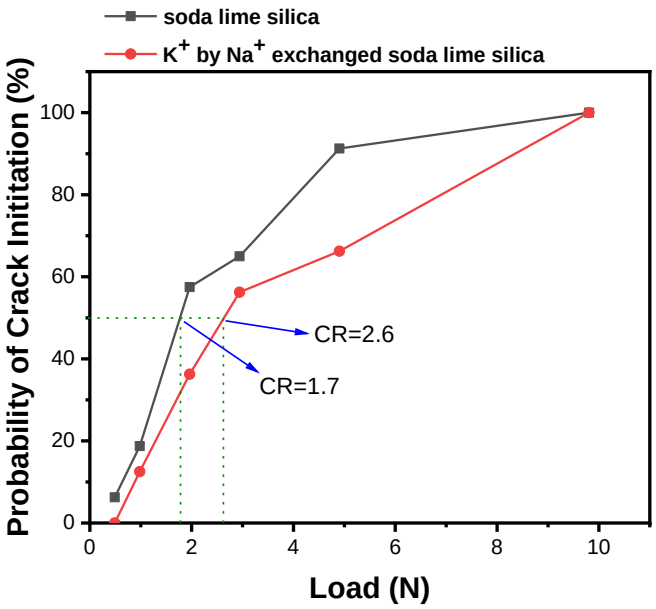

Figure 4. 65: Probability of crack initiation versus Indentation Load of non-ion-exchanged and ion-exchanged soda-lime-silica glasses

Ion exchange strengthening provides an increase in surface hardness and crack resistance. For the untreated glass specimen, lateral and radial cracking was observed to initiate at lower loads, and as the load increases cracks become increasingly more severe. At small indentation, loads crack initiation is remarkably low for ion-exchanged glasses. When the applied load increased step-by-step crack initiation was observed on ion-exchanged glasses but the length of the cracks was certainly smaller than the ones on the non-ion-exchanged glasses. Additionally, when reannealing takes place on ion-exchanged glasses the length of the cracks increased, respectively shown in Figure 4. 66.

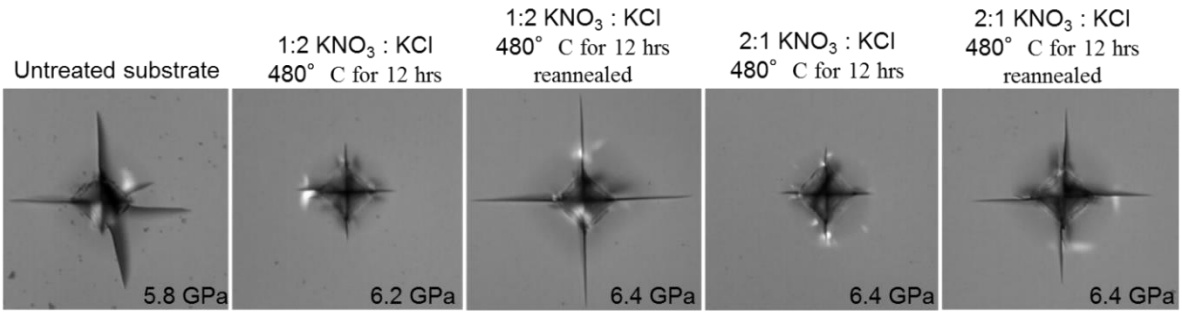

Figure 4. 66: Vickers Micro Hardness 10 indentations 9.8 N Load 15 s (50 µ)

An increase of approximately 10 % is observed in the hardness of the ion exchanged glass compared to the hardness results of untreated glasses. Similar findings have been reported in the literature for both ion exchanged aluminosilicate glasses (Kato *et al.*, 2010) and soda lime silica glass (Kese et al., 2004).

When the results of the ion exchange process were compared with the untreated sample, it was determined that the ion exchange process increased the crack formation limit load as indicated in the literature. However, a clear relationship has not been found between the crack resistance and Vickers hardness or fracture toughness Sehgal and Ito (1999). Because, residual stresses supress the crack initiation whereas they can cause a slight change in hardness.

The crack propagation begins for ion-exchange strengthened glass specimen at lower loads than 9.8 N and became gradually more severe with increasing the growing load. The crack lengths of strengthened glasses are definitely smaller than the untreated specimens. Vickers indentation images for different ion-exchange process temperatures, namely 420°C, 450°C and 480°C all applied for 12 hrs are shown in figure 4.68. The indentation loads were started at 0.49 N and increased 0.98 N, 1.96 N, 1.96 N, 4.9 N and 9.8 N, respectively.

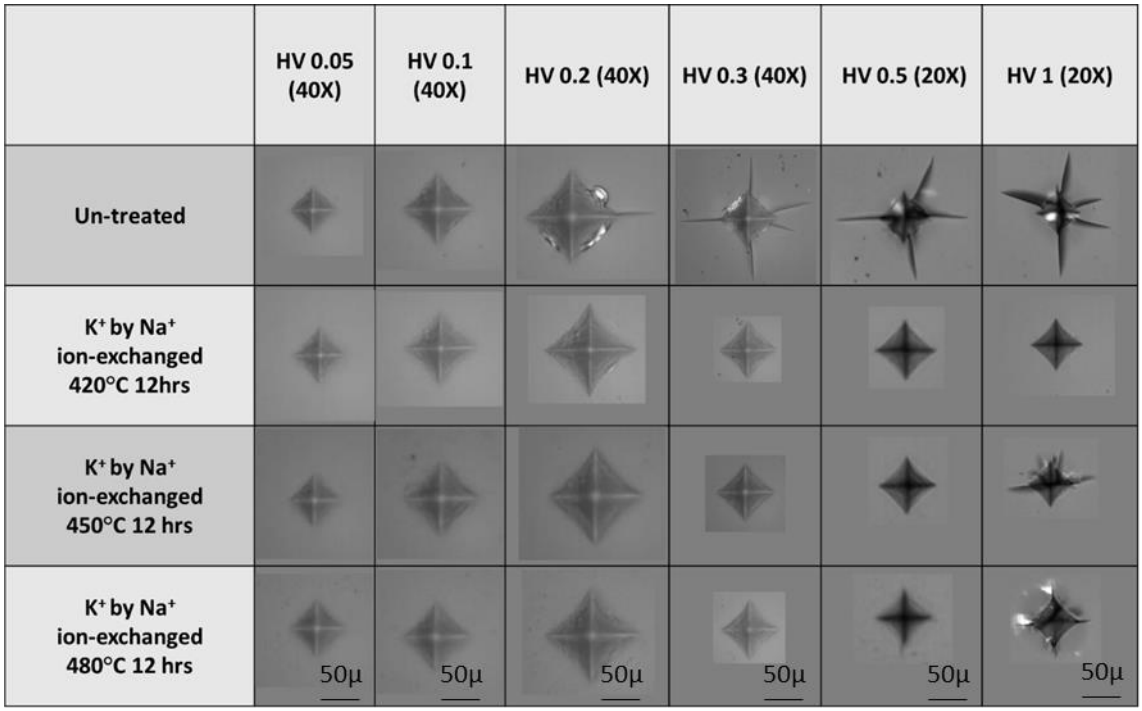

Figure 4. 67: Indentation crack formation of non-ion-exchanged and ion-exchanged soda-lime-silica glasses images

The decrease in hardness values by ion exchange can be explained by increased viscoelastic relaxation with increasing temperature for the processes applied for a fixed time. As the process temperature approaches the glass transition temperature of the glass, there will be increased relaxation of the glass structure during the process as indicated in previous studies(Bradshaw, 1979b; Wright *et al.*, 1989). With the relaxation of the glass structure, potassium ions can undergo local relaxation thereby allowing the potassium to be more readily accommodated.

With increased relaxation the structure of the glass surface might be expected to be similar to the structure of a glass containing a large amount of potassium in its main composition. In this case, the resulting structural compression and the resulting stress amount is less. This relaxation process, long-term processes obtained after the hardness of the values close to being able to explain the behaviour Sehgal and Ito (1999). The resistance of the surface to indentation decreases in proportion to the relaxation. As stated in the literature, crack formation and crack propagation are limited and prevented by the presence of compressive stresses on the glass surface. Crack lengths or the size of deformed regions under the same load are smaller in samples with high compressive stress. Thus, the effectiveness of the chemical tempering process can be interpreted. When the results of the ion-exchanged samples were compared with the non-ion-exchanged sample, it was determined that the ion exchange process increased the limit load for the crack, as indicated in the literature(Sehgal and Ito (1999).

The molar volume has effects on the fracture toughness of glass. For instance, according to Sehgal and Ito (1999) glasses with larger molar volume have higher fracture toughness; therefore, smaller brittleness, meaning they deform more easily. The molar volume of the ion-exchanged layer cannot be measured directly. Nevertheless, it has never been reported except some mechanisms from simulations have been suggested. One would observe that for an ion-exchanged but non-relaxed system the expected molar volume could be more than the equivalent relaxed composition.

4.7. Summary of the Results and Discussion

The results of experimental work discovered that compared to non-ion-exchanged reference soda-lime-silica glass sample, Na^+ - K^+ ion exchanged glasses provide increased surface microhardness / nanohardness, resistance to crack formation and strength. Based on the

results and discussion, it can be suggested that the ion – exchange process which had taken place by using salt paste was most successfully achieved on Na^+ - K^+ exchanged ones. Alterations in the Na^+ - K^+ ion – exchanged glasses are observed to be associated with structural band changes in the silica network structure. The structural changes are detected by a structural band shift on Si – O stretching band located at around 1000-1200 cm^{-1} as well as the new structural infrared band at around 950cm^{-1}. Raman spectra also show structural changes accordingly. Raman Spectra of the Na^+ - K^+ ion – exchanged glasses show a shift of the ~1100 cm^{-1} band to higher wavenumbers as the ion-exchange temperature increases. Alterations in the Na-K ion-exchanged glasses are assumed and observed to be associated with the structural changes in the silica network structure which are detected by a shift in the Si-O stretching infrared band located at 1000-1200 cm^{-1}.

It has been demonstrated that an increase in strength of soda-lime-silica glass slices can be achieved by applying Na – K ion exchange strengthening. The average four – point bending strength of ion-exchange strengthened soda lime silica glasses were up to a factor of 3.8 ± 0.2 times higher than the untreated soda lime silica glasses.

The results of mechanical properties suggested major differences between ion-exchanged and as melted equivalent potassium-containing glasses. Ion – exchange process aids to improve mechanical properties; however, as the amount of potassium content increases in the glass composition, toughness, hardness, Elastic Moduli, decrease respectively. This has been presented by the outcomes of Nanoindentation Figure 4. 16 and Figure 4. 33.

However, the structural peak position at around 1050 cm^{-1} which is assigned to symmetrical stretching modes of Si-O-Si, bridging oxygens shifts to lower wavenumbers, similarly on both potassium induced by ion exchange or added from the batch into the glass structure. The Q^n species assignments are also reasonably in the same trend and supported that reduction in connectivity is observed as a direct consequence of both ion exchange treatment and the addition of potassium into the glass batch.

The trends of the results of structural and mechanical property assignments of lithium-containing as melted glasses also supported the findings of as melted potassium-containing glasses as well as the ion-exchanged glass specimens.

Chapter 5. Conclusions and Suggestions for Further Work

5.1. Conclusions

1. Ion exchange of different alkali ions such as Na^+ for Li^+, K^+ for Na^+, Cs^+ for Na^+ or K^+ have been demonstrated using a salt paste method, although only the K^+ for Na^+ exchange yielded good products, as significant cracking was found in the Li/Na, K/Cs, Na/Cs samples. It has been demonstrated that an increase in strength of soda-lime-silica glass slides can be achieved by applying Na – K ion exchange strengthening using a salt paste method.
2. This Na – K ion exchange strengthening provided an increase in crack resistance. Compared to a reference sample, the chance of crack formation was reduced in ion-exchange treated samples. Vickers hardness and nanoindentation hardness also increased. The average four – point bending strength of ion-exchange strengthened soda lime silica glasses were up to a factor of 3.8 ±0.2 times higher than the untreated soda lime silica glasses.
3. Structural changes observed using FTIR suggested that network connectivity changes following ion-exchange treatment. Structural changes observed using Raman spectroscopy suggested that after ion-exchange treatment that the fraction of observed Q species slightly changed, indicating a small reduction in connectivity as a direct consequence of ion-exchange treatment.
4. The structural comparison between as melted potassium containing soda-lime-silica glass series and sodium-potassium ion exchange strengthened glasses suggested that addition of potassium in the structure resulted in similar trends in both FTIR spectra and Raman spectra. The FTIR reflectance spectra peak at ~1050 cm^{-1} shifted to lower wavenumbers with increasing potassium in the structure. However, the equivalent peak in the Raman spectra shifted to higher wavenumbers with increasing potassium in the structure. This change is claimed to be related the connectivity difference of sodium and potassium ions.
5. Similar overall trends were observed in the Raman and FTIR spectra for both as melted soda potassia lime silica glass series and as melted soda lithia lime silica glass series. The FTIR reflectance spectra peak at ~1050 cm^{-1} shifted to lower wavenumbers with increasing sodium in the structure. However, the equivalent peak in the Raman spectra shifted to higher wavenumbers with increasing sodium in the structure. This

indicates that the observed changes in the Raman spectra and the FTIR spectra are not simply due to induced residual stresses in the ion exchange process.

6. The overall trends in mechanical properties are similar for both as melted soda potassia lime silicate glass series and as melted soda lithia lime silicate glass series. As the potassium content increases in the glass composition, toughness, hardness, elastic moduli all decrease; as the amount of lithium content increases in the glass composition, toughness, hardness, elastic moduli all increase.
7. This work has also led to further research and development at the sponsoring company in terms of developing impact resistance. Preliminary pilot-scale tests have been done, further experiments are planned.

5.2. Suggestions for Further Work

- Although this study has clearly shown how structural and property changes differ from the compositional modifications inherent in ion-exchange more detailed structural investigation using Si-NMR is required to confirm the Q-speciation inferred from Raman spectroscopy and FTIR.
- Adjustment of processing parameters to produce uncracked samples for Li-Na, K-Cs and Na-Cs exchange would enable a more detailed investigation of the behaviour of these glasses.
- Further nanoindentation experiments to investigate the variation of the moduli and hardness with depth in the ion exchanged samples. These measurements should be coupled with EDS and Raman on cross-sections to provide both compositional and structural information.
- It would also be beneficial to conduct a similar study using MD simulations to be able to make more precise conclusions in terms of using the same glass compositions and ion-exchange parameters.

REFERENCES

Abrams, M. B., Green, D. J. and Glass, S. J. (2003) "Fracture behavior of engineered stress profile soda lime silicate glass," *Journal of Non-Crystalline Solids*, 321(1–2), pp. 10–19. doi: 10.1016/S0022-3093(03)00021-8.

Abrams, M., Shen, J. and Green, D. (2004) "Residual stress measurement in ion-exchanged glass by iterated birefringence and etching," *Journal of Testing and Evaluation*, 32(3), pp. 227–233. doi: 10.1016/j.cplett.2004.07.081.

A.Feltz (2001) "Oxide Glasses," in *Encyclopedia of Materials: Science and Technology (Second Edition)*. Elsevier, pp. 6614–6624.

Agarwal, A., Davis, K. M. and Tomozawa, M. (1995) "A simple IR spectroscopic method for determining fictive temperature of silica glasses," *Journal of Non-Crystalline Solids*, 185(1–2), pp. 191–198. doi: 10.1016/0022-3093(94)00676-8.

Agarwal, A. and Tomozawa, M. (1995) "Determination of Fictive Temperature of Soda???Lime Silicate Glass," *Journal of the American Ceramic Society*, pp. 827–829. doi: 10.1111/j.1151-2916.1995.tb08257.x.

Agarwal, A. and Tomozawa, M. (1997) "Correlation of silica glass properties with the infrared spectra," *Journal of Non-Crystalline Solids*, 209(1–2), pp. 166–174. doi: 10.1016/S0022-3093(96)00542-X.

Amidon, G. L. *et al.* (1983) "LOW PRESSURE LAMINATION OF SAFETY GLASS," *United States Patent*, (19). doi: 10.1016/j.(73).

Anderson, T. L. (2005) *Fracture Mechanics*. Taylor & Francis.

As, R., Mognato, E. and Schiavonato, M. (2005) "Correlation Between Strength and Measured Residual Stress in Tempered Glass Products," 2(3), pp. 1–10.

Barthel, E. *et al.* (2005) "The mechanics of glass and functionalised glass surfaces."

Beall, G. H. *et al.* (2016) "Ion-Exchange in Glass-Ceramics," *Frontiers in Materials*, 3(August), pp. 1–11. doi: 10.3389/fmats.2016.00041.

Beall, G. H., Pierson, J. E., Stookey, S. D. (1989) "Strengthened Glass Article and Method."

Bradshaw, W. (1979a) "Stress profile determination in chemically strengthened glass using scattered light," *Journal of Materials Science*, 14(12), pp. 2981–2988. doi: 10.1007/BF00611483.

Bradshaw, W. (1979b) "Stress profile determination in chemically strengthened glass using scattered light," *Journal of Materials Science*, 14(12), pp. 2981–2988. doi: 10.1007/BF00611483.

Brawer, S. A. and White, W. B. (1975) "Raman spectroscopic investigation of the structure of silicate glasses. I. The binary alkali silicates," *The Journal of Chemical Physics*, 63(6), pp. 2421–2432. doi: 10.1063/1.431671.

Brzesowsky, R. H. *et al.* (1998) "Glass strengthening by silica particle reinforced organic-inorganic coatings," *Journal of Non-Crystalline Solids*, 241(1), pp. 27–37. doi: 10.1016/S0022-3093(98)00750-9.

Burkhard*, D. J. M. (1997) "Elastic properties of Alkali Silicate Glasses with Iron Oxide: Relation to Glass Structure," *Solid State Communication*, 35(5), pp. 1332–1336.

Burns, A., Brack, H. P. and Risen, W. M. (1991) “Dielectric and infrared reflectance studies of inorganic oxide glasses,” *Journal of Non-Crystalline Solids*, 131–133(PART 2), pp. 994–1000. doi: 10.1016/0022-3093(91)90714-H.

Calahoo, C. (2016a) *Structure-Property Relations of Mixed-Alkali and Ion-Exchange Silicate Glasses*.

Calahoo, C. (2016b) *Structure-Property Relations of Mixed-Alkali and Ion-Exchange Silicate Glasses*.

Calahoo, C., Zwanziger, J. W. and Butler, I. S. (2016) “Mechanical-Structural Investigation of Ion-Exchanged Lithium Silicate Glass using Micro-Raman Spectroscopy,” *Journal of Physical Chemistry C*, 120(13), pp. 7213–7232. doi: 10.1021/acs.jpcc.6b01720.

CHARLES, R. J. (1966) “Metastable Liquid Immiscibility in Alkali Metal Oxide–Silica Systems,” *Journal of the American Ceramic Society*, 49(2), pp. 55–62. doi: 10.1111/j.1151-2916.1966.tb13208.x.

Chen, X. and Ellis, B. (1995) “Strengthening of glass rods with ormosil polymeric coatings,” *Journal of Non-Crystalline Solids*, 185, pp. 1–17. doi: 10.1016/0022-3093(94)00647-4.

Chisholm, R. S., Sleighter, G. E., Heights, N., Ernsberger, F. M. (1966) “Method of Strengthening Glass by Ion Exchange and Articles Therefrom.”

Colomban, P. (2003) “Polymerization degree and Raman identification of ancient glasses used for jewelry, ceramic enamels and mosaics,” *Journal of Non-Crystalline Solids*, 323(1–3), pp. 180–187. doi: 10.1016/S0022-3093(03)00303-X.

COOPER, A. R. and KROHN, D. A. (1969) “Strengthening of Class Fibers: 11, Ion Exchange,” *Journal of the American Ceramic Society*, 52(12), pp. 665–669. doi: 10.1111/j.1151-2916.1969.tb16073.x.

Cornel, Jeroen; Lindenberg, Christian; Scholl, Jochen and Mazzotti, M. (2012) “Raman Spectroscopy,” in *Industrial Crystallization Process Monitoring and Control*. John Wiley & Sons, Incorporated.

Corning (2016) *Corning. Corning Gorilla Glass 4 Product Information. Technical report, 2016*.

DAY, D. E. and RINDONE, G. E. (1962) “Properties of Soda Aluminosilicate Glasses: Coordination of Aluminum Ions,” *Journal of the American Ceramic Society*, 45(12), pp. 579–581. doi: 10.1111/j.1151-2916.1962.tb11063.x.

Dériano, S. *et al.* (2004) “Mechanical strength improvement of a soda-lime-silica glass by thermal treatment under flowing gas,” *Journal of the European Ceramic Society*, 24(9), pp. 2803–2812. doi: 10.1016/j.jeurceramsoc.2003.09.019.

Dimitrova, M. *et al.* (2016) “Modifying of Float Glass Surface with Silver Nanoparticles by Ion - Exchange,” 5(12), pp. 63–70.

Donald, I. W. (1989) “Methods for improving the mechanical properties of oxide glasses,” *Journal of Materials Science*, 24(12), pp. 4177–4208. doi: 10.1007/BF00544488.

DOREMUS, R. H. (1974) “Mixed-Alkali Effect and Interdiffusion of Na and K Ions in Glass,” *Journal of the American Ceramic Society*, 57(11), pp. 478–480. doi: 10.1111/j.1151-2916.1974.tb11395.x.

Eckert, H. (2015) “Modern Glass Characterization,” *Modern Glass Characterization*, pp. 345–390.

Ellison, A. J., Gomez, S. (2010) “Down-Drawable, Chemically Strengthened Glass for Cover Plate” US 7,666,511 B2

El-Sayed, T. and Hand, R. J. (2011) “Modelling the strengthening of glass using epoxy based coatings,” *Journal of the European Ceramic Society*, 31(15), pp. 2783–2791. doi: 10.1016/j.jeurceramsoc.2011.05.033.

El-Sayed, T. and Hand, R. J. (2012) “Fractographic analysis of epoxy coated glass,” *Ceramics International*, 38(3), pp. 2543–2549. doi: 10.1016/j.ceramint.2011.11.025.

Erdem, İ., Guldiren, D. and Aydin, S. (2017) “Chemical tempering of soda lime silicate glasses by ion exchange process for the improvement of surface and bulk mechanical strength,” *Journal of Non-Crystalline Solids*, 473(May), pp. 170–178. doi: 10.1016/j.jnoncrysol.2017.08.010.

EVANS, A. G. and CHARLES, E. A. (1976) “Fracture Toughness Determinations by Indentation,” *Journal of the American Ceramic Society*, 59(7–8), pp. 371–372. doi: 10.1111/j.1151-2916.1976.tb10991.x.

Fabes, B. D. *et al.* (1986) “Strengthening of silica glass by gel-derived coatings,” *Journal of Non-Crystalline Solids*, 82(1–3), pp. 349–355. doi: 10.1016/0022-3093(86)90151-1.

Fabes, B. D. and Uhlmann, D. R. (1990) “Strengthening of Glass by Sol-Gel Coatings,” *Journal of the American Ceramic Society*, 73(4), pp. 978–988. doi: 10.1111/j.1151-2916.1990.tb05146.x.

Ferraro, J. (2002) *Introductory Raman Spectroscopy*. Academic Press Inc.

Ferraro, J. R. and Manghnani, M. H. (1972) “Infrared absorption spectra of sodium silicate glasses at high pressures,” *Journal of Applied Physics*, 43(11), pp. 4595–4599. doi: 10.1063/1.1660971.

Fett, T. *et al.* (2007) “Ring-on-ring strength measurements on rectangular glass slides,” *Journal of Materials Science*, 42(1), pp. 393–395. doi: 10.1007/s10853-006-1102-8.

Fett, T., Guin, J. P. and Wiederhorn, S. M. (2005) “Stresses in ion-exchange layers of soda-lime-silicate glass,” *Fatigue and Fracture of Engineering Materials and Structures*, 28(6), pp. 507–514. doi: 10.1111/j.1460-2695.2005.00888.x.

Findakly, T. (1985) “Glass Glass waveguides by ion exchange: a review,” *Optical Engineering*, 24(2), pp. 244–250.

Florent DOMINE * and Bernard PIRIOU (1983) “STUDY OF SODIUM SILICATE MELT AND GLASS BY INFRARED REFLECTANCE SPECTROSCOPY,” *Journal of Non-Crystalline Solids*, 62(5), pp. 5–10. doi: 10.3138/ptc.2009-09-s1.

Fluegel, A. *et al.* (2008) “Density and thermal expansion calculation of silicate glass melts from 1000°C to 1400°C,” *Physics and Chemistry of Glasses: European Journal of Glass Science and Technology Part B*, 49(5), pp. 245–257.

Fu, A. I. and Mauro, J. C. (2013) “Mutual diffusivity, network dilation, and salt bath poisoning effects in ion-exchanged glass,” *Journal of Non-Crystalline Solids*, 363(1), pp. 199–204. doi: 10.1016/j.jnoncrysol.2012.12.037.

Furukawa, T., Fox, K. E. and White, W. B. (1981) “Raman spectroscopic investigation of the structure of silicate glasses. III. Raman intensities and structural units in sodium silicate glasses,” *The Journal of Chemical Physics*, 75(7), pp. 3226–3237. doi: 10.1063/1.442472.

Garfinkel, H. M. (1968) “Ion exchange equilibria between glass and molten salts,” *Journal of Non-Crystalline Solids*, 318(3), pp. 262–267. doi: 10.1016/S0022-3093(02)01888-4.

Garza-Méndez, F. J. *et al.* (2007) “Scaling properties of fracture surfaces on glass strengthened by ionic exchange,” *Applied Surface Science*, 254(5), pp. 1471–1474. doi: 10.1016/j.apsusc.2007.07.019.

Gervais, F; Blin A; Massiot, D. C. J. P. C. M. H. N. F. (1987) “Infrared Reflectivity Spectroscopy of Silılcate Glasses,” *Journal of Non-Crystalline Solids*, 89, pp. 384–401.

G.G. Liversidge J.F. Bishop, D.A. Czekai, K. C. C. (1983) “STRENGTHENED GLASS-CERAMIC ARTICLE AND METHOD,” 96(19), pp. 62–66. doi: US005485919A.

Gonzalez Rodriguez, J. a. and Hand, R. J. (2013) “Evolution of the modulus and hardness of the tin and air sides of float glass as a function of hydration time,” *Glass Technology: European Journal of Glass Science and Technology Part A*, 54(1), pp. 36–41.

Gordon, R., Kramer, K., & Liu, X. (1996) “Chemical Vapor Deposition and Properties of Amorphous Aluminum Oxide Films,” *MRS Proceedings*, pp. 446, 383.

Green, D. J. (1998) *An Introduction to the Mechanical Properties of Ceramics*. Cambridge University Press.

Griffith, A. A. (1921) “The Phenomenon of rupture and flow in solids,” *Philosophical Transactions of the Royal Society of London. Series A,* 221(1921), pp. 163–198.

Guldiren, D., Erdem, I. and Aydin, S. (2016a) “Influence of silver and potassium ion exchange on physical and mechanical properties of soda lime glass,” *Journal of Non-Crystalline Solids*, 441, pp. 1–9. doi: 10.1016/j.jnoncrysol.2016.03.007.

Guldiren, D., Erdem, I. and Aydin, S. (2016b) “Influence of silver and potassium ion exchange on physical and mechanical properties of soda lime glass,” *Journal of Non-Crystalline Solids*, 441, pp. 1–9. doi: 10.1016/j.jnoncrysol.2016.03.007.

Guldiren, D., Erdem, I. and Aydin, S. (2016c) “Influence of silver and potassium ion exchange on physical and mechanical properties of soda lime glass,” *Journal of Non-Crystalline Solids*, 441, pp. 1–9. doi: 10.1016/j.jnoncrysol.2016.03.007.

Gy, R. (2008a) “Ion exchange for glass strengthening,” *Materials Science and Engineering B: Solid-State Materials for Advanced Technology*, 149(2), pp. 159–165. doi: 10.1016/j.mseb.2007.11.029.

Gy, R. (2008b) “Ion exchange for glass strengthening,” *Materials Science and Engineering: B*, 149(2), pp. 159–165. doi: 10.1016/j.mseb.2007.11.029.

Hale, D. K. (1968) “Strengthening of silicate glasses by ion exchange,” *Nature*, 217(5134), pp. 1115–1118. doi: 10.1038/2171115a0.

Hammer, F. W. (1970) “MANUFACTURE OF CHEMICALLY STRENGTHENED GLASS ARTICLES.” doi: 10.1111/j.1559-3584.1927.tb04229.x.

Hand, R. J. *et al.* (2003) “Epoxy based coatings on glass: Strengthening mechanisms,” *Journal of Non-Crystalline Solids*, 315(3), pp. 276–287. doi: 10.1016/S0022-3093(02)01611-3.

Hand, R. J. and Tadjiev, D. R. (2010) “Mechanical properties of silicate glasses as a function of composition,” *Journal of Non-Crystalline Solids*, 356(44–49), pp. 2417–2423. doi: 10.1016/j.jnoncrysol.2010.05.007.

Hand, R. J., Wang, F. H. and Ellis, B. (1998) “Glass Strengthening Using Ormosil Polymeric Coatings,” *Journal of Sol-Gel Science and Technology*, 13, pp. 695–699.

Hanna, R. and SU, G. -J (1964) “Infrared Absorption Spectra of Sodium Silicate Glasses from 4 to 30μ,” *Journal of the American Ceramic Society*, 47(12), pp. 597–601. doi: 10.1111/j.1151-2916.1964.tb13113.x.

Hassani, H. and Sglavo, V. M. (2015) “Effect of KNO 3 Molten Bath Na Enrichment on the Mechanical Performances of Ion-exchanged Soda-Lime- Silicate Glass,” *Ion Exchange - Studies and Applications*, (September). doi: 10.5772/60976.

Hassani, H. and Sglavo, V. M. (2019) “Effect of Na contamination on the chemical strengthening of soda-lime silicate float glass by ion-exchange in molten potassium nitrate,” *Journal of Non-Crystalline Solids*, 515(February), pp. 143–148. doi: 10.1016/j.jnoncrysol.2019.04.013.

Hermansen, C. *et al.* (2013) “Densification and plastic deformation under microindentation in silicate glasses and the relation to hardness and crack resistance,” *Journal of Non-Crystalline Solids*, 364(1), pp. 40–43. doi: 10.1016/j.jnoncrysol.2012.12.047.

Hödemann, S. *et al.* (2016) “Gradient scattered light method for non-destructive stress profile determination in chemically strengthened glass,” *Journal of Materials Science*, 51(12), pp. 5962–5978. doi: 10.1007/s10853-016-9897-4.

Hornschuh, S. *et al.* (2004) “Silver ion exchange in glasses of the system Na2O/Al 2O3/B2O3/SiO2,” *Journal of Non-Crystalline Solids*, 347(1–3), pp. 121–127. doi: 10.1016/j.jnoncrysol.2004.09.021.

Husung, R. D. and Doremus, R. H. (1990) “The infrared transmission spectra of four silicate glasses before and after exposure to water,” *Journal of Materials Research*, 5(10), pp. 2209–2217. doi: 10.1557/JMR.1990.2209.

Inglis, C. E. (1913) “Stresses in a Plate due to the Presence of Cracks and Sharp Corners,” *Trans. Inst. Naval Architects*, 55, p. 219.

Irwin, G. R. (1958) *‘Fracture’, in Handbook der Physik*. Vol. 79, Springer-Verlag, Berlin.

James, P. F., Chen, M. and Jones, F. R. (1993) “Strengthening of soda-lime-silica glass by sol-gel- and melt-derived coatings,” *Journal of Non-Crystalline Solids*, 155(2), pp. 99–109. doi: 10.1016/0022-3093(93)91313-R.

Jannotti, P. *et al.* (2011) “Photoelastic Measurement of High Stress Profiles in Ion-Exchanged Glass,” *International Journal of Applied Glass Science*, 2(4), pp. 275–281. doi: 10.1111/j.2041-1294.2011.00066.x.

Jannotti, P. *et al.* (2012) “Influence of ultra-high residual compressive stress on the static and dynamic indentation response of a chemically strengthened glass,” *Journal of the European Ceramic Society*, 32(8), pp. 1551–1559. doi: 10.1016/j.jeurceramsoc.2012.01.002.

Jannotti, P., Subhash, G. and Varshneya, A. K. (2014) “Ball impact response of unstrengthened and chemically strengthened glass bars,” *Journal of the American Ceramic Society*, 97(1), pp. 189–197. doi: 10.1111/jace.12704.

Karlsson, S. (2012) *Modification of Float Glass Surfaces by Ion Exchange*.

Karlsson, S. *et al.* (2015) “Alkali salt vapour deposition and in-line ion exchange on flat glass surfaces,” 56(6), pp. 203–213. doi: 10.13036/1753-3546.56.6.203.

Karlsson, S. *et al.* (2017) “Trends in Effective Diffusion Coefficients for Ion-Exchange Strengthening of Soda-Lime-Silicate Glasses” 4(April). doi: 10.3389/fmats.2017.00013.

Karlsson, S.;Jonson, B.;Stalhandske, C. (2010) “The technology of chemical glass strengthening - a review,” *Glass Technology - European Journal of Glass Science and Technology*, 356((44-49)), pp. 2289–2294.

Karlsson, Stefan; Jonson, Bo; Johansson, Marie; Enquist, B. (2013) “The effect of single-side ion exchange on the flexural strength of plain and holed float glass,” *Glass Technology - European Journal of Glass Science and Technology Part A*, 54(2), pp. 66–1(6).

Kato, Y. *et al.* (2010) “Effect of densification on crack initiation under Vickers indentation test,” *Journal of Non-Crystalline Solids*, 356(35–36), pp. 1768–1773. doi: 10.1016/j.jnoncrysol.2010.07.015.

Kearns, K. L. *et al.* (2010) “High-modulus organic classes prepared by physical vapor deposition,” *Advanced Materials*, 22(1), pp. 39–42. doi: 10.1002/adma.200901673.

Kese, K. O. (2004) *Relaxation and Nanomechanical Studies of the Vickers Residual Stress Field in Glass*. Thesis

Kese, K. O., Li, Z. C. and Bergman, B. (2004) “Influence of residual stress on elastic modulus and hardness of soda-lime glass measured by nanoindentation,” *Journal of Materials Research*, 19(10), pp. 3109–3119. doi: 10.1557/JMR.2004.0404.

Kese, K. and Rowcliffe, D. J. (2003) “Nanoindentation method for measuring residual stress in brittle materials,” *Journal of the American Ceramic Society*, 86(5), pp. 811–816. doi: 10.1111/j.1151-2916.2003.tb03380.x.

Kese, K., Tehler, M. and Bergman, B. (2006) “Contact residual stress relaxation in soda-lime glass Part I . Measurement using nanoindentation,” 26, pp. 1003–1011. doi: 10.1016/j.jeurceramsoc.2004.12.029.

Kilinc, E. (2016) *Mechanical and structural properties of soda lime silica glasses as a function of composition*. Thesis

Kilinc, E. and Hand, R. J. (2015) “Mechanical properties of soda-lime-silica glasses with varying alkaline earth contents,” *Journal of Non-Crystalline Solids*, 429, pp. 190–197. doi: 10.1016/j.jnoncrysol.2015.08.013.

Kingston, J. G. R. and Hand, R. J. (2000a) “Compositional effects on the fracture behaviour of alkali-silicate glasses,” *Fatigue and Fracture of Engineering Materials and Structures*, 23(8), pp. 685–690. doi: 10.1046/j.1460-2695.2000.00274.x.

Kingston, J. G. R. and Hand, R. J. (2000b) “Compositional effects on the fracture behaviour of alkali-silicate glasses,” *Fatigue and Fracture of Engineering Materials and Structures*, 23(8), pp. 685–690. doi: 10.1046/j.1460-2695.2000.00274.x.

Kishii, T. (1983) “Surface stress meters utilising the optical waveguide effect of chemically tempered glasses,” *Optics and Lasers in Engineering*, 4(1), pp. 25–38. doi: 10.1016/0143-8166(83)90004-0.

Kistler, S. S. (1962) “Stresses in Glass Produced by Nonuniform Exchange of Monovalent Ions,” *Journal of the American Ceramic Society*, 45(2), pp. 59–68. doi: 10.1111/j.1151-2916.1962.tb11081.x.

Koike, A. *et al.* (2012) “Difference of cracking behavior due to Vickers indentation between physically and chemically tempered glasses,” *Journal of Non-Crystalline Solids*, 358(24), pp. 3438–3444. doi: 10.1016/j.jnoncrysol.2012.02.020.

Kreski, P. K., Varshneya, A. K. and Cormack, A. N. (2012) “Investigation of ion-exchange ‘stuffed’ glass structures by molecular dynamics simulation,” *Journal of Non-Crystalline Solids*, 358(24), pp. 3539–3545. doi: 10.1016/j.jnoncrysol.2012.05.025.

Kurkjian, C. R. (1985a) “From griffith flaws to perfect fibers a history of glass research,” *Journal of Non-Crystalline Solids*, 73(1–3), pp. 265–271. doi: 10.1016/0022-3093(85)90352-7.

Kurkjian, C. R. (1985b) *Strength of Inorganic Glass*. Nato Advanced Research Workshop . Algarve: Plenum Press, New York.

Kurkjian, C. R. *et al.* (2003) “The intrinsic strength and fatigue of oxide glasses,” *Journal of Non-Crystalline Solids*, 316(1), pp. 114–124. doi: 10.1016/S0022-3093(02)01943-9.

Kurkjian, C. R., Gupta, P. K. and Brow, R. K. (2010) “The Strength of Silicate Glasses: What Do We Know, What Do We Need to Know?,” *International Journal of Applied Glass Science*, 1(1), pp. 27–37. doi: 10.1111/j.2041-1294.2010.00005.x.

LaCourse, W. C. (1987) “How surface flaws affect glass strength,” *The Glass industry*, 68(7), pp. 14–23.

LaCourse, W. C., A. M. (1989) “Process for Strengthening Glass.”

Lakin, M. J. (1991) *Glass:Nature, Structure, and Properties*. Springer - Verlag, New York.

Lawn, B. (1993) *Fracture of Brittle Solids*. Cambridge University Press.

LAWN, B. R. and MARSHALL, D. B. (1979a) “Hardness, Toughness, and Brittleness: An Indentation Analysis,” *Journal of the American Ceramic Society*, 62(7–8), pp. 347–350. doi: 10.1111/j.1151-2916.1979.tb19075.x.

LAWN, B. R. and MARSHALL, D. B. (1979b) “Hardness, Toughness, and Brittleness: An Indentation Analysis,” *Journal of the American Ceramic Society*, 62(7–8), pp. 347–350. doi: 10.1111/j.1151-2916.1979.tb19075.x.

Leboeuf, V. *et al.* (2013) “Potassium ionic exchange in glasses for mechanical property improvement,” *Journal of Non-Crystalline Solids*, 377, pp. 60–65. doi: 10.1016/j.jnoncrysol.2013.04.046.

Lee, L. G. M., Quintal, J. M. and Yan, Y. (2012) “DUAL STAGE ION EXCHANGE FOR CHEMICAL STRENGTHENING OF GLASS.” doi: 10.1038/incomms1464.

Lee, Y., Peng, Y. and Tomozawa, M. (1997) “IR reflection spectroscopy of a soda-lime glass surface during ion-exchange,” *Journal of non-crystalline solids*, 222, pp. 125–130. doi: 10.1016/S0022-3093(97)90104-6.

Macdonald, S. A. *et al.* (2000) “Dispersion analysis of FTIR reflection measurements in silicate glasses,” *Journal of Non-Crystalline Solids*, 275, pp. 72–82. doi: 10.1016/S0022-3093(00)00121-6.

Macrelli, G. (2015) “Glass Chemical Strengthening by Ion Exchange Glass Chemical strengthening by Ion Exchange,” (June).

Macrelli, G. (2017) “Chemical Strengthening of Glass by Ion-Exchange,” in *ICG Annual meeting and 32nd Sisecam Glass Symposium . Istanbul.*

Makishima, A. and Mackenzie, J. D. (1973a) “Direct calculation of Young’s modulus of glass,” *Journal of Non-Crystalline Solids*, 12(1), pp. 35–45. doi: 10.1016/0022-3093(73)90053-7.

Makishima, A. and Mackenzie, J. D. (1973b) “Direct calculation of Young’s moidulus of glass,” *Journal of Non-Crystalline Solids*, 12(1), pp. 35–45. doi: 10.1016/0022-3093(73)90053-7.

Makishima, A. and Mackenzie, J. D. (1975) “Calculation of bulk modulus, shear modulus and Poisson’s ratio of glass,” *Journal of Non-Crystalline Solids*, 17(2), pp. 147–157. doi: 10.1016/0022-3093(75)90047-2.

Mallick, K. K. and Holland, D. (2005) “Strengthening of container glasses by ion-exchange dip coating,” *Journal of Non-Crystalline Solids*, 351(30–32), pp. 2524–2536. doi: 10.1016/j.jnoncrysol.2005.06.040.

Matson, D. W., Sharma, S. K. and Philpotts, J. A. (1983) “The structure of high-silica alkali-silicate glasses. A Raman spectroscopic investigation,” *Journal of Non-Crystalline Solids*, 58(2–3), pp. 323–352. doi: 10.1016/0022-3093(83)90032-7.

Mazzoldi, P. *et al.* (2013) “Ion exchange process: History, evolution and applications,” *Rivista del Nuovo Cimento*, 36(9), pp. 397–460. doi: 10.1393/ncr/i2013-10092-1.

McMillan, P. (1984) “Structural Studies of Silicate Glasses and Melts - Applications and Limitations of Raman Spectroscopy.,” *American Mineralogist*, 69(6–8), pp. 622–644.

McMillan, P. F. (1984) “Structural Studies of Silicate Glasses and Melts-Applications and Limitations of Raman Spectroscopy,” *American Mineralogist*, 69, pp. 622–644. doi: 0003-004x/84/070E-0622$0.

Mognato, E. *et al.* (2014) “Thermally toughened safety glass,” pp. 1–9.

Mognato, E., Brocca, S. and Comiati, F. (2018) “Which is the Right Reference Surface Compression Value for Heat Treated Glass ?,” in *Challenging Glass 6 - Conference on Architectural and Structural Applications of Glass Louter, Bos, Belis, Veer, Nijsse (Eds.), Delft University of Technology*.

Morozumi, H. *et al.* (2015) “Crack Initiation Tendency of Chemically Strengthened Glasses,” *International Journal of Applied Glass Science*, 6(1), pp. 64–71. doi: 10.1111/ijag.12089.

Morris, D. J., Myers, S. B. and Cook, R. F. (2004) “Indentation crack initiation in ion-exchanged aluminosilicate glass,” *Journal of Materials Science*, 39(7), pp. 2399–2410. doi: 10.1023/B:JMSC.0000020002.06117.46.

N. SOGA, H. YAMANAKA, C. H. and M. K. (1976) “Elastic Properties and Structure of Alkaline-Earth Silicate Glasses,” 22, pp. 67–76.

Nordberg, M. E. *et al.* (1964) “Strengthening by ion exchange,” *Journal of the American Ceramic Society*, 47(5), pp. 215–219. doi: 10.1111/j.1151-2916.1964.tb14399.x.

Di Nunzio, S. *et al.* (2004) “Silver containing bioactive glasses prepared by molten salt ion-exchange,” *Journal of the European Ceramic Society*, 24(10–11), pp. 2935–2942. doi: 10.1016/j.jeurceramsoc.2003.11.010.

Olcott, J. S. (1963) “Chemical Strengthening of Glass Chemical Strengthening of Glass,” *Science*, 140(3572), pp. 1189–1193.

Oven, R., Batchelor, S. and Ashworth, D. G. (1999) “Effects of annealing electric field assisted K+-Na+ ion exchanged soda-lime glass guides,” *Journal of Physics D: Applied Physics*, 32(6), pp. 650–655. doi: 10.1088/0022-3727/32/6/009.

Özdemir Yanık, M. C. *et al.* (2018) “Influence of different process conditions on mechanical, optical and surface properties of silver ion exchanged soda-lime silicate glass,” *Journal of Non-Crystalline Solids*, 493(April), pp. 1–10. doi: 10.1016/j.jnoncrysol.2018.04.024.

Pantano, C. G. (no date) “The Role of Coatings and Other Surface Treatments in the Strength of Glass.”

Park, J.W. ; Chen, H. (1980) “an Infrared Study of Crystallization in Sodium-Disilicate Glasses Containing Iron-Oxide,” *Journal of Non-Crystalline Solids*, 40(1980), pp. 515–525.

Patschger, Marek; Rüssel, C. (2014) “Equilibria fromed during sodium/potasiium ion exchange between a salt melt and a soda lime silica glass as well as a sodium aluminosilicate glass,” *Journal of Physical Chemistry B*, 55(4), pp. 161–166.

Patschger, Marek; Rüssel, C. (2016) “Strengthening of a soda–lime–silica glass by ion exchange using an adherent potassium salt coating,” *Glass Technology - European Journal of Glass Science and Technology Part A, Volume 57, Number 1, February 2016, pp. 6-14(9)*, 57, pp. 6–14.

Ponton, C. B. and Rawlings, R. D. (1989) “Vickers indentation fracture toughness test Part 1 Review of literature and formulation of standardised indentation toughness equations,” *Materials Science and Technology*, 5(9), pp. 865–872. doi: 10.1179/mst.1989.5.9.865.

Quaranta, A. *et al.* (2012) “Spectroscopic investigation of structural rearrangements in silver ion-exchanged silicate glasses,” *Journal of Physical Chemistry C*, 116(5), pp. 3757–3764. doi: 10.1021/jp2095399.

Ragoen, C. *et al.* (2017) “Effect of Al2O3 content on the mechanical and interdiffusional properties of ion-exchanged Na-aluminosilicate glasses,” *Journal of Non-Crystalline Solids*, 458, pp. 129–136. doi: 10.1016/j.jnoncrysol.2016.12.019.

Ragoen, C. *et al.* (2018) “A XANES investigation of the network-modifier cations environment before and after the Na+/K+ion-exchange in silicate glasses,” *Journal of Non-Crystalline Solids*, 479(September 2017), pp. 97–104. doi: 10.1016/j.jnoncrysol.2017.10.021.

Ramaswamy R. V., S. R. (1988) “Ion-Exchanged Glass Waveguides : A Review,” *Journal of Lightwave Technology*, 6(6).

Ray, N. H. (1974) “Composition-property relationships in inorganic oxide glasses,” *Journal of Non-Crystalline Solids*, 15(3), pp. 423–434. doi: 10.1016/0022-3093(74)90148-3.

SANE, A. Y. and COOPER, A. R. (1987) “Stress Buildup and Relaxation During Ion Exchange Strengthening of Glass,” *Journal of the American Ceramic Society*, 70(2), pp. 86–89. doi: 10.1111/j.1151-2916.1987.tb04934.x.

Schott (no date) “SCHOTT Xensation ® Cover.”

Sehgal, J. and Ito, S. (1998) “A New Low-Brittleness Glass in the Soda-Lime-Silica Glass Family,” *Journal of the American Ceramic Society*, 81(9), pp. 2485–2488. doi: 10.1111/j.1151-2916.1998.tb02649.x.

Sehgal, J. and Ito, S. (1999) “Brittleness of glass,” *Journal of Non-Crystalline Solids*, 253(1–3), pp. 126–132. doi: 10.1016/S0022-3093(99)00348-8.

Sglavo, V. M. *et al.* (2014) “Analysis of the surface structure of soda lime silicate glass after chemical strengthening in different KNO3 salt baths,” *Journal of Non-Crystalline Solids*, 401, pp. 105–109. doi: 10.1016/j.jnoncrysol.2014.01.026.

Sglavo, V. M. (2015) “Chemical Strengthening of Soda Lime Silicate Float Glass: Effect of Small Differences in the KNO3 Bath,” *International Journal of Applied Glass Science*, 6(1), pp. 72–82. doi: 10.1111/ijag.12101.

Sglavo, V. M., Bonafini, M. and Prezzi, A. (2005) “Procedure for residual stress profile determination by curvature measurements,” *Mechanics of Materials*, 37(8), pp. 887–898. doi: 10.1016/j.mechmat.2004.09.003.

Sglavo, V. M. and Green, D. J. (2001) “Flaw-Insensitive Ion-Exchanged Glass: II, Production and Mechanical Performance,” 38(188774), pp. 1832–1838.

Sglavo, V. M., Larentis, L. and Green, D. J. (2001) “Flaw-Insensitive Ion-Exchanged Glass: I, Theoretical Aspects,” *Journal of the American Ceramic Society*, 84(8), pp. 1827–1831. doi: 10.1111/j.1151-2916.2001.tb00922.x.

Sglavo, V. M., Prezzi, A. and Zandonella, T. (2004) “Engineered stress-profile silicate glass: High strength material insensitive to surface defects and fatigue,” *Advanced Engineering Materials*, 6(5), pp. 344-349+276. doi: 10.1002/adem.200300509.

Shaisha, E. E. and Cooper, A. R. (1981) “Ion Exchange of Soda Lime Glass with Univalent Cations,” *Journal of the American Ceramic Society*, 64(5), pp. 278–283. doi: 10.1111/j.1151-2916.1981.tb09602.x.

Sharaf, N. a., Condrate, R. a. and Ahmed, a. a. (1991) “FTIR spectral/structural investigation of the ion exchange/thermal treatment of silver ions into a silicate glass,” *Materials Letters*, 11(3–4), pp. 115–118. doi: 10.1016/0167-577X(91)90097-P.

Shelby, J. E. (1989) “Properties and structure of soda-lime aluminosilicate glasses,” *Journal of Applied Physics*, 66(5), pp. 1947–1950. doi: 10.1063/1.344330.

Shelby, J. E. (2005) *Introduction to Glass Science and Technology*. Royal Society of Chemistry.

Shen, J. *et al.* (2003) “Stress relaxation of a soda lime silicate glass below the glass transition temperature,” *Journal of Non-Crystalline Solids*, 324(3), pp. 277–288. doi: 10.1016/S0022-3093(03)00260-6.

Shen, J. and Green, D. J. (2004) “Prediction of stress profiles in ion exchanged glasses,” *Journal of Non-Crystalline Solids*, 344(1–2), pp. 79–87. doi: 10.1016/j.jnoncrysol.2004.07.026.

SlMON and H. 0. McMAHON (1952) “Study of Some Binary Silicate Glasses by Means of Reflection in Infrared,” *Journal of American Ceramic Society*, 36(5), pp. 1–5.

Speranza, G. *et al.* (2009) “Quantum confinement and matrix effects in silver-exchanged soda lime glasses,” *Journal of Physical Chemistry C*, 113(11), pp. 4445–4450. doi: 10.1021/jp810317q.

Stavrou, E. *et al.* (2014a) “Vibrational study of thermally ion-exchanged sodium aluminoborosilicate glasses,” *Journal of Non-Crystalline Solids*, 401, pp. 232–236. doi: 10.1016/j.jnoncrysol.2013.12.017.

Stavrou, E. *et al.* (2014b) “Vibrational study of thermally ion-exchanged sodium aluminoborosilicate glasses,” *Journal of Non-Crystalline Solids*, 401, pp. 232–236. doi: 10.1016/j.jnoncrysol.2013.12.017.

Sun, Y. H. (1947) “Fundametal Condition of Glass Formation,” *Journal of American Ceramic Society*, 123(6), pp. 415–426.

Sundberg, P. *et al.* (2019) “Simultaneous chemical vapor deposition and thermal strengthening of glass,” *Thin Solid Films*, 669(November 2018), pp. 487–493. doi: S0040609018307697.

Tadjiev, D. R., Hand, R. J. and Hayes, S. a. (2010) “Calibrating a nanoindenter for very shallow depth indentation using equivalent contact radius,” *Philosophical Magazine*, 90(13), pp. 1819–1832. doi: 10.1080/14786430903571420.

Talimian, A., Mariotto, G. and Sglavo, V. M. (2017) “Electric field-assisted ion exchange strengthening of borosilicate and soda lime silicate glass,” *International Journal of Applied Glass Science*, 8(3), pp. 291–300. doi: 10.1111/ijag.12266.

Talimian, A. and Sglavo, V. M. (2017) “Ion-exchange strengthening of borosilicate glass: Influence of salt impurities and treatment temperature,” *Journal of Non-Crystalline Solids*, 456, pp. 12–21. doi: 10.1016/j.jnoncrysol.2016.10.032.

Tandia, A. *et al.* (2012) “Atomistic understanding of the network dilation anomaly in ion-exchanged glass,” *Journal of Non-Crystalline Solids*, 358(2), pp. 316–320. doi: 10.1016/j.jnoncrysol.2011.09.034.

Tandia, A., Vargheese, K. D. and Mauro, J. C. (2012) “Elasticity of ion stuffing in chemically strengthened glass,” *Journal of Non-Crystalline Solids*, 358(12–13), pp. 1569–1574. doi: 10.1016/j.jnoncrysol.2012.04.021.

Teisseire, J. *et al.* (2011) “Glass strengthening by polymeric coatings: Combined effect of mechanical properties and confinement,” *International Journal of Fracture*, 170(2), pp. 115–121. doi: 10.1007/s10704-011-9606-x.

Terakado, N. *et al.* (2016) “Depth analysis of a compression layer in chemically strengthened glass using depth-resolved micro-Raman spectroscopy,” *Journal of the Ceramic Society of Japan*, 124(10), pp. 1164–1166. doi: 10.2109/jcersj2.16138.

Tyagi, V. and Varshneya, A. K. (1998) “Measurement of progressive stress buildup during ion exchange in alkali aluminosilicate glass,” *Journal of Non-Crystalline Solids*, 238(3), pp. 186–192. doi: 10.1016/S0022-3093(98)00691-7.

Uchino, T. *et al.* (1993) “Local structure of sodium aluminosilicate glass: An ab initio molecular orbital study,” *Journal of Physical Chemistry*, 97(38), pp. 9642–9649. doi: 10.1021/j100140a019.

Uhlmann, D. R. and K. N. J. (1980) *Glass Science and Technology: Elasticity and Strength in Glasses*. Academic Press Inc.

Urbain, O. M., Stemeri, W. R. and Charles, H. (1966) “Method of Fire Polishing Edges of Hollow Articles,” *United States Patent Office*, pp. 18–20.

Varma, R. S., Kothari, D. C. and Tewari, R. (2009) “Nano-composite soda lime silicate glass prepared using silver ion exchange,” *Journal of Non-Crystalline Solids*, 355(22–23), pp. 1246–1251. doi: 10.1016/j.jnoncrysol.2009.05.001.

Varshneya, A. K. (1975) “Kinetics of ion exchange in glasses,” *Journal of Non-Crystalline Solids*, 19(C), pp. 355–365. doi: 10.1016/0022-3093(75)90099-X.

Varshneya, A. K. (2001) “Chemical Strengthening of Glass Products,” *Transactions of the Indian Ceramic Society*, 60(1), pp. 1–6. doi: 10.1080/0371750X.2001.10799951.

Varshneya, A. K. (2006) *Fundamentals of Inorganic Glasses*. The Society of Glass Technology.

Varshneya, A. K. (2010a) “Chemical Strengthening of Glass,” *International Journal of Applied Glass Science*, 1(January), pp. 131–142. doi: 10.2307/1711232.

Varshneya, A. K. (2010b) “Chemical Strengthening of Glass: Lessons Learned and Yet To Be Learned,” *International Journal of Applied Glass Science*, 1(2), pp. 131–142. doi: 10.1111/j.2041-1294.2010.00010.x.

Varshneya, A. K. (2010c) “The physics of chemical strengthening of glass: Room for a new view,” *Journal of Non-Crystalline Solids*, 356(44–49), pp. 2289–2294. doi: 10.1016/j.jnoncrysol.2010.05.010.

Varshneya, A. K. (2012) “Chemically Strengthened Lithium Aluminosilicate Glass Having High Strength Effective to Resist Fracture Upon Flexing.” doi: 10.1038/incomms1464.

Varshneya, A. K. *et al.* (2015) “Buildup and relaxation of stress in chemically strengthened glass,” *Journal of Non-Crystalline Solids*, 427, pp. 91–97. doi: 10.1016/j.jnoncrysol.2015.07.037.

Varshneya, A. K. (2018) “Stronger glass products: Lessons learned and yet to be learned,” *International Journal of Applied Glass Science*, 9(2), pp. 140–155. doi: 10.1111/ijag.12341.

Verné, E. *et al.* (2009) “Surface silver-doping of biocompatible glass to induce antibacterial properties. Part I: Massive glass,” *Journal of Materials Science: Materials in Medicine*, 20(3), pp. 733–740. doi: 10.1007/s10856-008-3617-9.

Wang, F. H. *et al.* (1997) “Strengthening of glass rods and bottles \ Nith \ Nater based epoxy acrylate coatings,” 13(February), pp. 163–171.

Wang, M. *et al.* (2011) “Raman spectra of sodalimesilicate glass doped with rare earth,” *Physica B: Condensed Matter*, 406(20), pp. 3865–3869. doi: 10.1016/j.physb.2011.07.014.

Wang, P. W. (1997) “Formation of silver colloids in silver ion-exchanged soda-lime glasses during annealing,” *Applied Surface Science*, 120(3–4), pp. 291–298. doi: 10.1016/S0169-4332(97)00237-7.

WANG, R.-B. (2014) “METHOD FOR STRENGTHENING GLASS SUBSTRATE AND ARTICLE MANUFACTURED BY THE SAME.”

Warren, B. E. (1934) “X-Ray Determination of the structure of Glass,” *American Ceramic Society Bulletin*, 17(1–12), pp. 249–254.

Watanabe, M. (1980) “Method of Strengthening Chemically Aglass Container.”

Weber, N. (1965) “US Patent 3,218,220. 1965, Brockway Glass Company, Inc.”

Wen, M. *et al.* (2008) “Edge-strengthening of flat glass with acrylate coatings,” *Journal of Non-Crystalline Solids*, 354(45–46), pp. 5060–5067. doi: 10.1016/j.jnoncrysol.2008.08.004.

WIEDERHORN, S. M. (1969) “Fracture Surface Energy of Glass,” *Journal of the American Ceramic Society*, 52(2), pp. 99–105. doi: 10.1111/j.1151-2916.1969.tb13350.x.

Wojdyr, M. (2010) “Fityk: A general-purpose peak fitting program,” *Journal of Applied Crystallography*, 43(5 PART 1), pp. 1126–1128. doi: 10.1107/S0021889810030499.

Wright, A. C. *et al.* (1989) “Neutron scattering studies of network glasses,” *Journal of Non-Crystalline Solids*, 112(1–3), pp. 33–47. doi: 10.1016/0022-3093(89)90491-2.

X. Zhou, P. F. Johnson, R. A. Condrate Sr, Y. M. G. (1990) “Structural Invesitgation of Plasma-Enhanced Glass Surface Modifcation Using FTIR Spectroscopy,” *Materials Letters*, 9(5.6), pp. 207–210.

Xiang, Y. *et al.* (2013) “Structure and properties of sodium aluminosilicate glasses from molecular dynamics simulations,” *Journal of Chemical Physics*, 139(4). doi: 10.1063/1.4816378.

Yarema, S. Ya. (1995) “On the contribution of G. R. Irwin to fracture mechanics,” *Materials Science*, 31(5), pp. 617–623. doi: 10.1007/bf00558797.

Yunqiu, H., Duvigneaud, P. H. and Plumat, E. (1986) “Mechanical strength improvement of glass by ion exchange in the solid state,” *Journal of Non-Crystalline Solids*, 80(1–3), pp. 283–291. doi: 10.1016/0022-3093(86)90408-4.

Zachariasen, W. H. (1932) “The atomic arrangement in glass,” *Journal of the American Chemical Society*, 54(10), pp. 3841–3851. doi: 10.1021/ja01349a006.

Published Work

Conferences

- **SGT 2016 Centenary Conference**
  Diffusional Strengthening of Glass - Poster
- **ICG 2017 Annual Meeting & 32nd Şişecam Glass Symposium**
  Properties of Ion-Exchanged Glasses - Poster
- **ESG & PNCS 2018 15th International Conference on the Physics of Non-Crystalline Solids**
  Strengthening of Alkali Alkaline Earth Silicate Glasses by Ion Exchange - Oral
- **SGT 2018 Glass and the Meeting of Minds**
  Strengthening of Alkali Alkaline Earth Silicate Glasses by Ion-Exchange - Oral
- **ICG 2019 25th International Congress on Glass**
  Understanding the effects of compositional changes in ion exchange - Oral